

Optical and near-infrared kilonova emission - light r-process composition

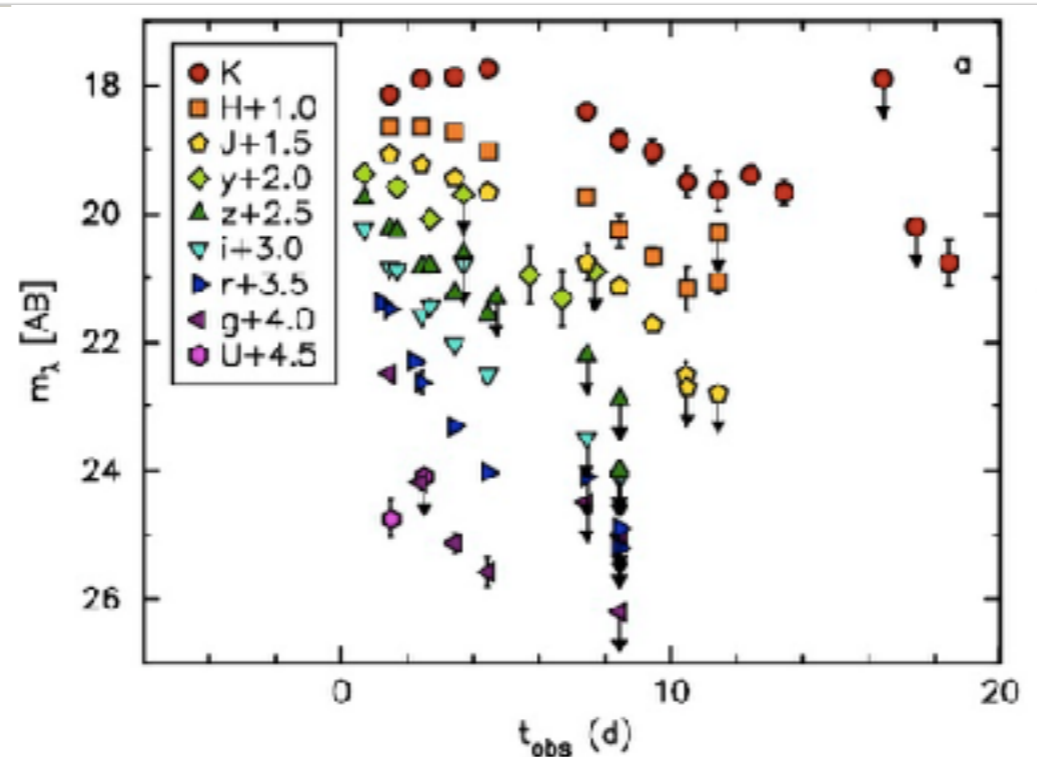
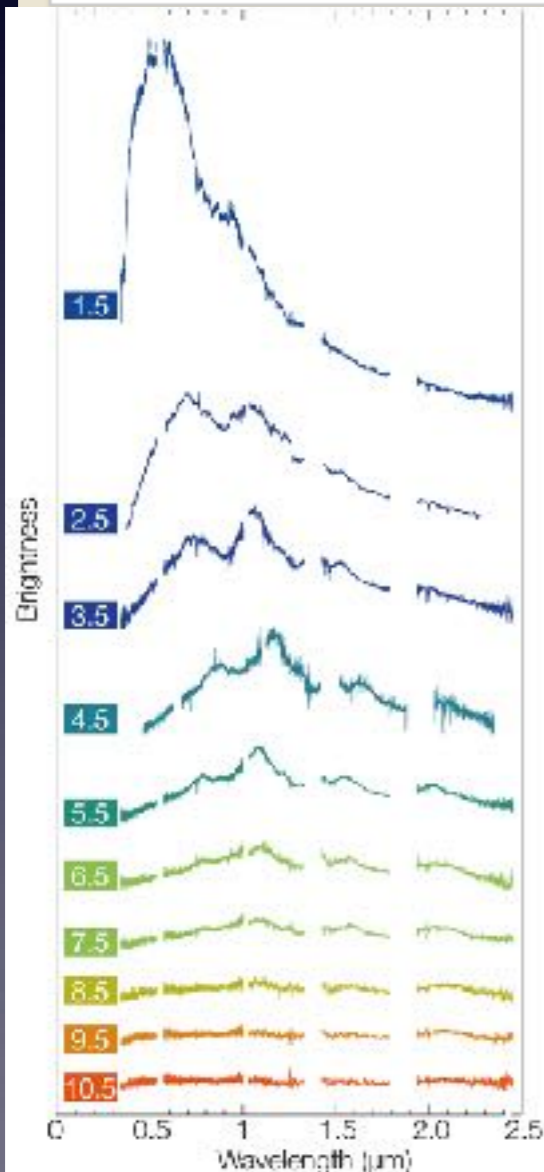
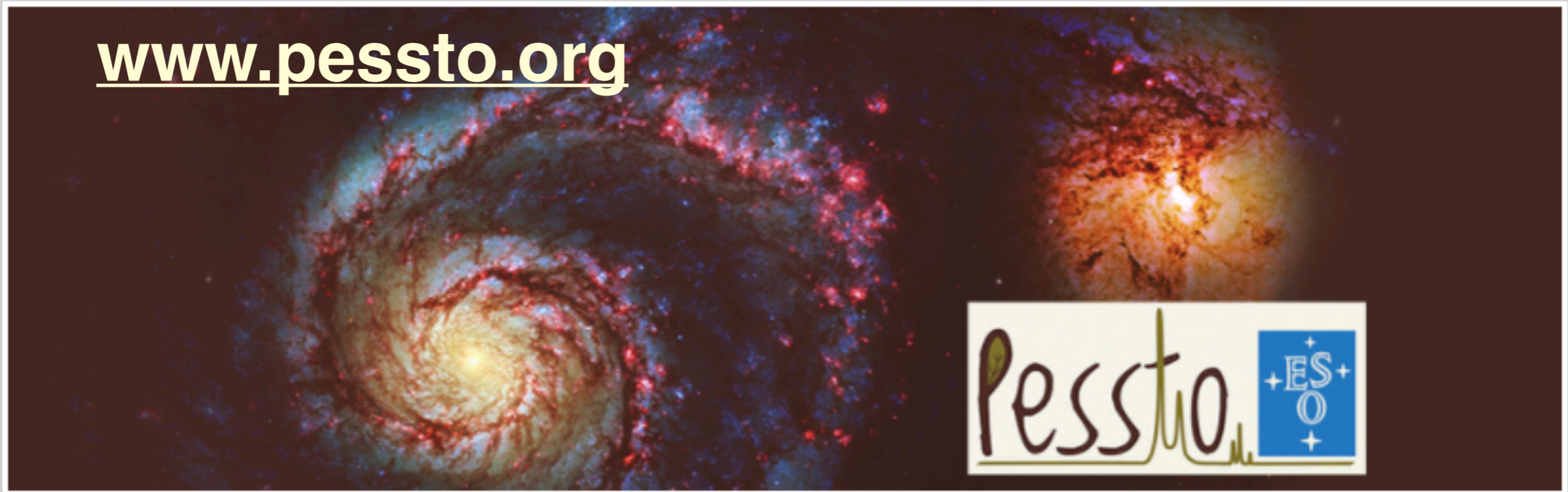
S. Smartt, A. Jerkstrand, G. Leloudas, M. Coughlin, E. Kankare

S. J. Smartt¹, T.-W. Chen², A. Jerkstrand³, M. Coughlin⁴, E. Kankare¹, S. A. Sim¹, M. Fraser⁵, C. Inerra⁶, K. Maguire¹, K. C. Chambers⁷, M. E. Huber⁷, T. Krühler², G. Leloudas⁸, M. Magee¹, L. J. Shingles¹, K. W. Smith¹, D. R. Young¹, J. Tonry⁷, R. Kotak¹, A. Gal-Yam⁹, J. D. Lyman¹⁰, D. S. Homan¹¹, C. Agliozzo^{12,13}, J. P. Anderson¹⁴, C. R. Angus⁶, C. Ashall¹⁵, C. Barbarino¹⁶, F. E. Bauer^{13,17,18}, M. Berton^{19,20}, M. T. Botticella²¹, M. Bulla²², J. Bulger⁷, G. Cannizzaro^{23,24}, Z. Cano²⁵, R. Cartier⁶, A. Cikota²⁶, P. Clark¹, A. De Cia²⁶, M. Della Valle^{21,27}, L. Denneau⁷, M. Dennefeld²⁸, L. Dessart²⁹, G. Dimitriadis⁶, N. Elias-Rosa³⁰, R. E. Firth⁶, H. Flewelling⁷, A. Flörs^{3,26,31}, A. Franckowiak³², C. Frohmaier³³, L. Galbany³⁴, S. González-Gaitán³⁵, J. Greiner², M. Gromadzki³⁶, A. Nicuesa Guelbenzu³⁷, C. P. Gutiérrez⁶, A. Hamanowicz^{26,36}, L. Hanlon⁵, J. Harmanen³⁸, K. E. Heintz^{3,39}, A. Heinze⁷, M.-S. Hernandez⁴⁰, S. T. Hodgkin⁴¹, I. M. Hook⁴², L. Izzo²⁵, P. A. James¹⁵, P. G. Jonker^{23,24}, W. E. Kerzendorf²⁶, S. Klose³⁷, Z. Kostrzewa-Rutkowska^{23,24}, M. Kowalski^{32,43}, M. Kromer^{44,45}, H. Kuncarayakti^{38,46}, A. Lawrence¹¹, T. B. Lowe⁷, E. A. Magnier⁷, I. Manulis⁹, A. Martin-Carrillo⁵, S. Mattila³⁸, O. McBrien¹, A. Müller⁴⁷, J. Nordin⁴³, D. O'Neill¹, F. Onori^{23,24}, J. T. Palmerio⁴⁸, A. Pastorello⁴⁹, F. Patat²⁶, G. Pignata^{12,13}, Ph. Podsiadlowski⁵⁰, M. L. Pumo^{49,51,52}, S. J. Prentice¹⁵, A. Rau², A. Razza^{14,53}, A. Rest^{54,55}, T. Reynolds³⁸, R. Roy^{16,56}, A. J. Ruiter^{57,58,59}, K. A. Rybicki³⁶, L. Salmon⁵, P. Schady², A. S. B. Schultz⁷, T. Schweyer², I. R. Seitenzahl^{57,58}, M. Smith⁶, J. Sollerman¹⁶, B. Stalder⁶⁰, C. W. Stubbs⁶¹, M. Sullivan⁶, H. Szegedi⁶², F. Taddia¹⁶, S. Taubenberger^{3,26}, G. Terreran^{49,63}, B. van Soelen⁶², J. Vos⁴⁰, R. J. Wainscoat⁷, N. A. Walton⁴¹, C. Waters⁷, H. Weiland⁷, M. Willman⁷, P. Wiseman², D. E. Wright⁶⁴, L. Wyrzykowski³⁶ & O. Yaron⁹

nature 551, 75–79 (2017) doi:10.1038/



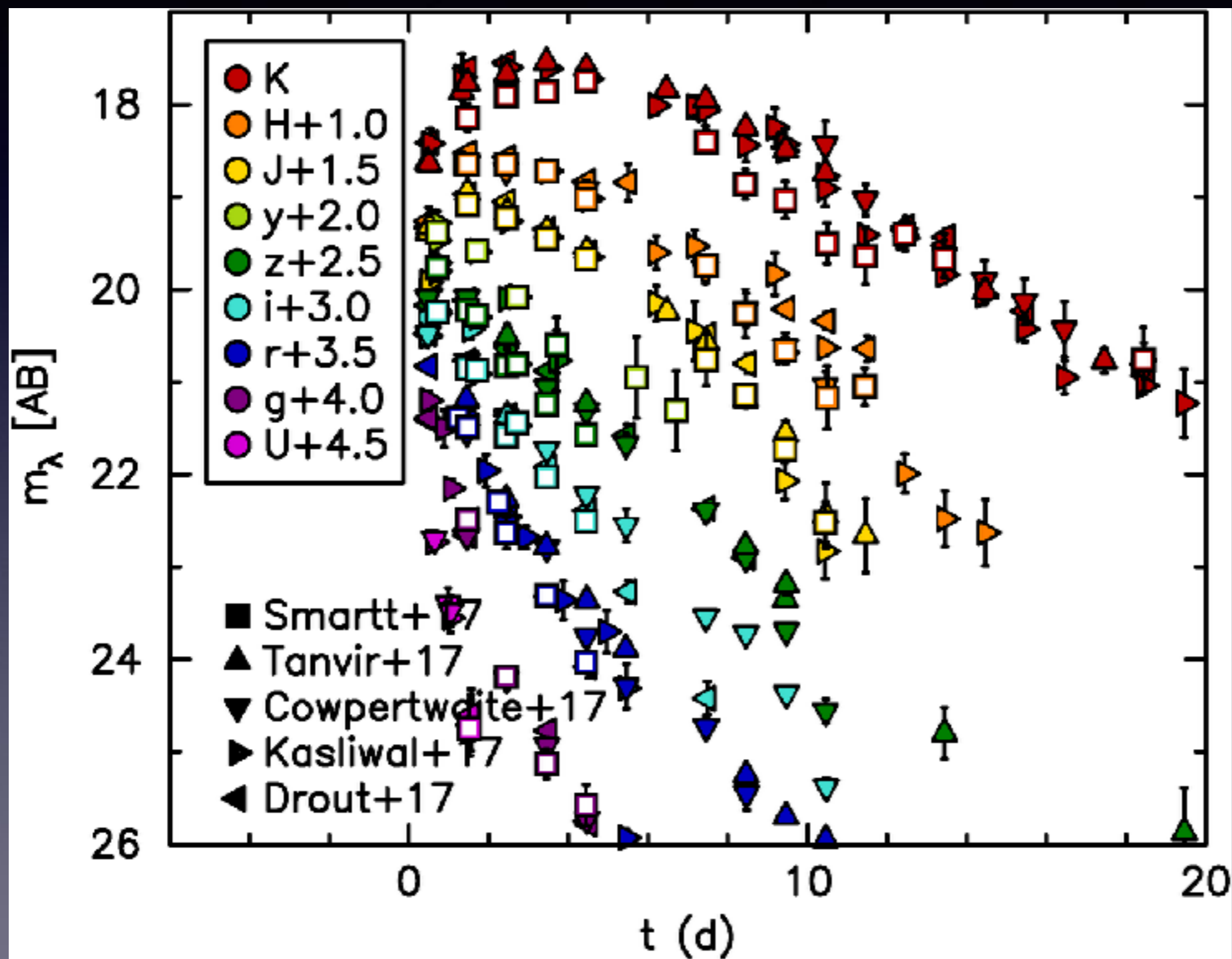
www.pessto.org



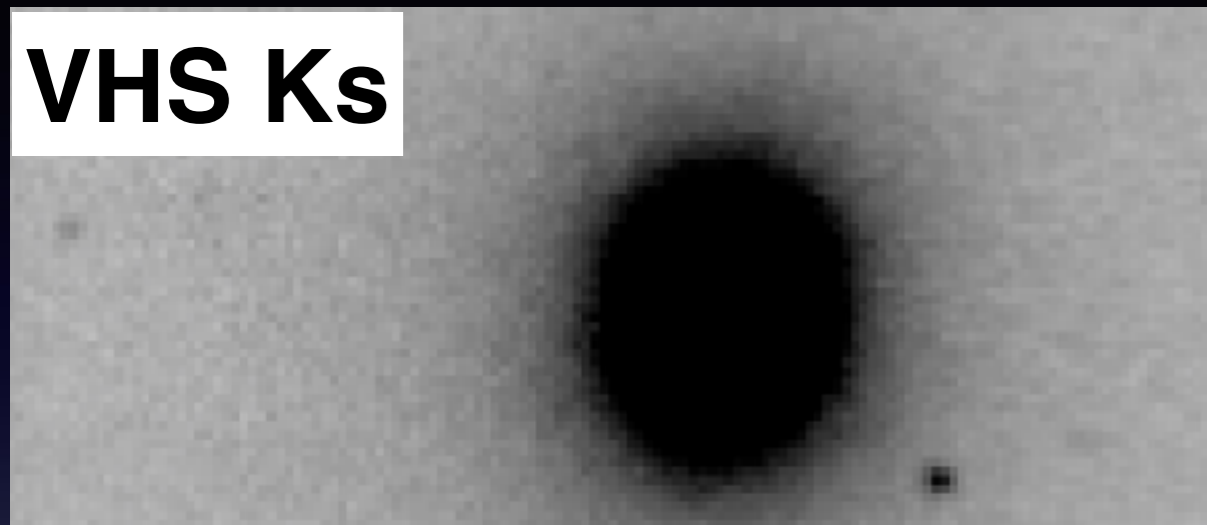
Smartt et al. 2017
Pian et al. 2017

- All data available on www.pessto.org (calibration notes)
- And <https://kilonova.space/>
- <https://wiserep.weizmann.ac.il/>

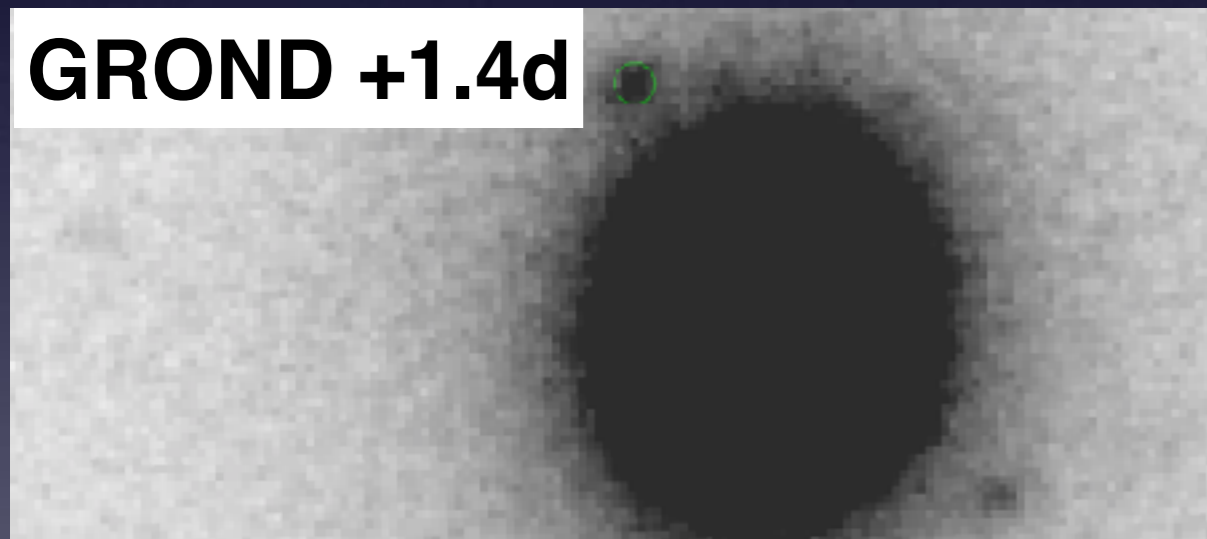
Impressive multi-band data



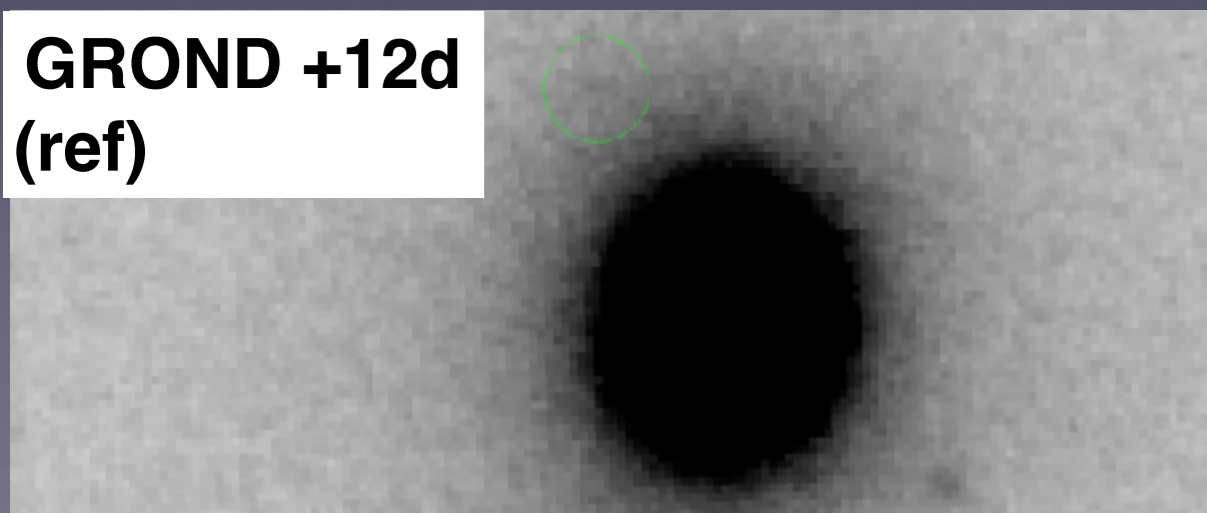
VHS Ks



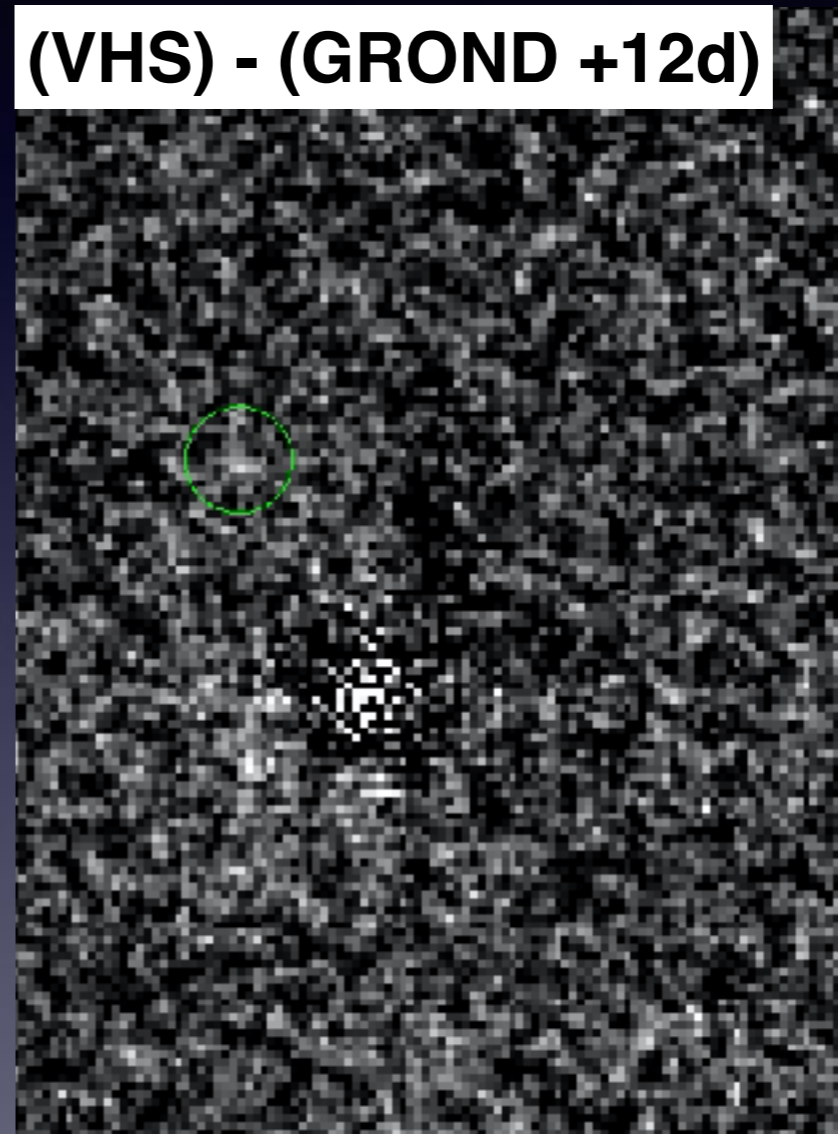
GROND +1.4d

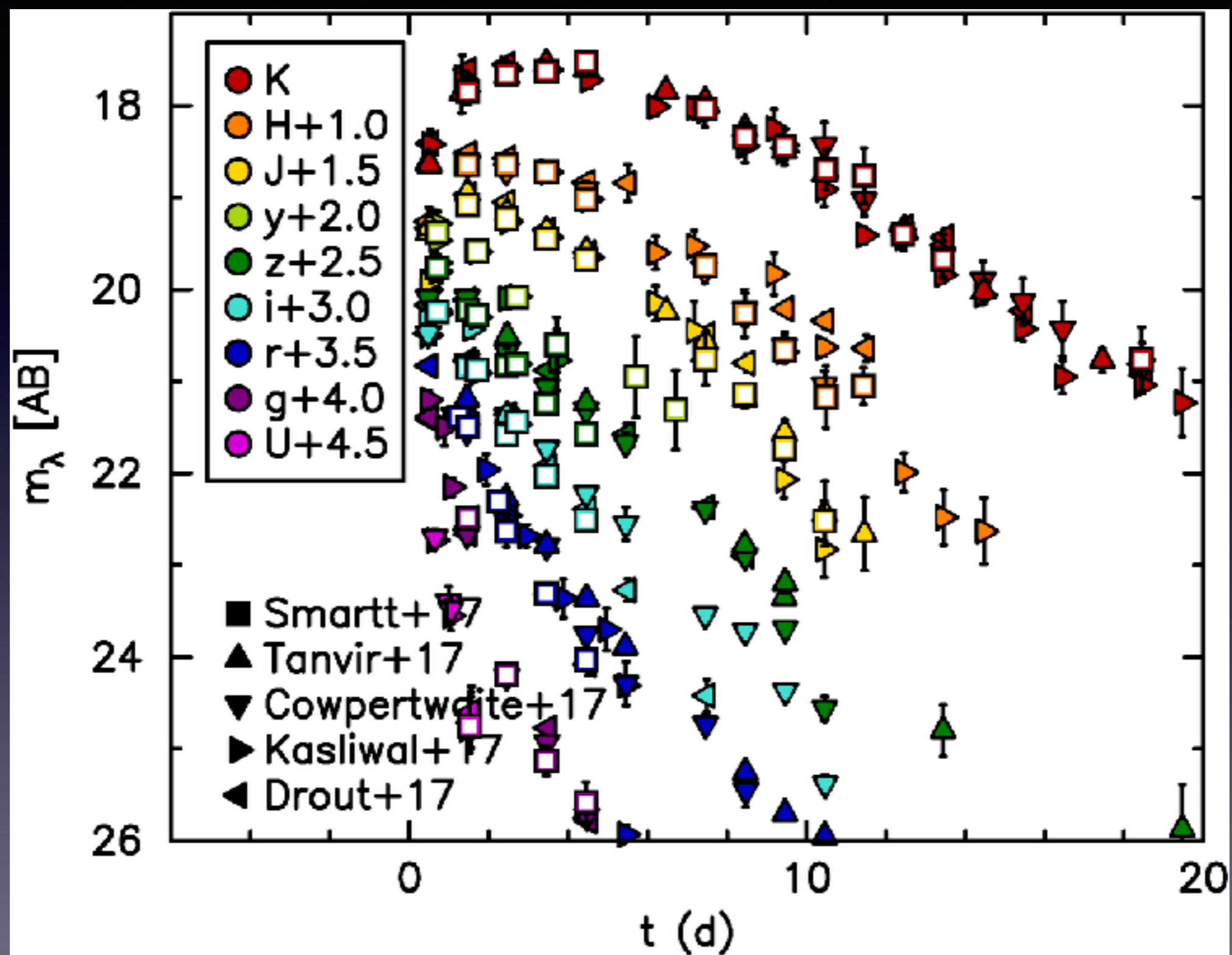


**GROND +12d
(ref)**

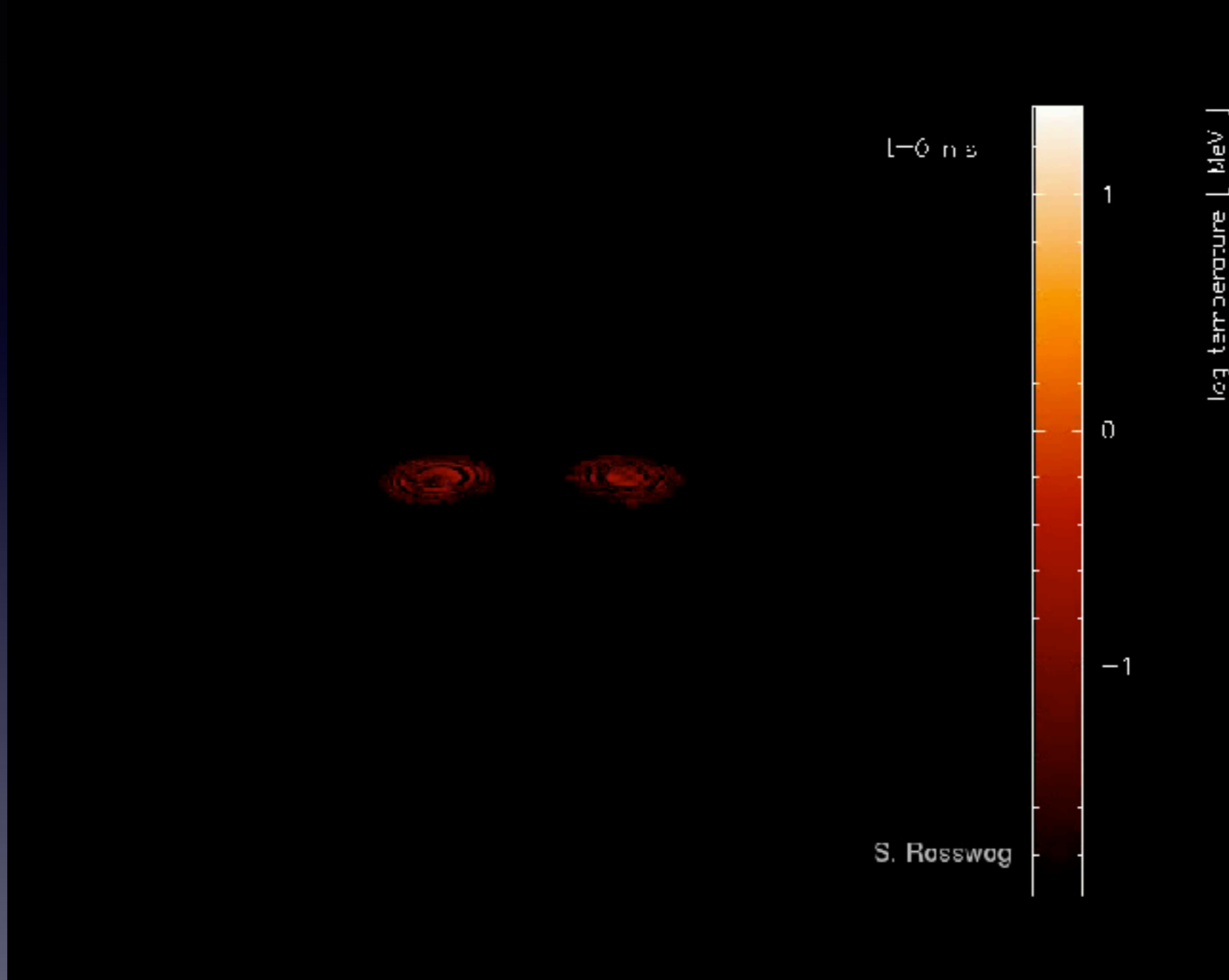


(VHS) - (GROND +12d)





NS-NS mergers - what do we expect to see ?



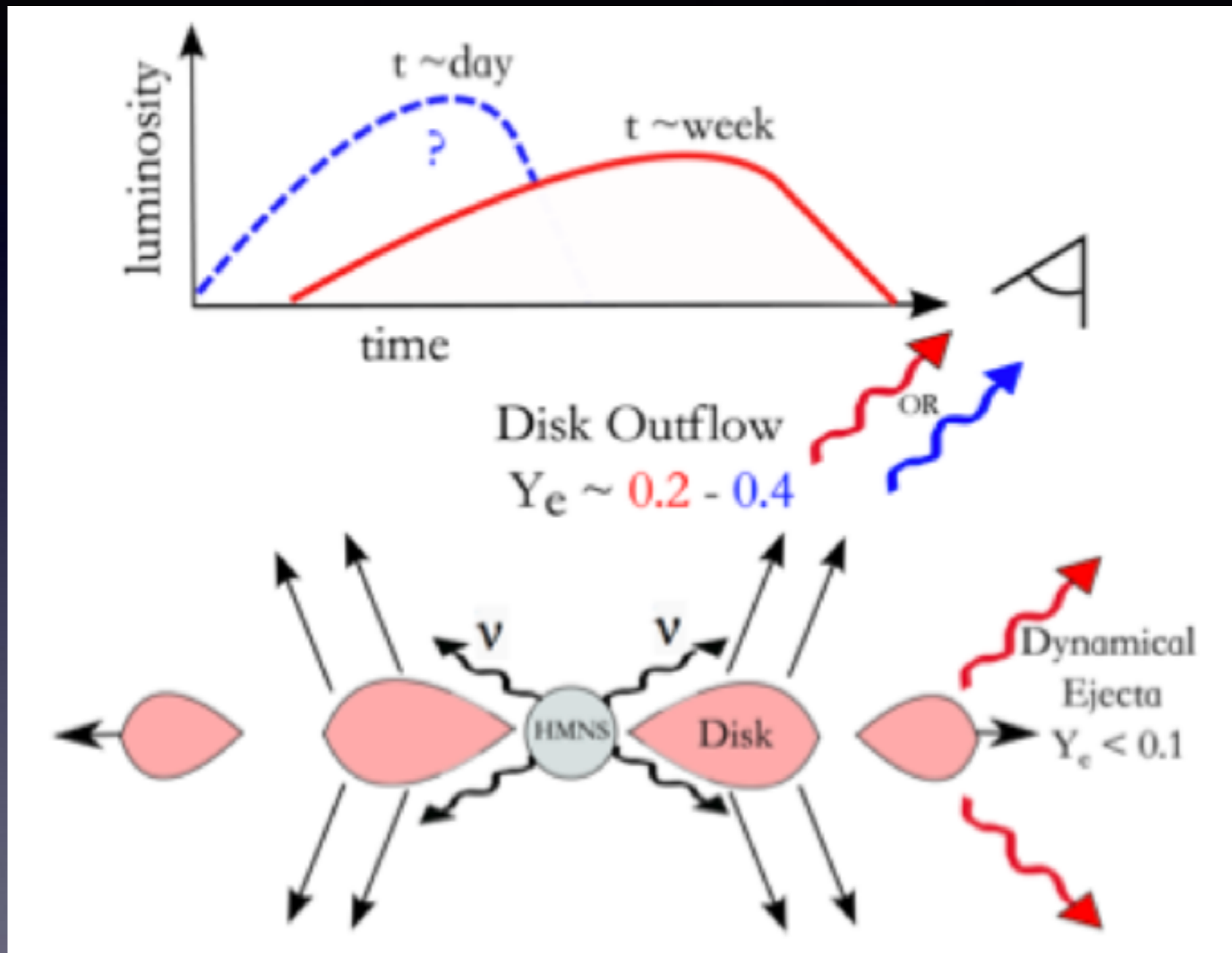
- Short GRBs : working model is NS-NS mergers, Gamma rays are beamed from relativistic jet
- Beam opening angle $\sim 10^\circ$ (see Berger ARA&A 2014)

1.4+1.3 M_\odot neutron stars

<http://compact-merger.astro.su.se/>

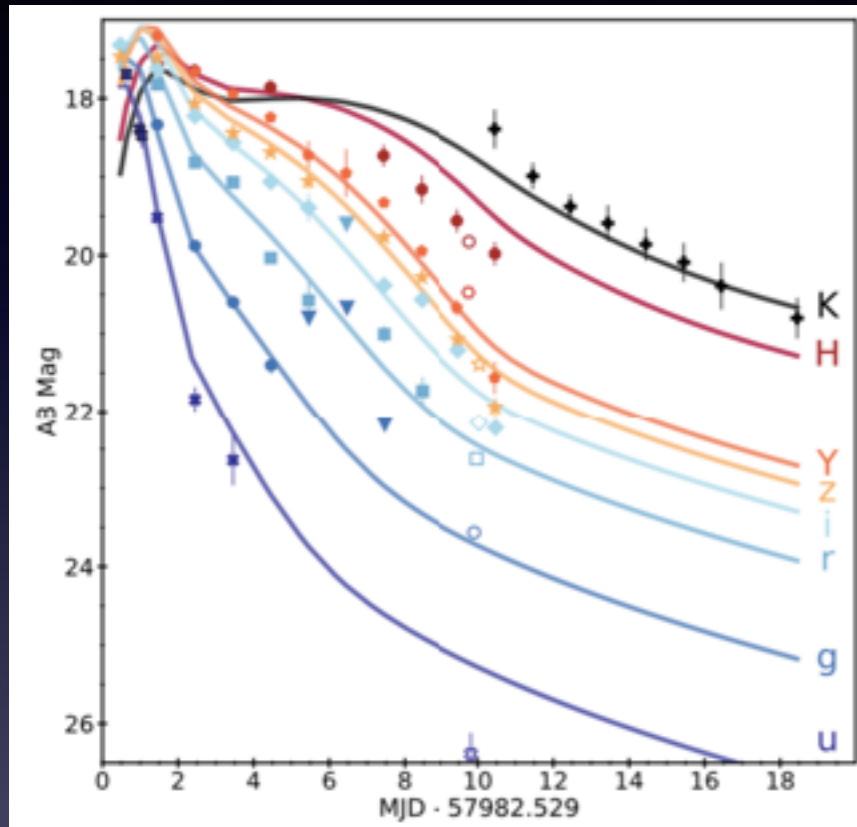
6 See Rosswog, Piran & Nakar 2013

Multiple components



Metzger 2014

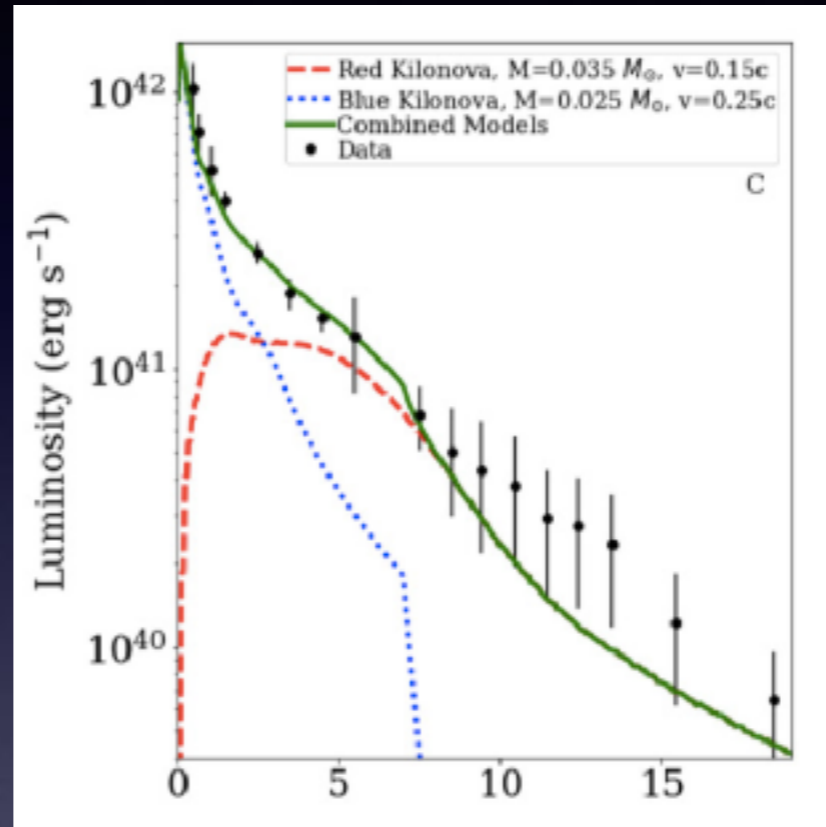
Multiple components or 1?



$$M_{ej}^{blue} \approx 0.01 M_{\odot} \text{ and } v_{ej}^{blue} \approx 0.3 c$$

$$M_{ej}^{red} \approx 0.04 M_{\odot} \text{ and } v_{ej}^{red} \approx 0.1 c$$

DECam team
Cowperthwaite et al.



Red Kilonova, $M=0.035 M_{\odot}$, $v=0.15c$
Blue Kilonova, $M=0.025 M_{\odot}$, $v=0.25c$

Swope/Carnegie
team
Kilpatrick et al. +
Drout et al.

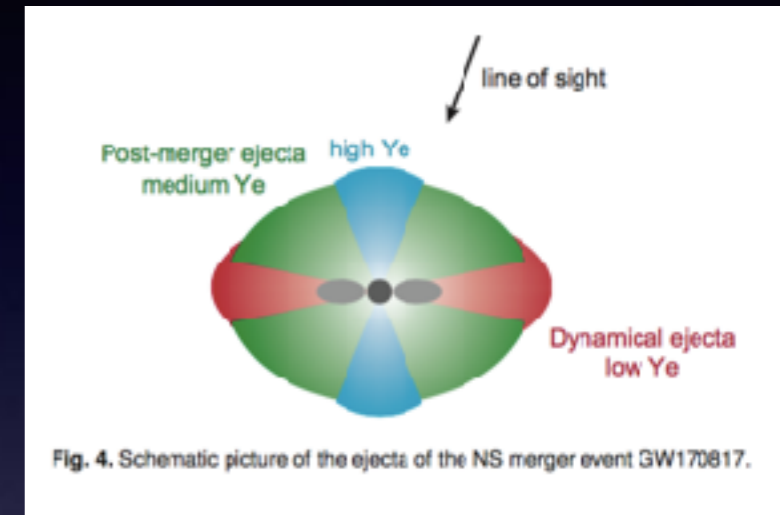


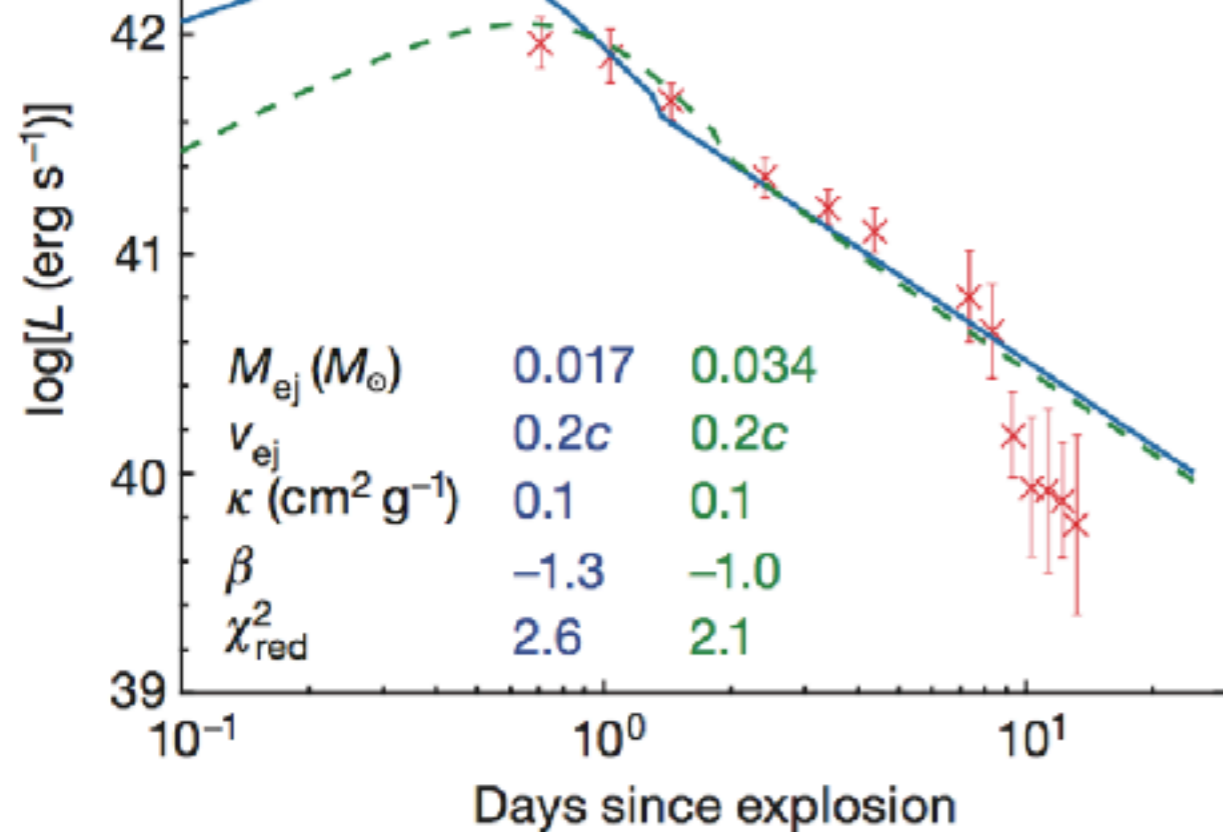
Fig. 4. Schematic picture of the ejecta of the NS merger event GW170817.

Tanaka et al.

AT2017fgo

nature

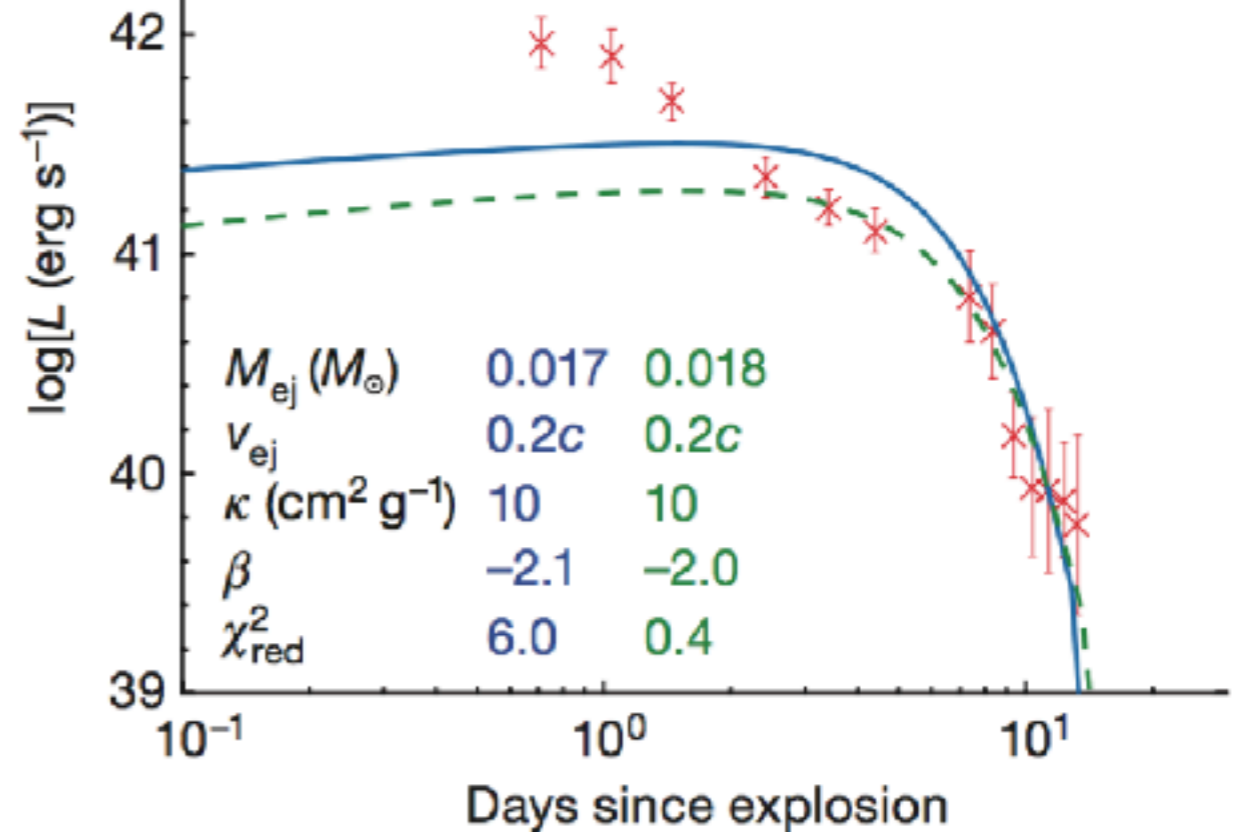
Low opacity model



b

Smartt et al. 551, 75–79 (2017)

High opacity model



2 lightcurve models: our own Arnett formulation and Metzger

See also Rosswog et al. 2017, A&A, Waxman et al. 2017

Heating rates $P(t) = A t^{-\beta}$ (Lippuner & Roberts 2015)

r-process radioactivity

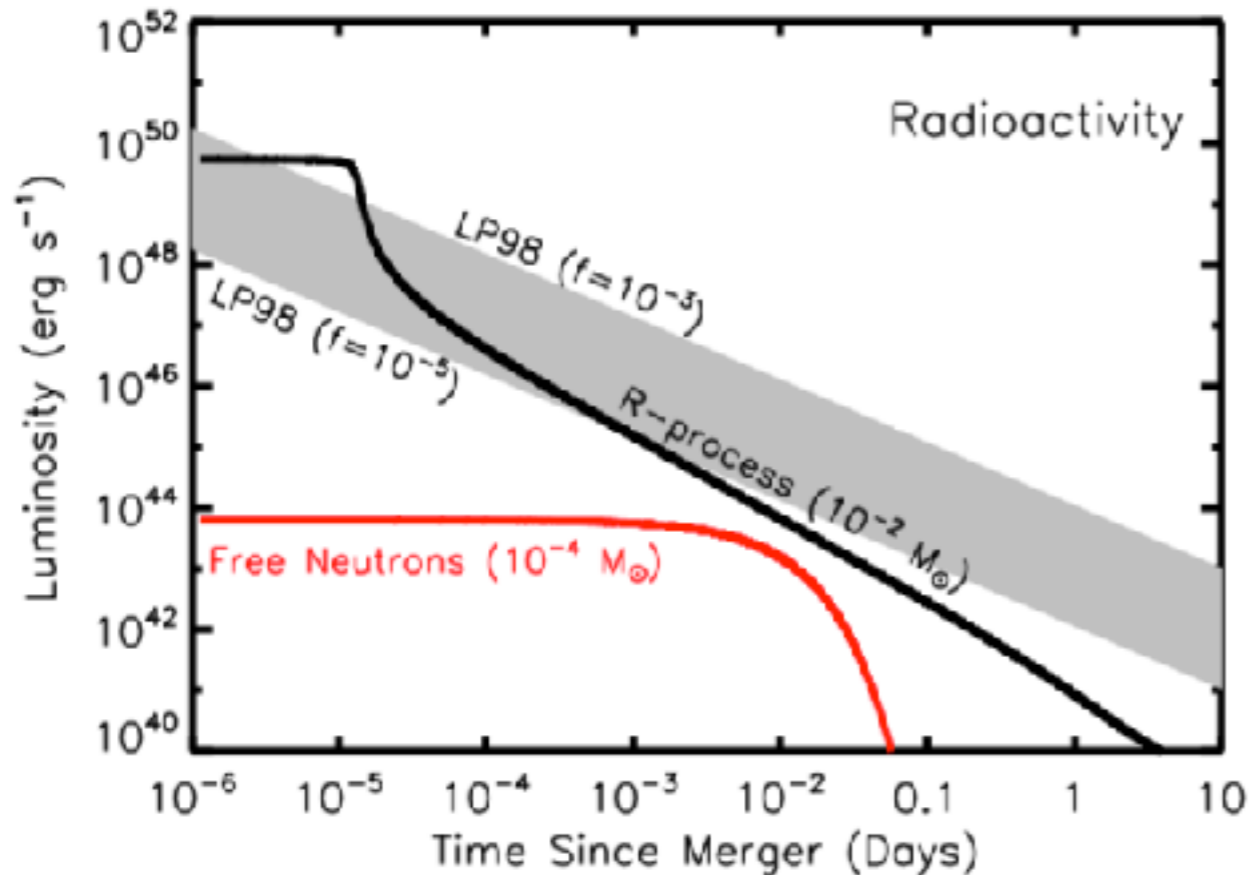


Table 1. Properties of the dominant β -decay nuclei at $t \sim 1$ d.

Isotope	$t_{1/2}$ (h)	Q^a (MeV)	ϵ_e^b	ϵ_ν^c	ϵ_γ^d	$E_\gamma^{avg e}$ (MeV)
^{135}I	6.57	2.65	0.18	0.18	0.64	1.17
^{129}Sb	4.4	2.38	0.22	0.22	0.55	0.86
^{128}Sb	9.0	4.39	0.14	0.14	0.73	0.66
^{129}Te	1.16	1.47	0.48	0.48	0.04	0.22
^{132}I	2.30	3.58	0.19	0.19	0.62	0.77
^{135}Xe	9.14	1.15	0.38	0.40	0.22	0.26
^{127}Sn	2.1	3.2	0.24	0.23	0.53	0.92
^{134}I	0.88	4.2	0.20	0.19	0.61	0.86
$^{56}\text{Ni}^f$	146	2.14	0.10	0.10	0.80	0.53

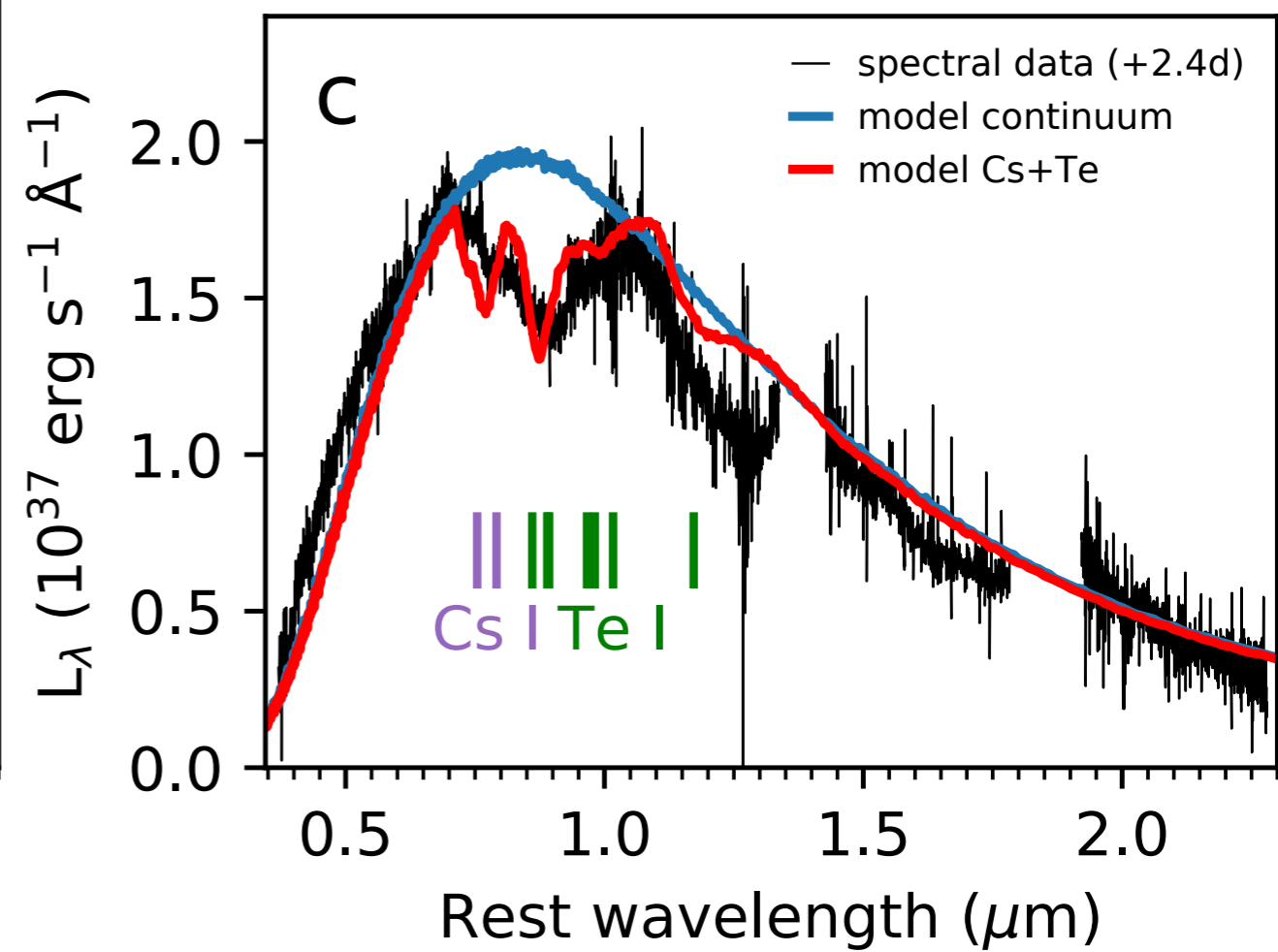
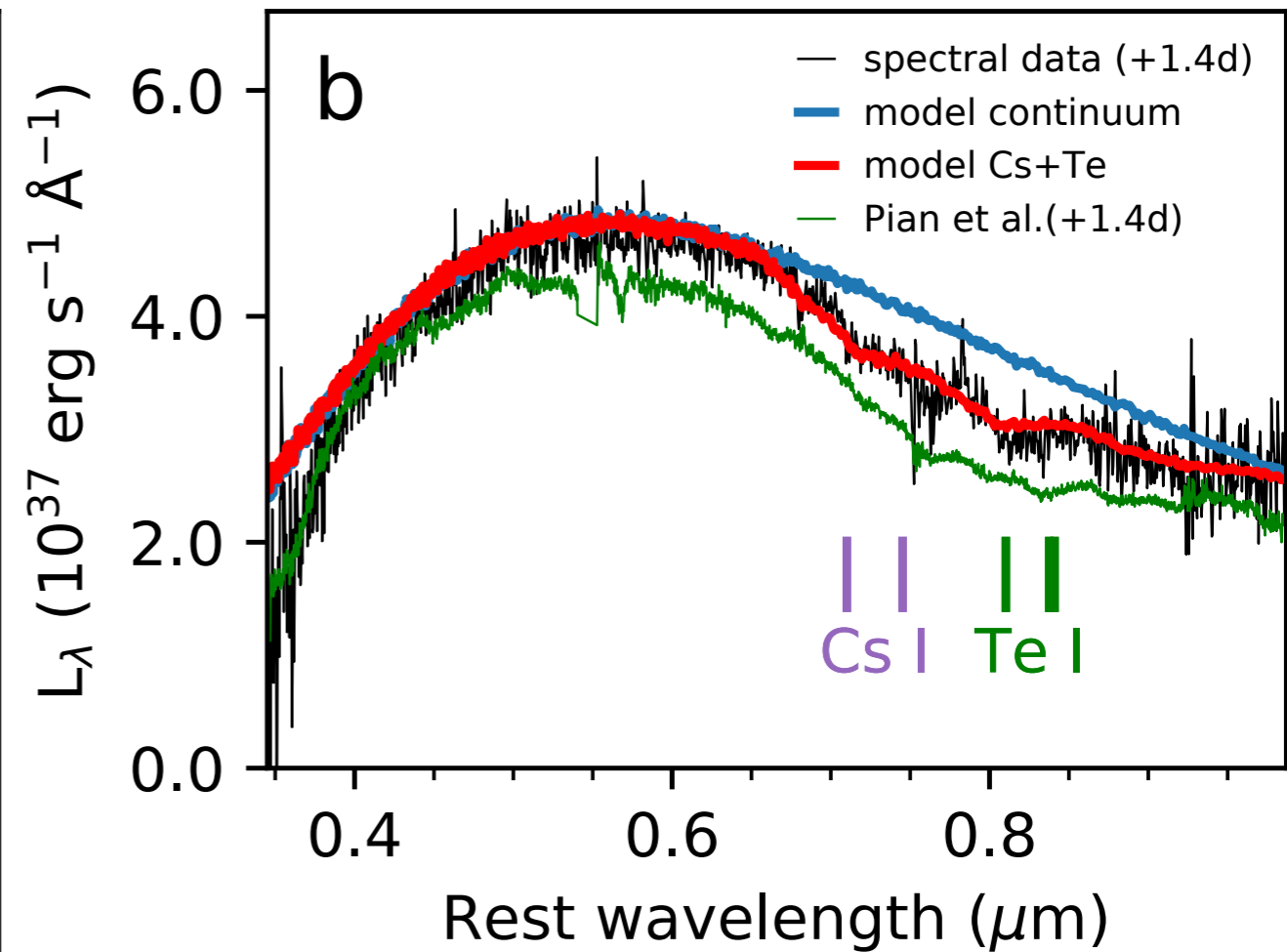
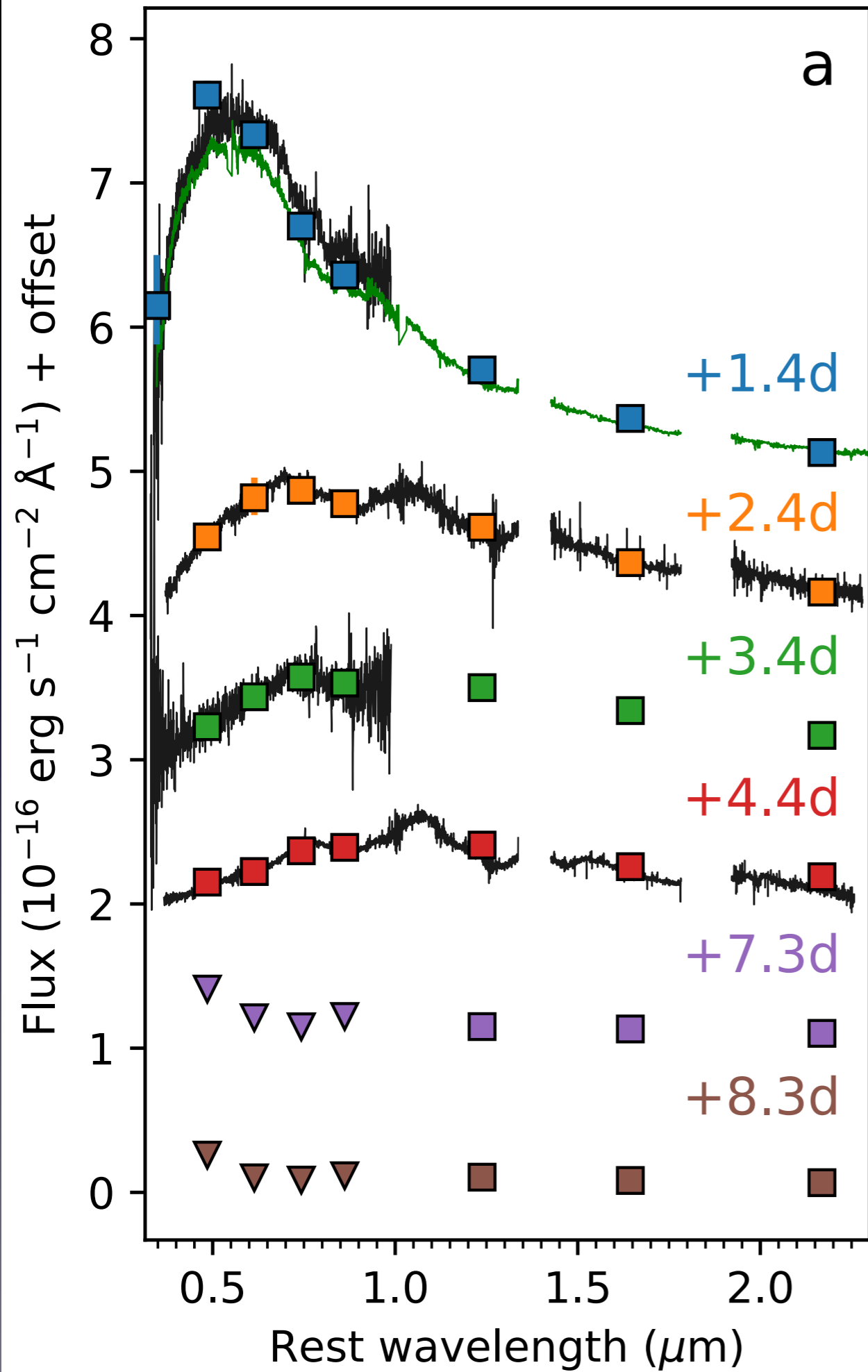
^aTotal energy released in the decay.

^{b,c,d}Fraction of the decay energy released in electrons, neutrinos and γ -rays.

^eAverage photon energy produced in the decay.

^fNote: ^{56}Ni is not produced by the r -process and is only shown for comparison [although a small abundance of ^{56}Ni may be produced in accretion disc outflows from NS–NS/NS–BH mergers (Metzger et al. 2008b)].

- Metzger 2017, Living Reviews in Relativity, 20, 3 “Kilonovae”
- Metzger et al. 2010, MNRAS, 406, 2650, “EM counterparts of compact object mergers powered by the radioactive decay of r-process material”
- Heating rates $P(t) = A t^{-\beta}$: also see Lippuner & Roberts 2015



Periodic Table of the Elements

Atomic Number
Symbol
 Name
 Atomic Mass

1 1A H Hydrogen 1.008	2 2A He Helium 4.003																	3 3A B Boron 10.811	4 4A C Carbon 12.011	5 5A N Nitrogen 14.007	6 6A O Oxygen 15.999	7 7A F Fluorine 18.998	8 8A Ne Neon 20.180
9 1A Li Lithium 6.941	10 2A Be Beryllium 9.012																	13 3A Al Aluminum 26.987	14 4A Si Silicon 28.086	15 5A P Phosphorus 30.974	16 6A S Sulfur 32.368	17 7A Cl Chlorine 35.453	18 8A Ar Argon 39.948
11 1A Na Sodium 22.990	12 2A Mg Magnesium 24.305	3 3B Sc Scandium 44.956	4 4B Ti Titanium 47.867	5 5B V Vanadium 50.942	6 6B Cr Chromium 51.996	7 7B Mn Manganese 54.938	8 8 Fe Iron 55.845	9 9 Co Cobalt 58.933	10 10 Ni Nickel 58.693	11 11 Cu Copper 63.546	12 12 Zn Zinc 65.38	31 3A Ga Gallium 69.723	32 4A Ge Germanium 72.631	33 5A As Arsenic 74.922	34 6A Se Selenium 78.972	35 7A Br Bromine 79.904	36 8A Kr Krypton 83.798						
19 1A K Potassium 39.098	20 2A Ca Calcium 40.078	21 3B Sc Scandium 44.956	22 4B Ti Titanium 47.867	23 5B V Vanadium 50.942	24 6B Cr Chromium 51.996	25 7B Mn Manganese 54.938	26 8 Fe Iron 55.845	27 9 Co Cobalt 58.933	28 10 Ni Nickel 58.693	29 11 Cu Copper 63.546	30 12 Zn Zinc 65.38	49 3A In Indium 114.818	50 4A Sn Tin 118.710	51 5A Sb Antimony 121.757	52 6A Te Tellurium 127.6	53 7A I Iodine 126.905	54 8A Xe Xenon 131.294						
37 1A Rb Rubidium 85.468	38 2A Sr Strontium 87.62	39 3B Y Yttrium 88.906	40 4B Zr Zirconium 91.224	41 5B Nb Niobium 92.906	42 6B Mo Molybdenum 95.94	43 7B Tc Technetium 98.906	44 8 Ru Ruthenium 101.07	45 9 Rh Rhodium 101.07	46 10 Pd Palladium 106.42	47 11 Ag Silver 107.868	48 12 Cd Cadmium 112.411	81 3A Tl Thallium 204.383	82 4A Pb Lead 207.2	83 5A Bi Bismuth 208.980	84 6A Po Polonium [209]	85 7A At Astatine [210]	86 8A Rn Radon 222.018						
55 1A Cs Cesium 132.905	56 2A Ba Barium 137.327	57-71 Lanthanide Series	72 4B Hf Hafnium 178.49	73 5B Ta Tantalum 180.948	74 6B W Tungsten 183.84	75 7B Re Rhenium 186.207	76 8 Os Osmium 190.23	77 9 Ir Iridium 192.222	78 10 Pt Platinum 195.084	79 11 Au Gold 196.967	80 12 Hg Mercury 200.596	113 3A Nh Nihonium 284	114 4A Fl Flerovium 289	115 5A Mc Moscovium 288	116 6A Lv Livermorium 293	117 7A Ts Tennessine [294]	118 8A Og Oganesson [294]						
87 1A Fr Francium 223.021	88 2A Ra Radium 226.025	89-103 Actinide Series	104 4B Rf Rutherfordium [261]	105 5B Db Dubnium [262]	106 6B Sg Seaborgium [266]	107 7B Bh Bohrium [264]	108 8 Hs Hassium [277]	109 9 Mt Meitnerium [276]	110 10 Ds Darmstadtium [281]	111 11 Rg Roentgenium [282]	112 12 Cn Copernicium [285]	113 3A Nh Nihonium [284]	114 4A Fl Flerovium [289]	115 5A Mc Moscovium [288]	116 6A Lv Livermorium [293]	117 7A Ts Tennessine [294]	118 8A Og Oganesson [294]						

Alkali Metal

Alkaline Earth

Transition Metal

Basic Metal

Semimetal

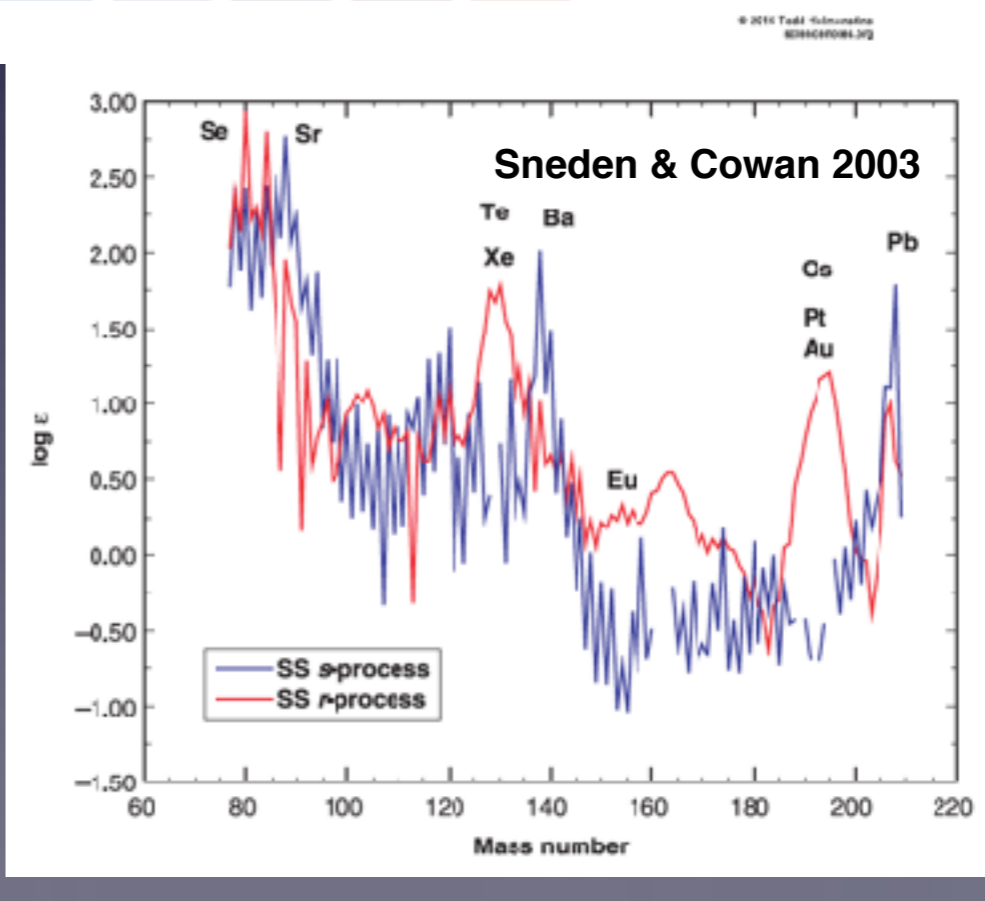
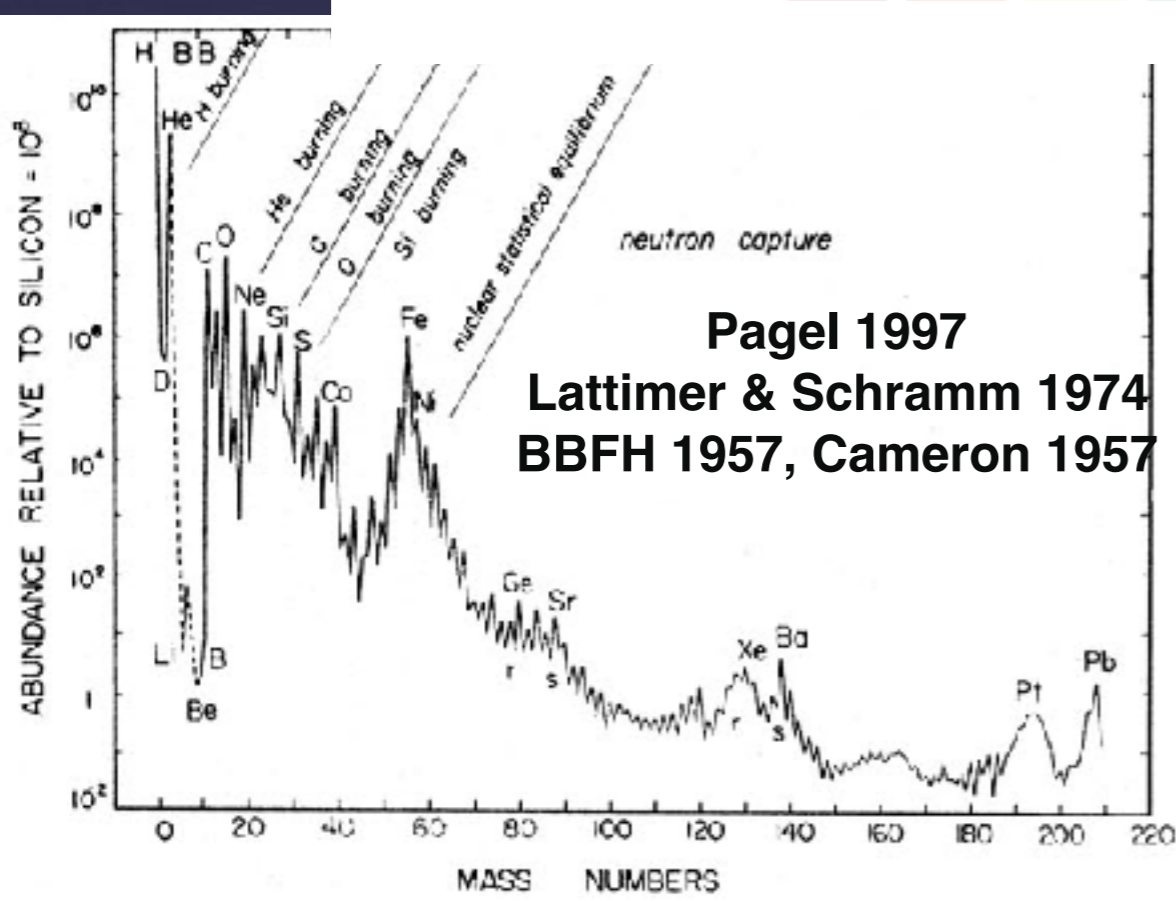
Nonmetal

Halogen

Noble Gas

Lanthanide

Actinide

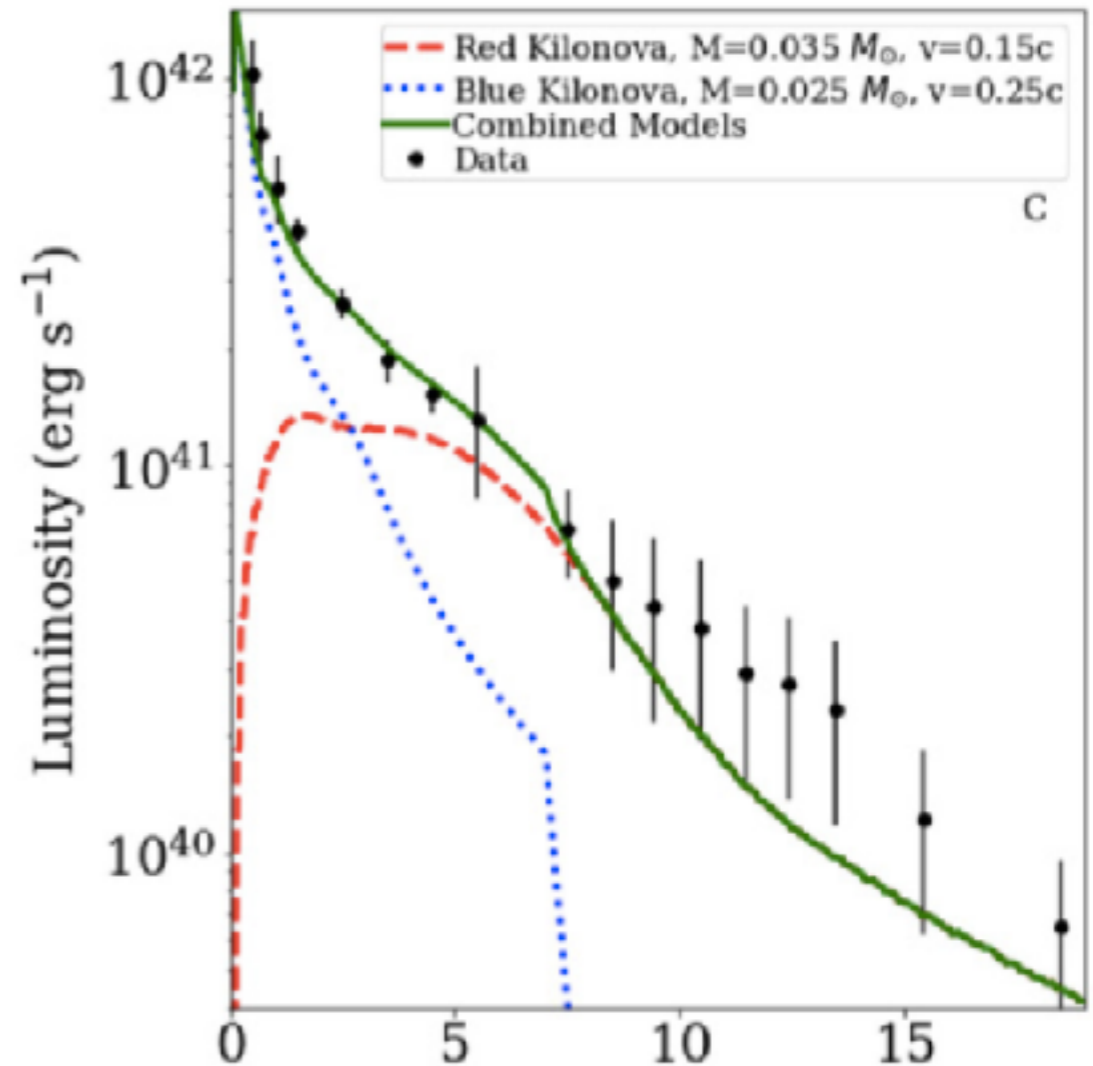
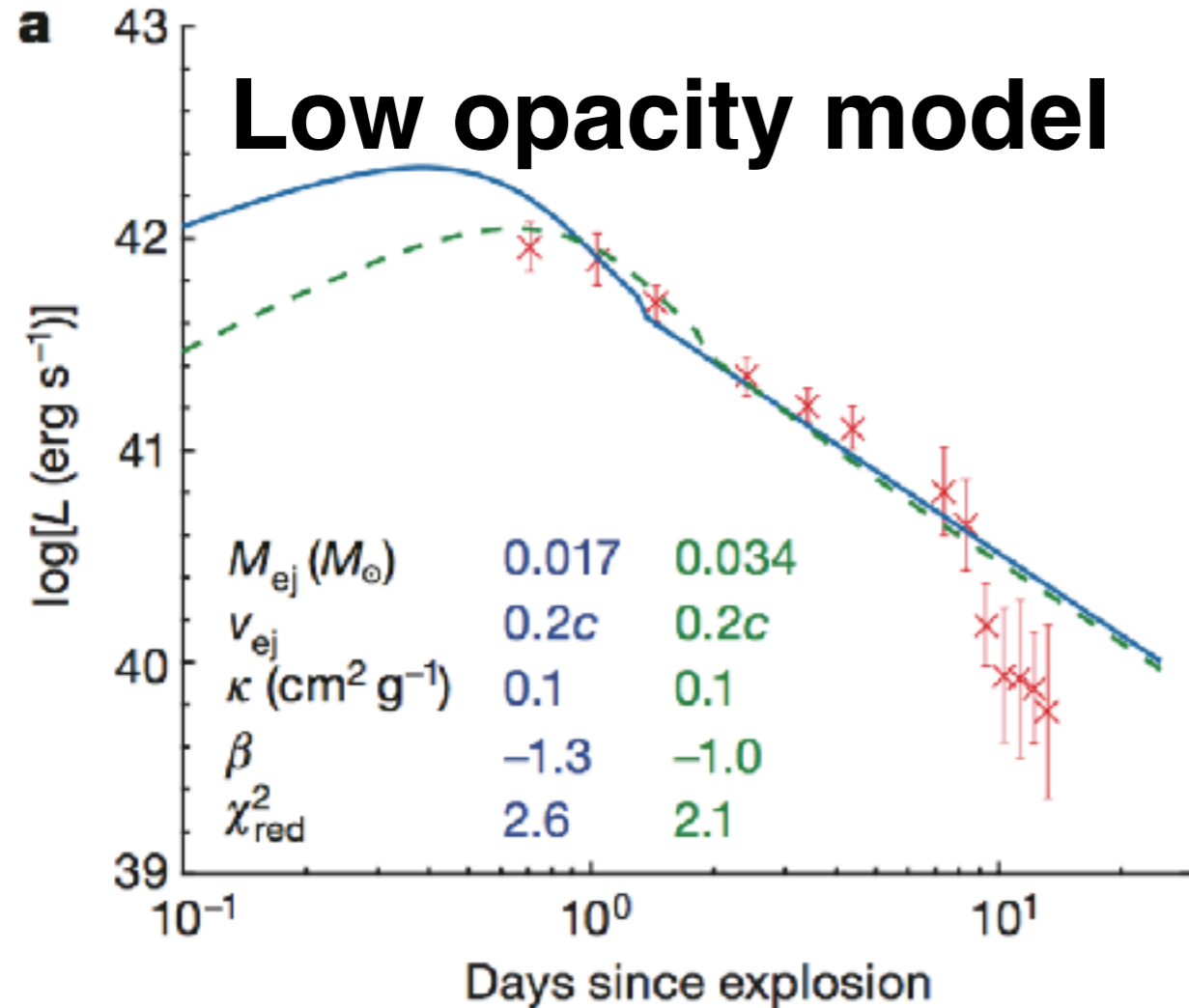


Reasonable criticisms - and implications for future

- Our models are too simple - Metzger 2017 “toy model” and Arnett-Jerkstrand semi-analytic model
- We do not use the SED/spectral information available when fitting the lightcurve (L_{bol} only)
- We have underestimated K-band at $> 10\text{d}$. Therefore underestimated the contribution to a high opacity component
- We have only integrated our L_{bol} out to 2.5microns, there is clearly **(some)** flux beyond that. Therefore underestimated the contribution to a high opacity component
- **The thermalisation function and/or heating rate we apply for radioactive decay particles (leptons) are either wrong or unknown**

1-component or 2 ?

nature



See also Rosswog et al. 2017, A&A,
Waxman et al. 2017, submitted

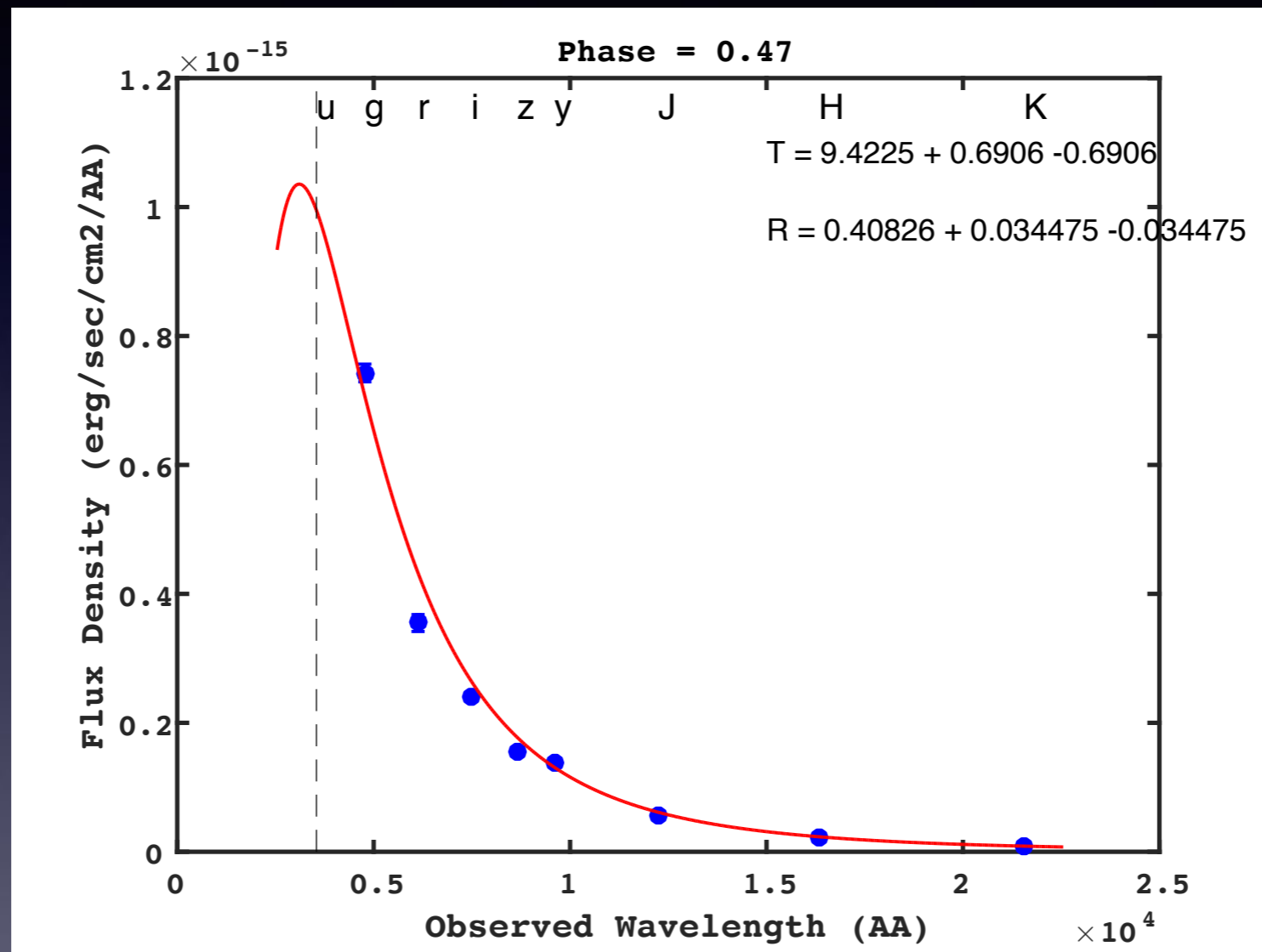
$$P(t) = A t^{-\beta}$$

Kilpatrick et al. 2017
Drout et al. 2017

Combined photometry for SED fitting +0.47d to +14.3d

MJD	Phase	U	U_err	g	g_err	r	r_err	i	i_err	z	z_err	y	y_err	Tel	Phase	J	J_err	H	H_err	K_s	K_err	Telescope
57983.0	0.467	NaN	NaN	17.41	0.02	17.56	0.04	17.48	0.03	17.59	0.03	17.46	0.01	various		17.88	0.03	18.26	0.15	18.62	0.11	4star/VISTA/GS
57983.23125	0.696	NaN	NaN	NaN	NaN	NaN	NaN	17.24	0.05	17.25	0.06	17.38	0.10	PS1		NaN	NaN	NaN	NaN	NaN	NaN	
57983.42	0.88	NaN	NaN	17.46	0.08	17.32	0.07	17.42	0.05	NaN	NaN	NaN	NaN	Skymapper		NaN	NaN	NaN	NaN	NaN	NaN	
57983.75833	1.218	NaN	NaN	18.05	0.12	17.89	0.03	NaN	NaN	NaN	NaN	NaN	NaN	1.58/LCO		17.51	0.03	17.54	0.04	17.91	0.05	Sirius
57983.96875	1.427	NaN	NaN	18.49	0.04	17.99	0.01	17.85	0.05	17.72	0.03	17.32	0.03	GROND/DECam	1.427	17.58	0.07	17.54	0.08	18.14	0.15	GROND
57984.04811	1.505	20.25	0.29	NaN	NaN	NaN	NaN	NaN	NaN	NaN	NaN	NaN	NaN	NTT		NaN	NaN	NaN	NaN	NaN	NaN	
57984.23125	1.686	NaN	NaN	NaN	NaN	NaN	NaN	17.87	0.05	17.78	0.07	17.58	0.11	PS1		NaN	NaN	NaN	NaN	NaN	NaN	
57984.37	1.82	NaN	NaN	19.28	0.17	18.34	0.11	18.32	0.14	NaN	NaN	NaN	NaN	Skymapper/LCO		NaN	NaN	NaN	NaN	NaN	NaN	
57984.76111	2.211	NaN	NaN	19.87	0.21	18.80	0.07	18.3	0.15	18.25	0.3	NaN	NaN	1.58/LCO		17.69	0.04	17.52	0.04	17.61	0.04	Sirius
57984.96897	2.417	19.6	9999	20.19	0.11	19.13	0.17	18.58	0.04	18.33	0.06	17.77	0.03	GROND	2.417	17.73	0.09	17.54	0.08	17.90	0.10	GROND
57985.23125	2.676	NaN	NaN	NaN	NaN	NaN	NaN	18.44	0.09	18.31	0.07	18.08	0.11	PS1		NaN	NaN	NaN	NaN	NaN	NaN	
57985.38	2.83	NaN	NaN	20.43	0.16	19.34	0.09	18.62	0.07	NaN	NaN	NaN	NaN	Skymapper/LCO		NaN	NaN	NaN	NaN	NaN	NaN	
57985.77639	3.216	NaN	NaN	NaN	NaN	19.64	0.13	18.80	0.2	18.42	0.34	NaN	NaN	1.58/LCO		17.78	0.05	17.57	0.04	17.55	0.05	Sirius
57985.97433	3.412	NaN	NaN	21.13	0.16	19.81	0.02	19.03	0.01	18.74	0.02	18.05	0.03	GROND/DECam	3.413	17.95	0.07	17.72	0.07	17.86	0.10	GROND
57986.23556	3.671	NaN	NaN	NaN	NaN	NaN	NaN	17.8	9999	18.10	0.30	17.7	9999	PS1		NaN	NaN	NaN	NaN	NaN	NaN	
57986.71	4.14	NaN	NaN	NaN	NaN	20.30	0.31	NaN	NaN	NaN	NaN	NaN	NaN	LCO		18.13	0.12	17.77	0.04	17.57	0.07	SIRIUS
57986.97426	4.402	NaN	NaN	21.58	0.22	20.53	0.05	19.51	0.04	19.07	0.06	18.35	0.03	GROND	4.403	18.17	0.07	18.02	0.10	17.74	0.11	GROND
57987.98	5.4	NaN	NaN	NaN	NaN	20.79	0.24	19.55	0.18	19.17	0.11	18.83	0.18	DECam		NaN	NaN	NaN	NaN	NaN	NaN	
57988.99	6.4	NaN	NaN	22.08	0.52	20.95	0.35	NaN	NaN	NaN	NaN	19.06	0.31	DECam	6.4	18.74	0.04	NaN	NaN	17.84	0.03	VISTA
57989.00	7.4	NaN	NaN	23.28	0.34	21.23	0.11	20.54	0.05	19.89	0.05	19.44	0.05	DECam	7.383	19.26	0.28	18.74	0.06	18.40	0.12	GROND
57991.00	8.4	NaN	NaN	NaN	NaN	21.95	0.18	20.72	0.05	20.40	0.06	20.06	0.07	DECam	8.358	19.64	0.11	19.26	0.26	18.85	0.16	GROND
57992.00	9.4	NaN	NaN	NaN	NaN	22.2	0.04	21.37	0.06	21.19	0.07	20.78	0.11	DECam/VIMOS	9.350	20.23	0.10	19.66	0.14	19.03	0.20	GROND
57993.00	10.4	NaN	NaN	NaN	NaN	22.45	0.07	22.38	0.10	22.06	0.13	21.67	0.21	DECam/VIMOS	10.386	21.62	0.22	20.17	0.34	19.50	0.22	GROND
57993.94	11.3	NaN	NaN	24.1	0.2	23.0	0.2	22.5	0.2	NaN	NaN	NaN	NaN	HST	11.322	NaN	NaN	20.05	0.20	19.64	0.30	NTT/GROND
57994.97	12.31	NaN	NaN	NaN	NaN	NaN	NaN	NaN	NaN	NaN	NaN	NaN	NaN			NaN	NaN	20.57	0.19	19.40	0.14	NTT/GS
57995.97	13.21	NaN	NaN	NaN	NaN	NaN	NaN	NaN	NaN	22.3	0.28	NaN	NaN	VIMOS		NaN	NaN	21.01	0.14	19.67	0.20	GS/NTT
57996.99	14.32	NaN	NaN	NaN	NaN	NaN	NaN	NaN	NaN	23.34	0.37	NaN	NaN	FORS		NaN	NaN	21.63	0.36	20.02	0.13	GS/VISTA
57997.979	15.30	NaN	NaN	NaN	NaN	NaN	NaN	NaN	NaN	NaN	NaN	NaN	NaN			NaN	NaN	NaN	NaN	20.17	0.08	GS/Magellan (average)
57999.98	17.28	NaN	NaN	NaN	NaN	NaN	NaN	NaN	NaN	NaN	NaN	NaN	NaN			NaN	NaN	NaN	NaN	20.77	0.13	HAWKI
58000.966	18.26	NaN	NaN	NaN	NaN	NaN	NaN	NaN	NaN	NaN	NaN	NaN	NaN			NaN	NaN	NaN	NaN	20.76	0.35	NTT
58003.969	21.23	NaN	NaN	NaN	NaN	NaN	NaN	NaN	NaN	NaN	NaN	NaN	NaN			NaN	NaN	NaN	NaN	21.45	0.08	HAWKI
58007.960	25.19	NaN	NaN	NaN	NaN	NaN	NaN	NaN	NaN	NaN	NaN	NaN	NaN			NaN	NaN	NaN	NaN	22.05	0.22	HAWKI

+0.47d Chile



Opt:
LCO, Magellan, DECam

IR:
Magellan, VISTA, GS

Arcavi et al, 2017

Drout et al. 2017

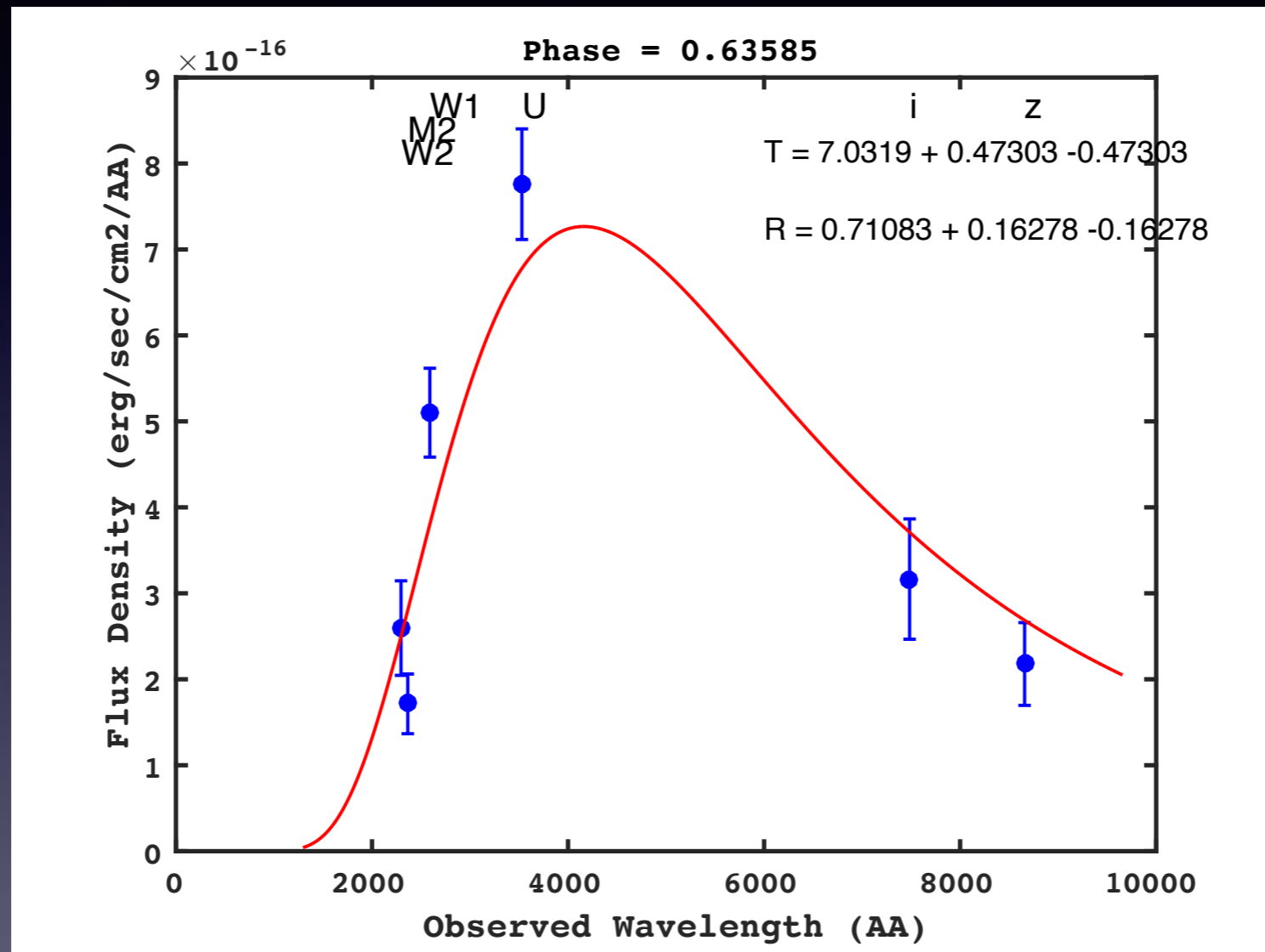
Cowperthwaite et al./Soares-Santos et al. 2017

Tanvir et al. 2017

Drout et al. 2017

Kasliwal et al. 2017

+0.64d Space - Swift



UV:
Swift

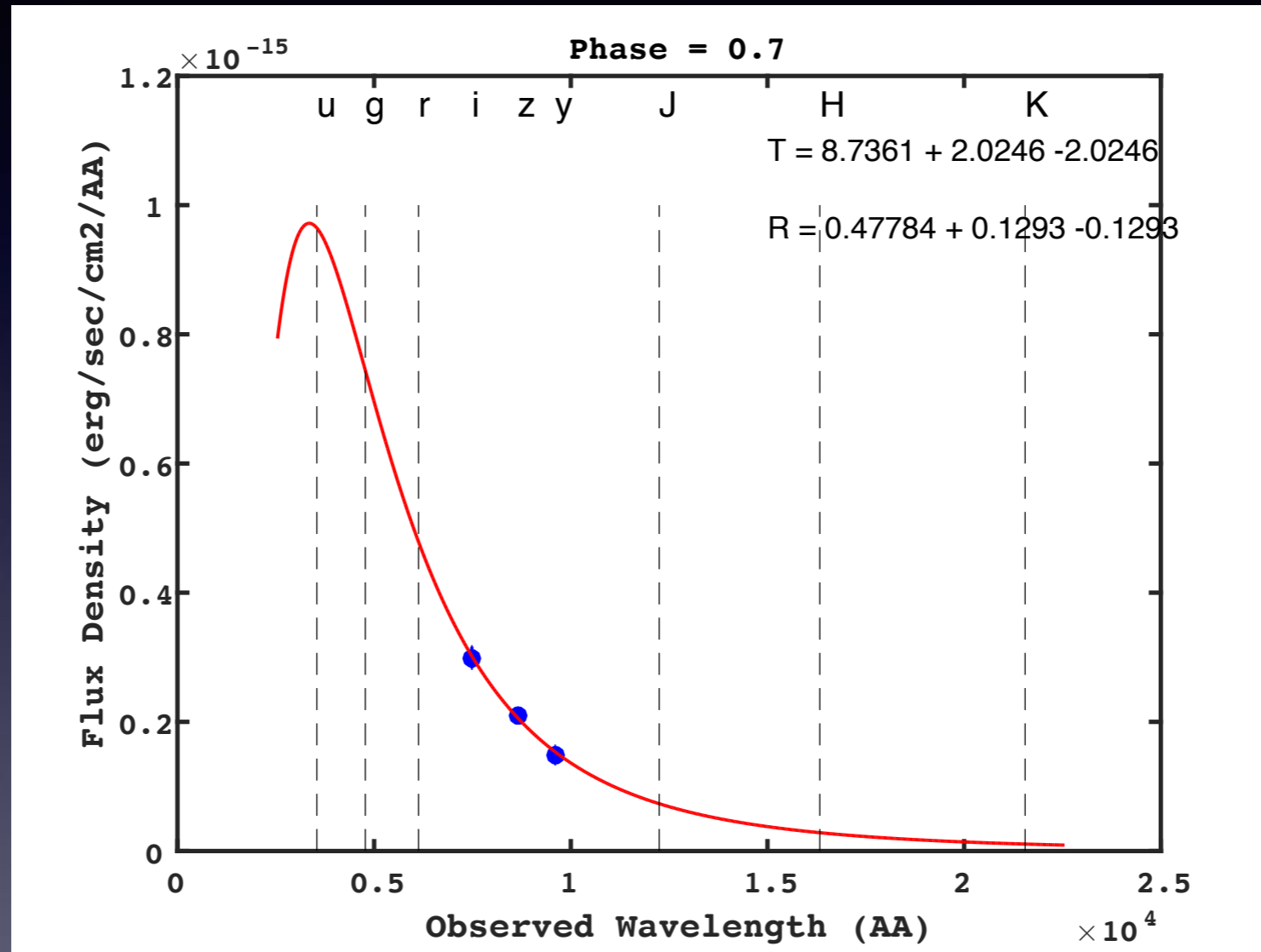
Evans et al. 2017

Optical:
Interpolated Pan-STARRS/DECam

Smartt et al. 2017

Soares-Santos et al. 2017

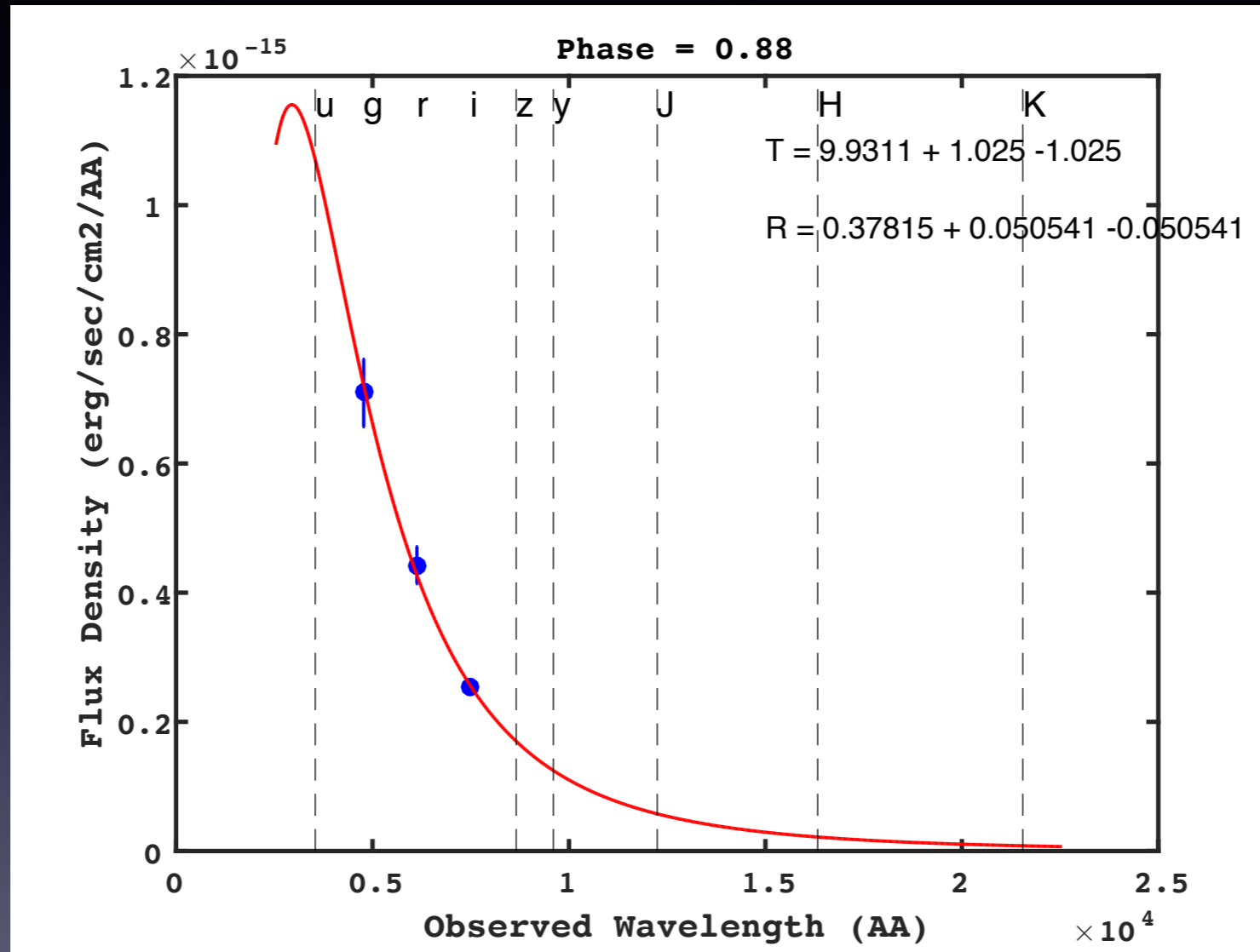
+0.70d Hawaii



Optical/NIR: Pan-STARRS

Smartt et al. 2017

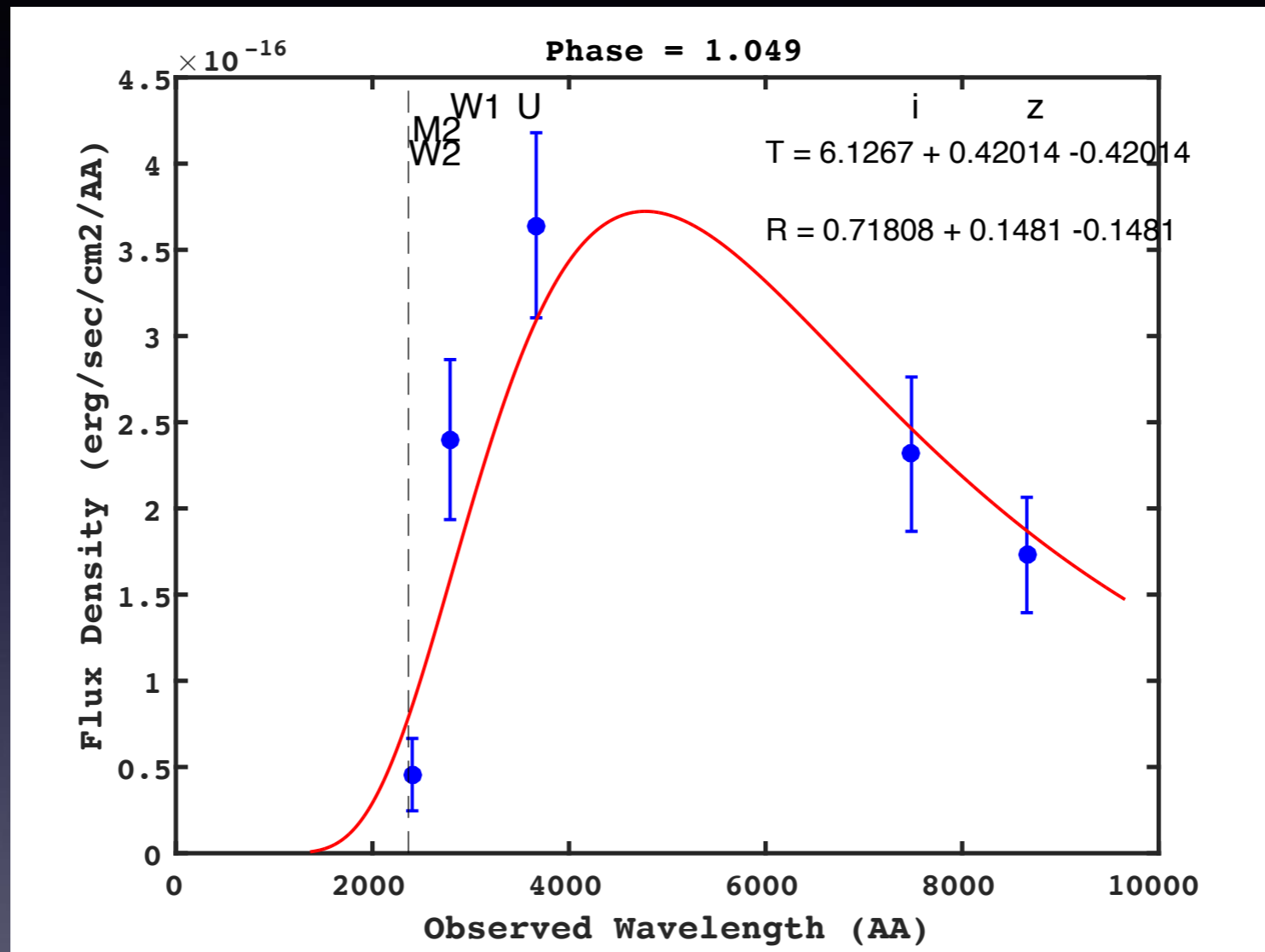
+0.88d Australia



Opt: SkyMapper

Andreoni et al. 2017

+1.05d Space - Swift



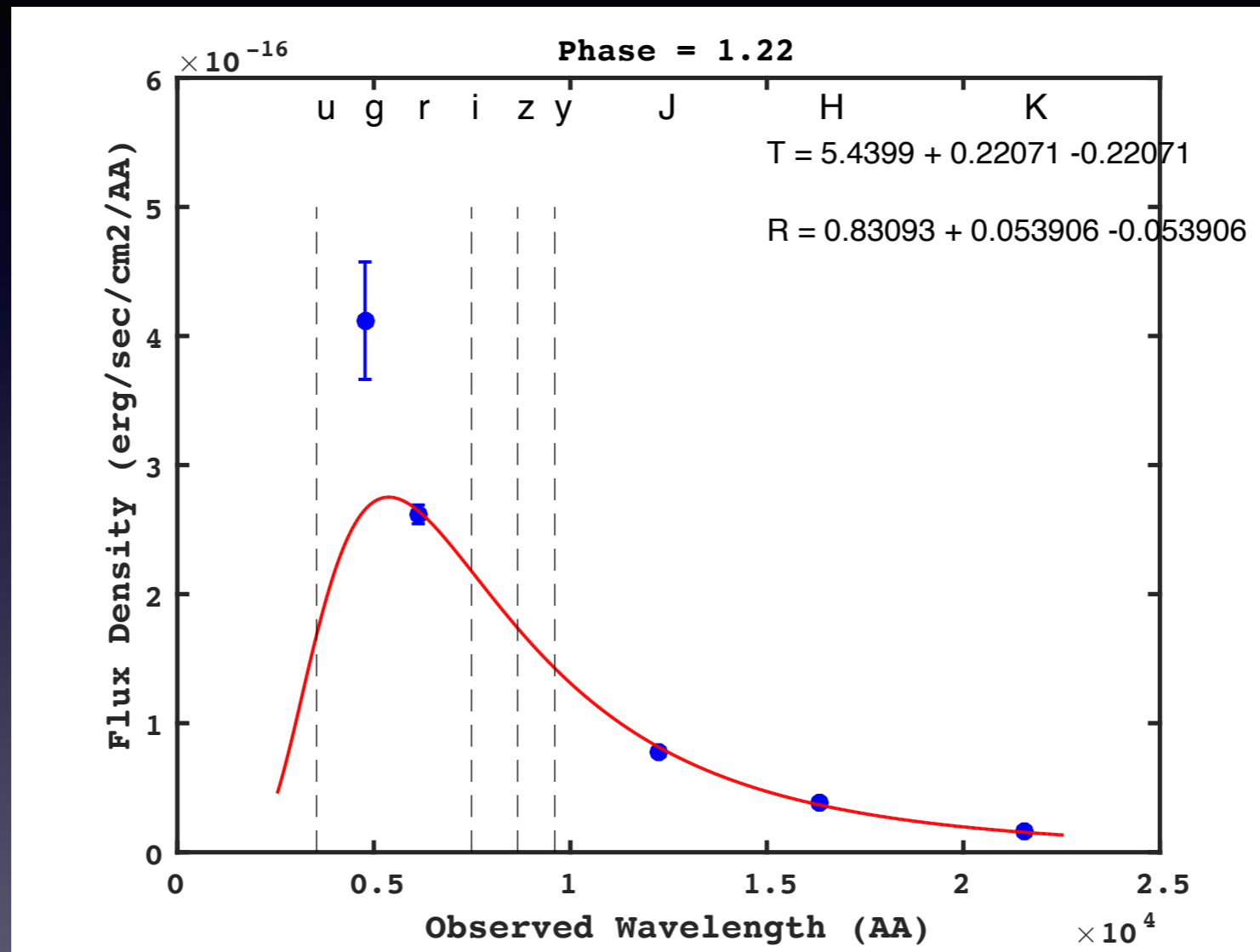
UV: Swift

Optical/NIR: Pan-STARRS
(interpolated)

Evans et al. 2017

Smartt et al. 2017

+1.22d South Africa



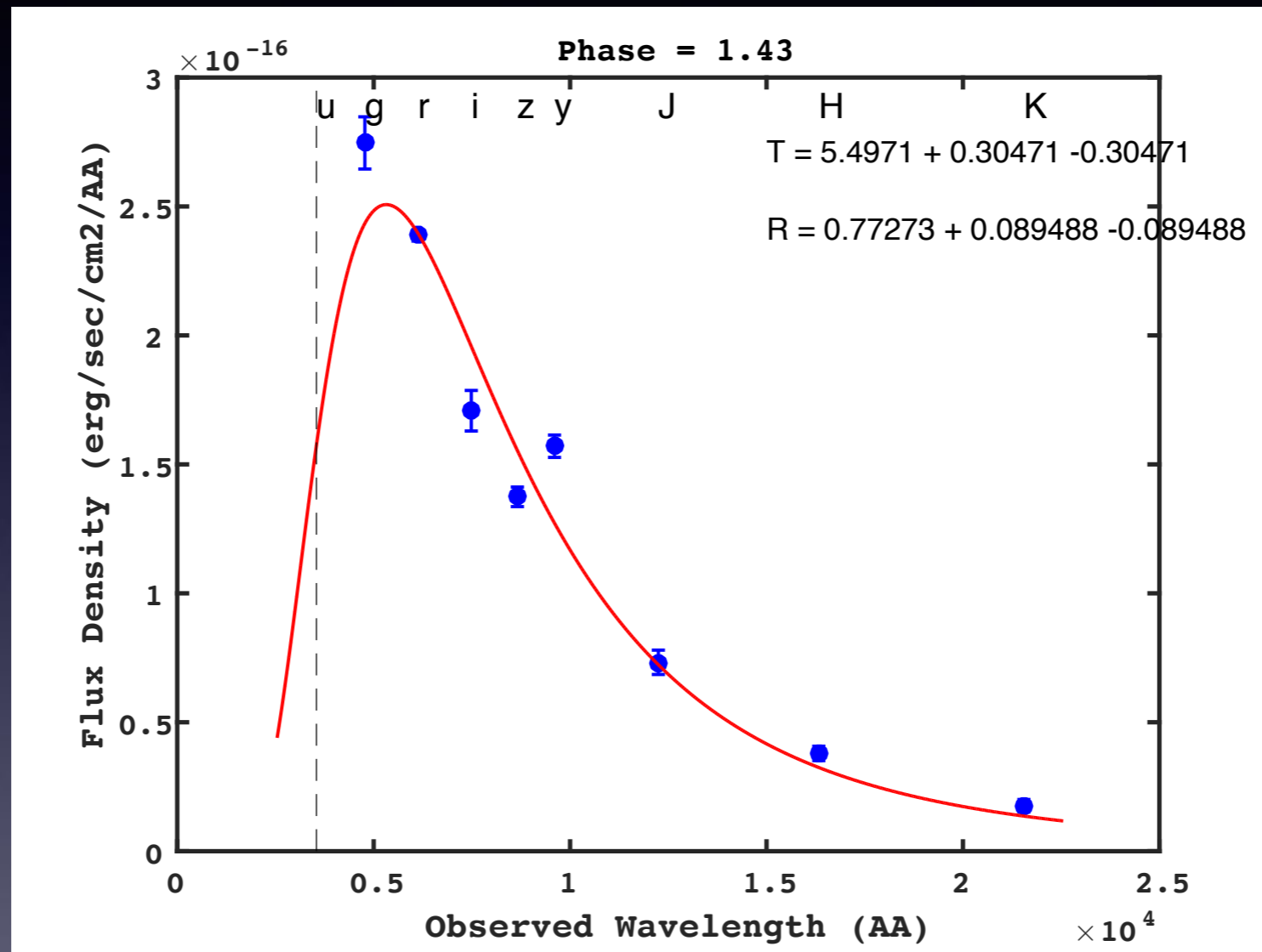
Optical : LCO, 1.5m Boyden

NIR: IRSF

Arcavi et al, 2017
Smartt et al, 2017

Utomi et al. 2017

+1.43d Chile



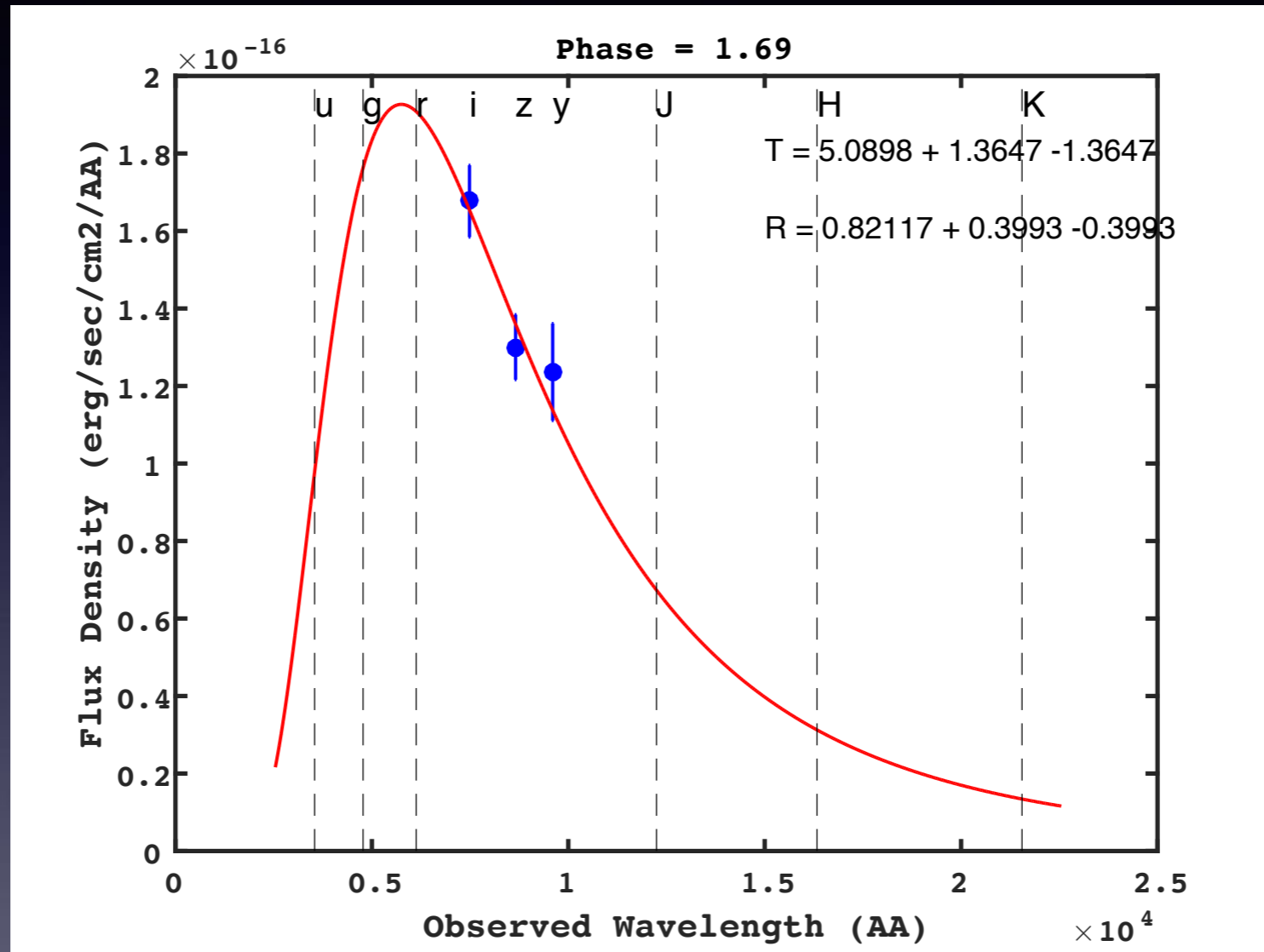
Opt: GROND, DECam

NIR: GROND

Smartt et al. 2017
Cowperthwaite et al./Soares-
Santos et al. 2017

Smartt et al. 2017

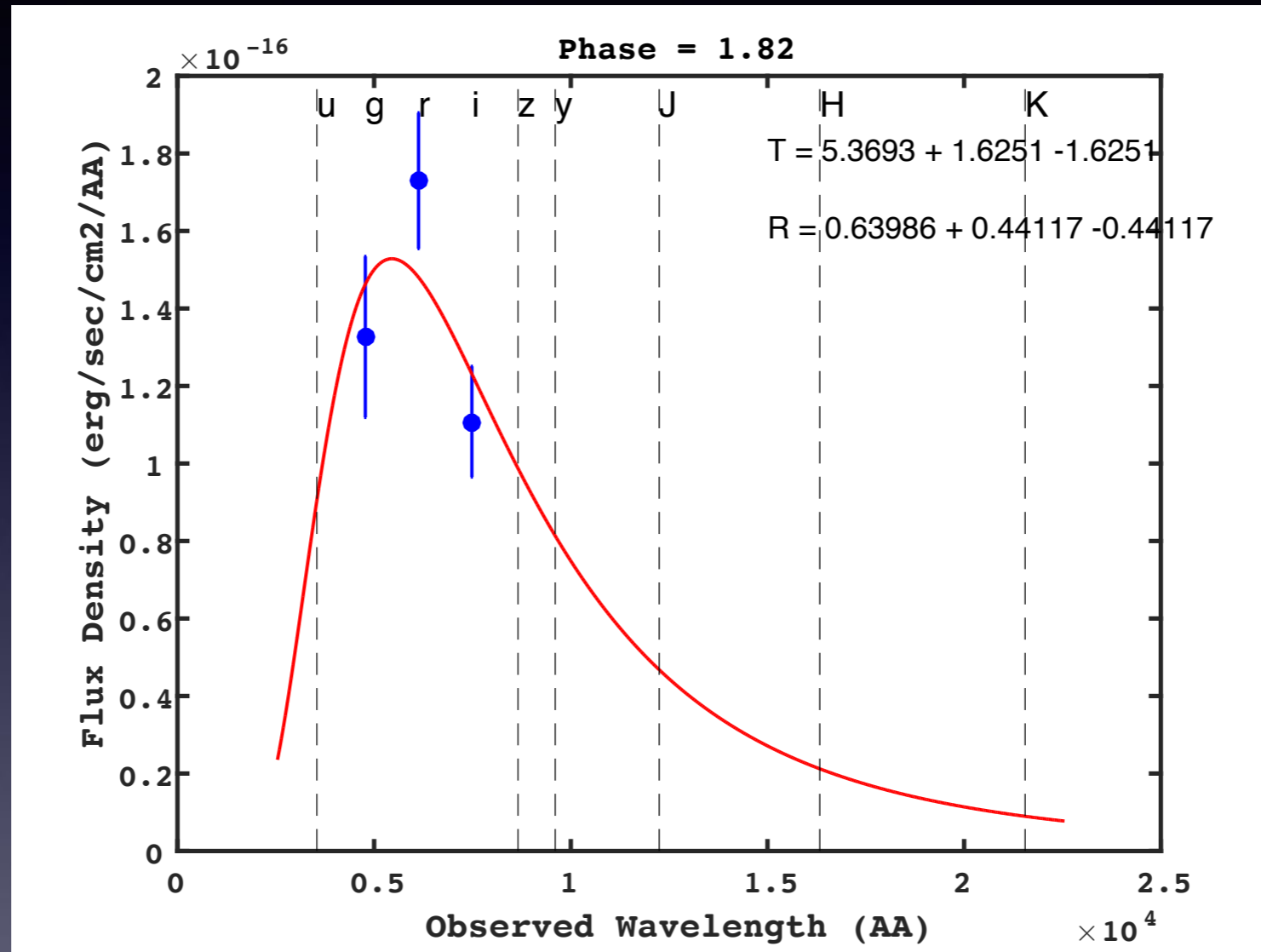
+1.69d Hawaii



Optical/NIR: Pan-STARRS

Smartt et al. 2017

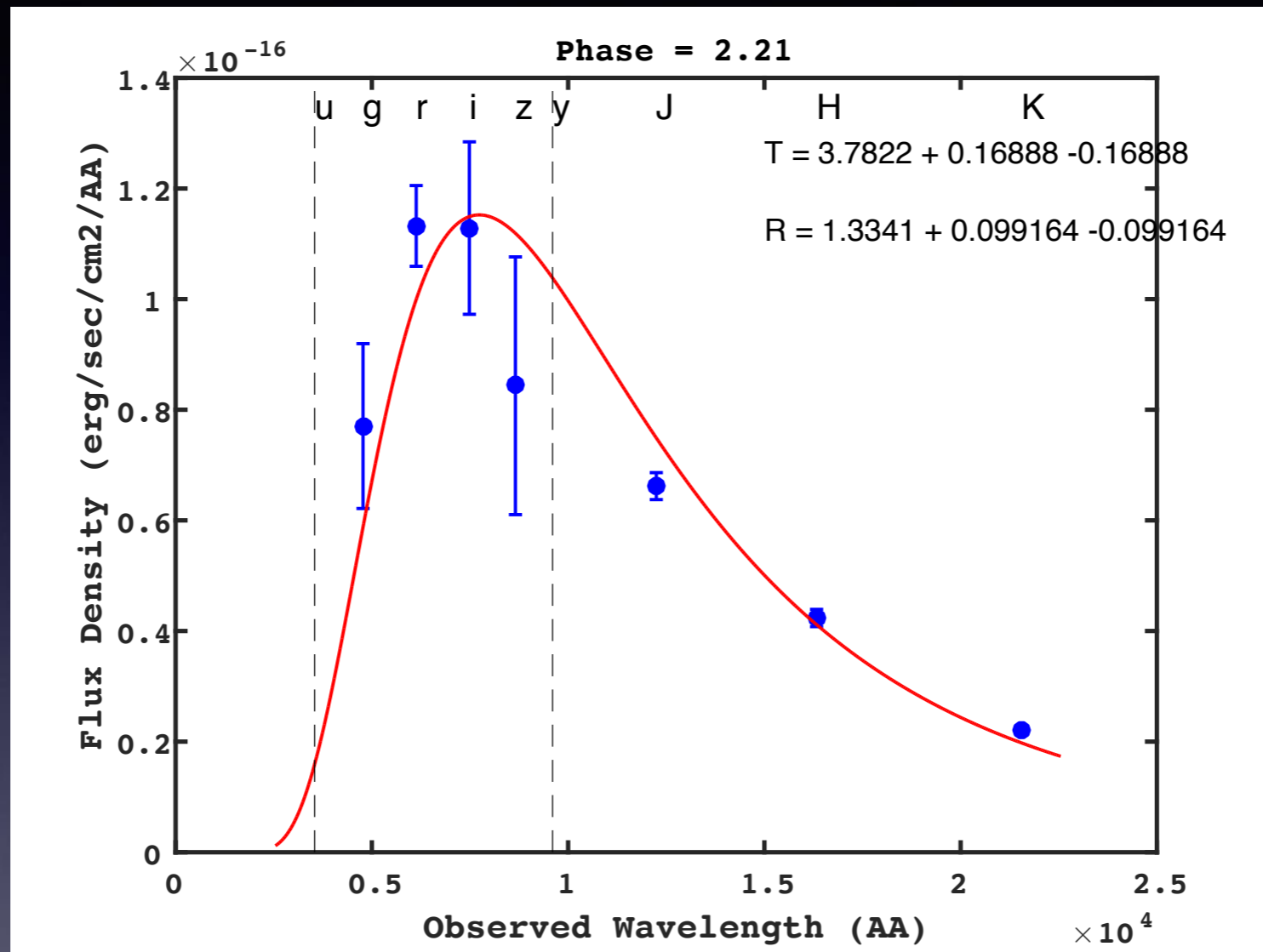
+1.82d Australia



Opt: SkyMapper

Andreoni et al. 2017

+2.21d South Africa



Optical : LCO, 1.5m Boyden

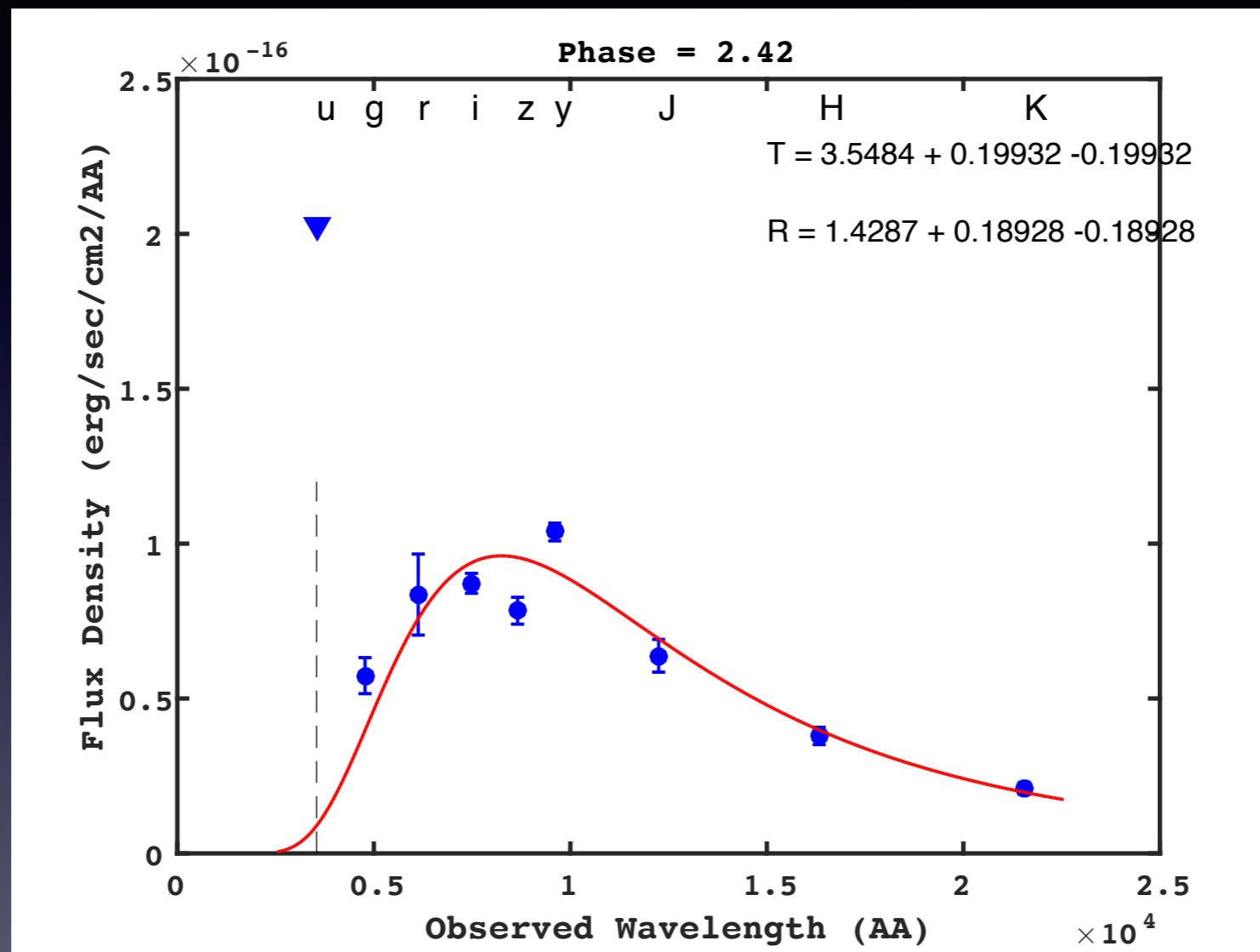
NIR: IRSF

Arcavi et al, 2017

Utomi et al. 2017

Smartt et al, 2017

+2.42d Chile



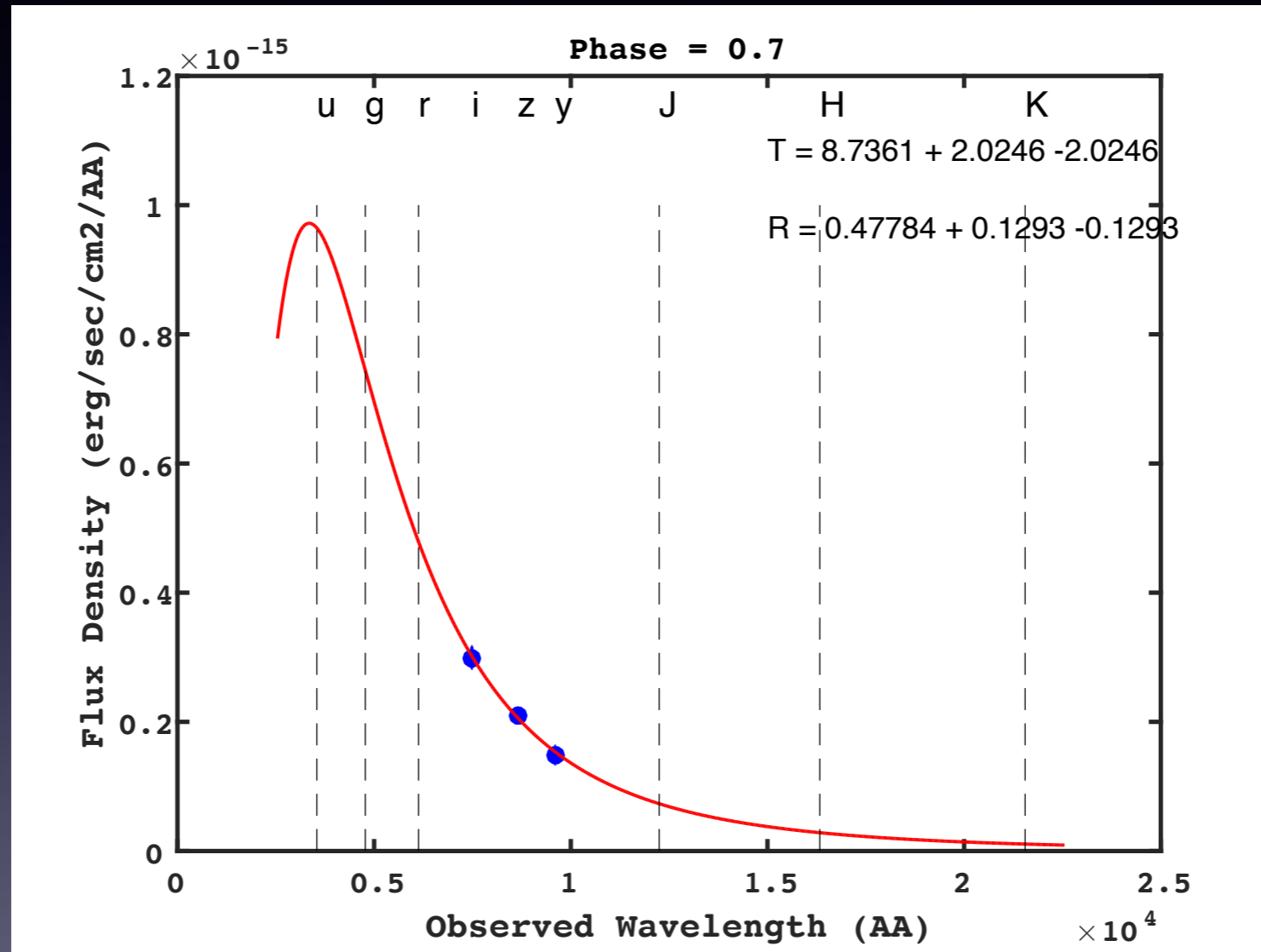
Opt: GROND, DECam

NIR: GROND

Smartt et al. 2017
Cowperthwaite et al./Soares-
Santos et al. 2017

Smartt et al. 2017

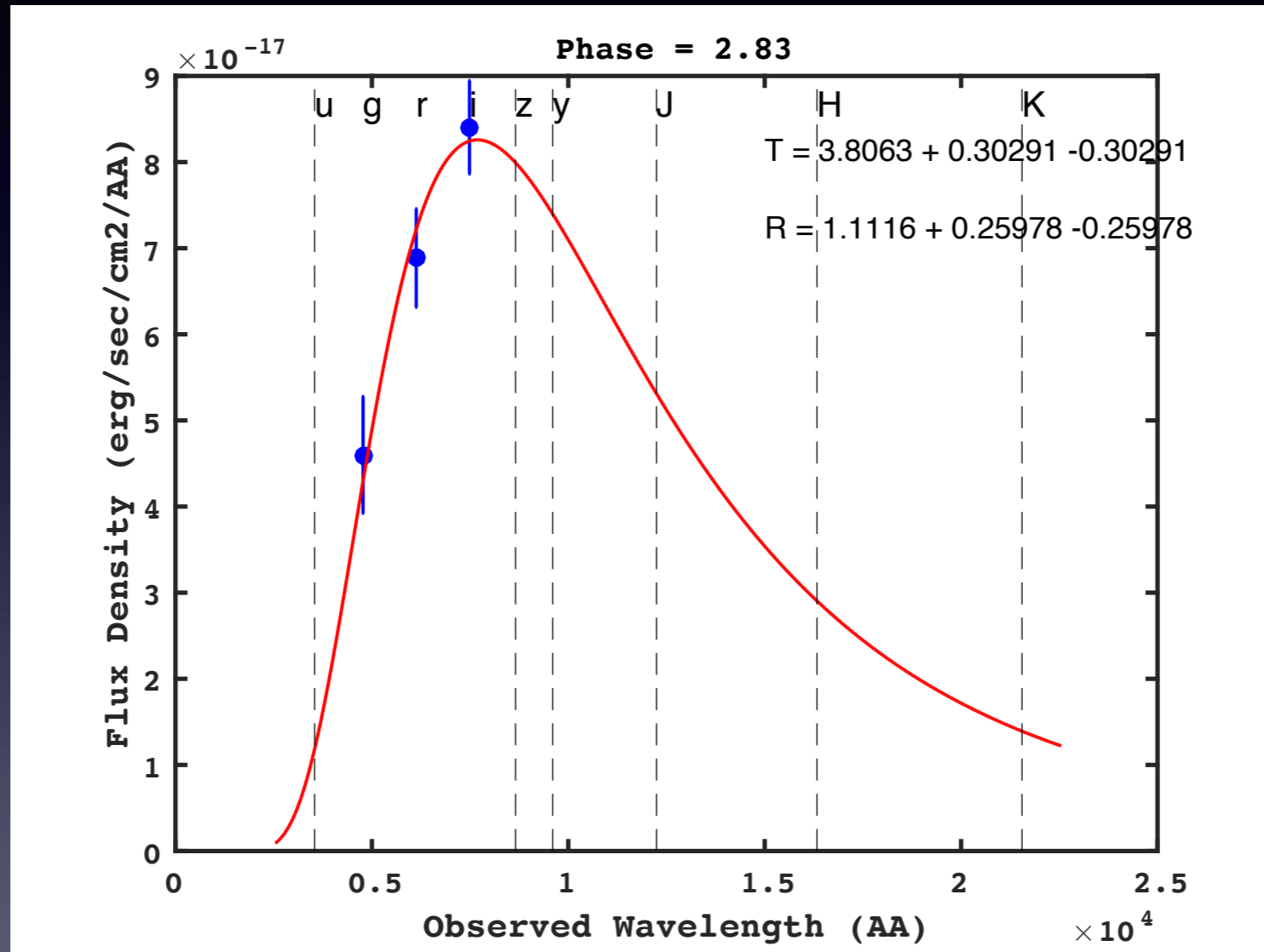
+2.68d Hawaii



Optical/NIR: Pan-STARRS

Smartt et al. 2017

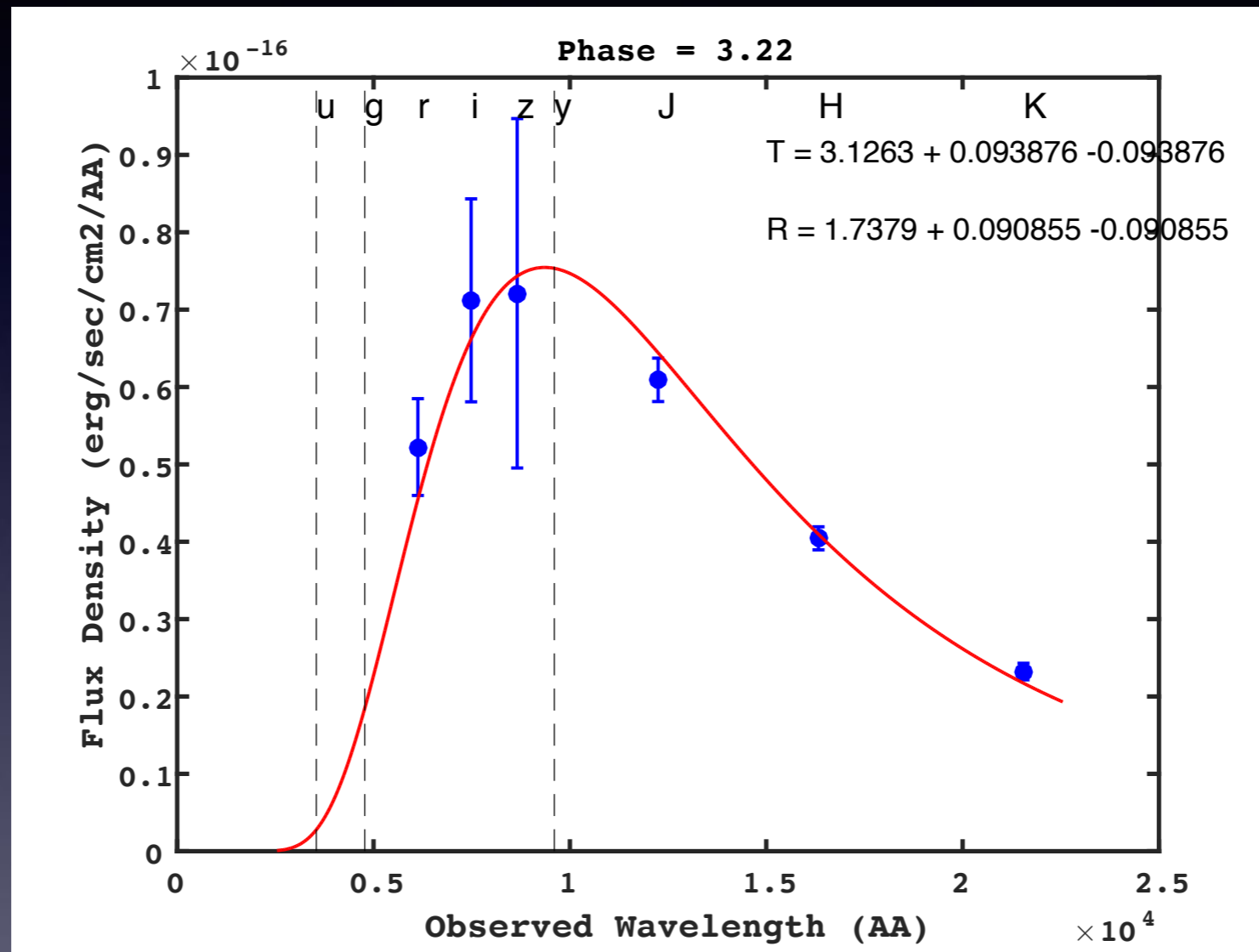
+2.83d Australia



Opt: SkyMapper

Andreoni et al. 2017

+3.22d South Africa



Optical : LCO, 1.5m Boyden

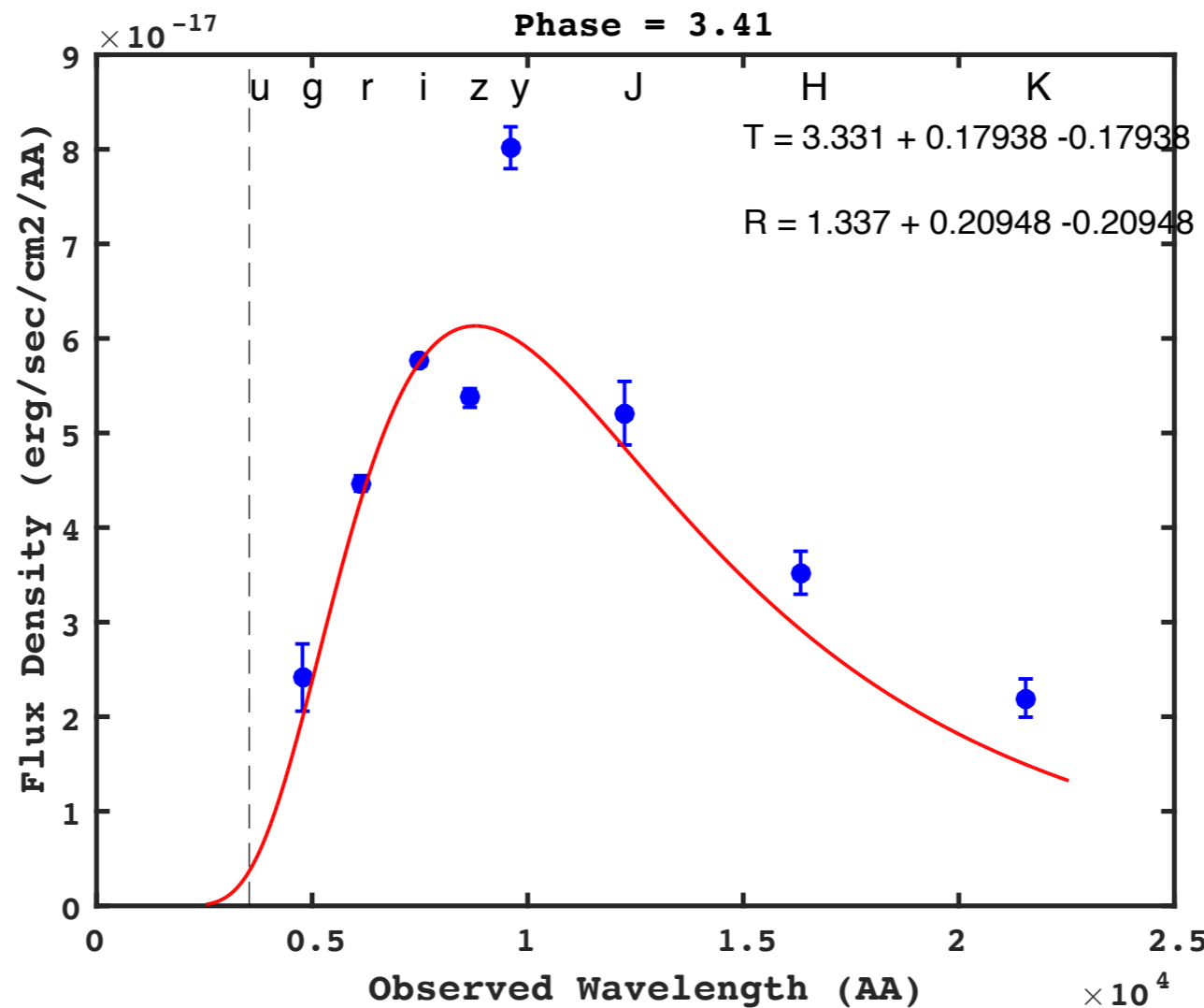
NIR: IRSF

Arcavi et al, 2017

Utomi et al. 2017

Smartt et al, 2017

+3.41d Chile



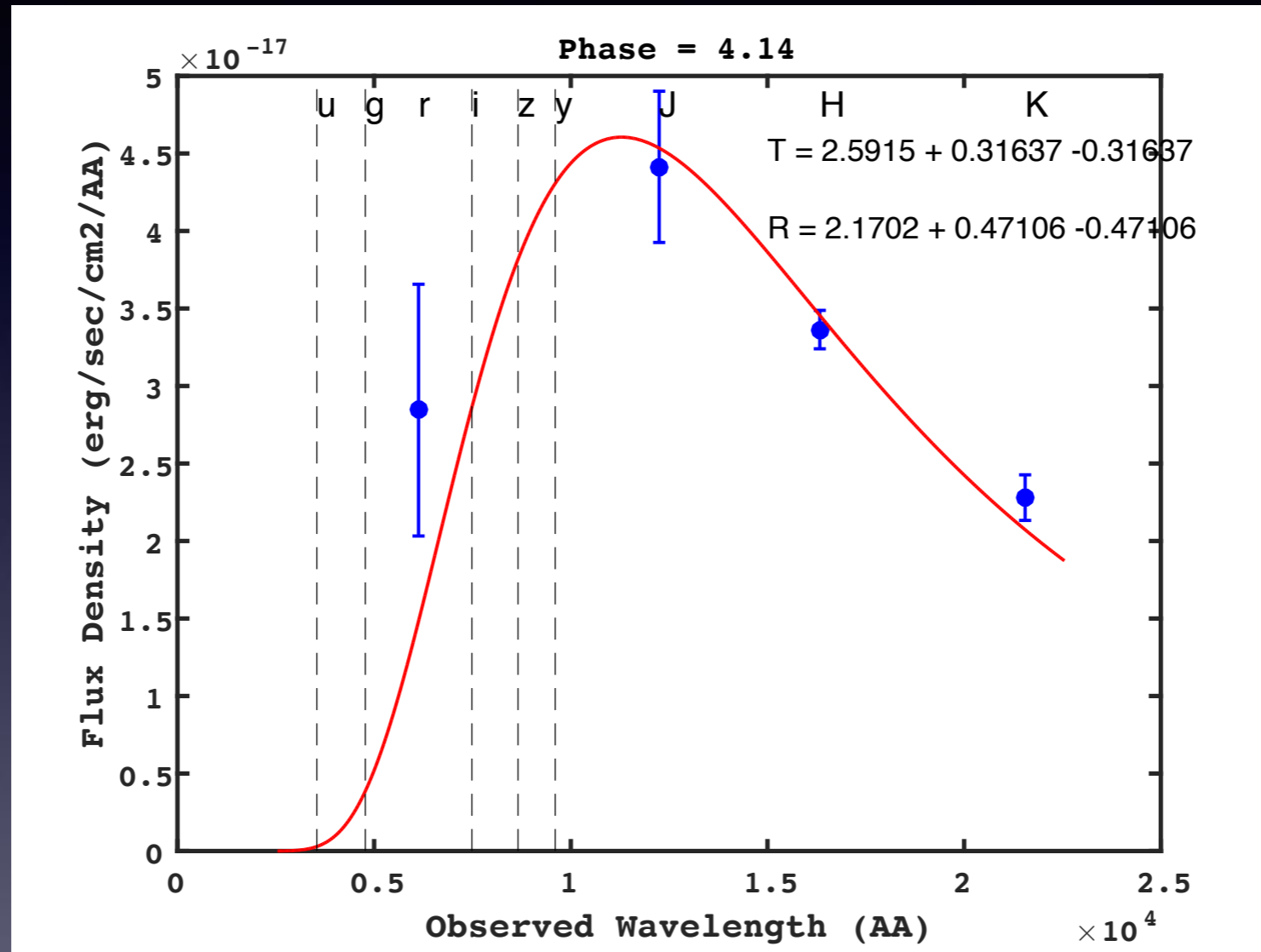
Opt: GROND, DECam

NIR: GROND

Smartt et al. 2017
Cowperthwaite et al./Soares-
Santos et al. 2017

Smartt et al. 2017

+4.14d South Africa



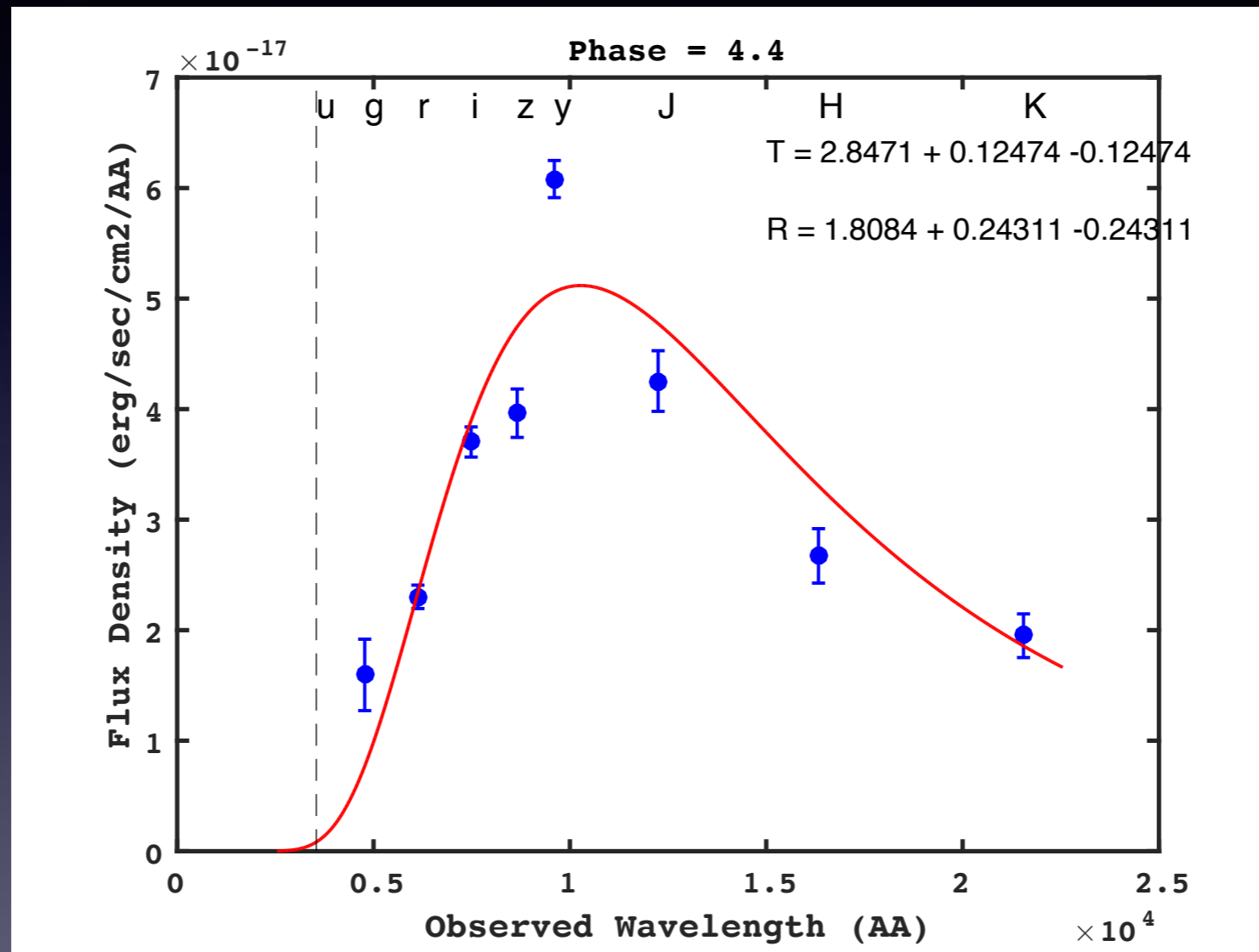
Optical : LCO

Arcavi et al, 2017

NIR: IRSF

Utomi et al. 2017

+4.4d Chile



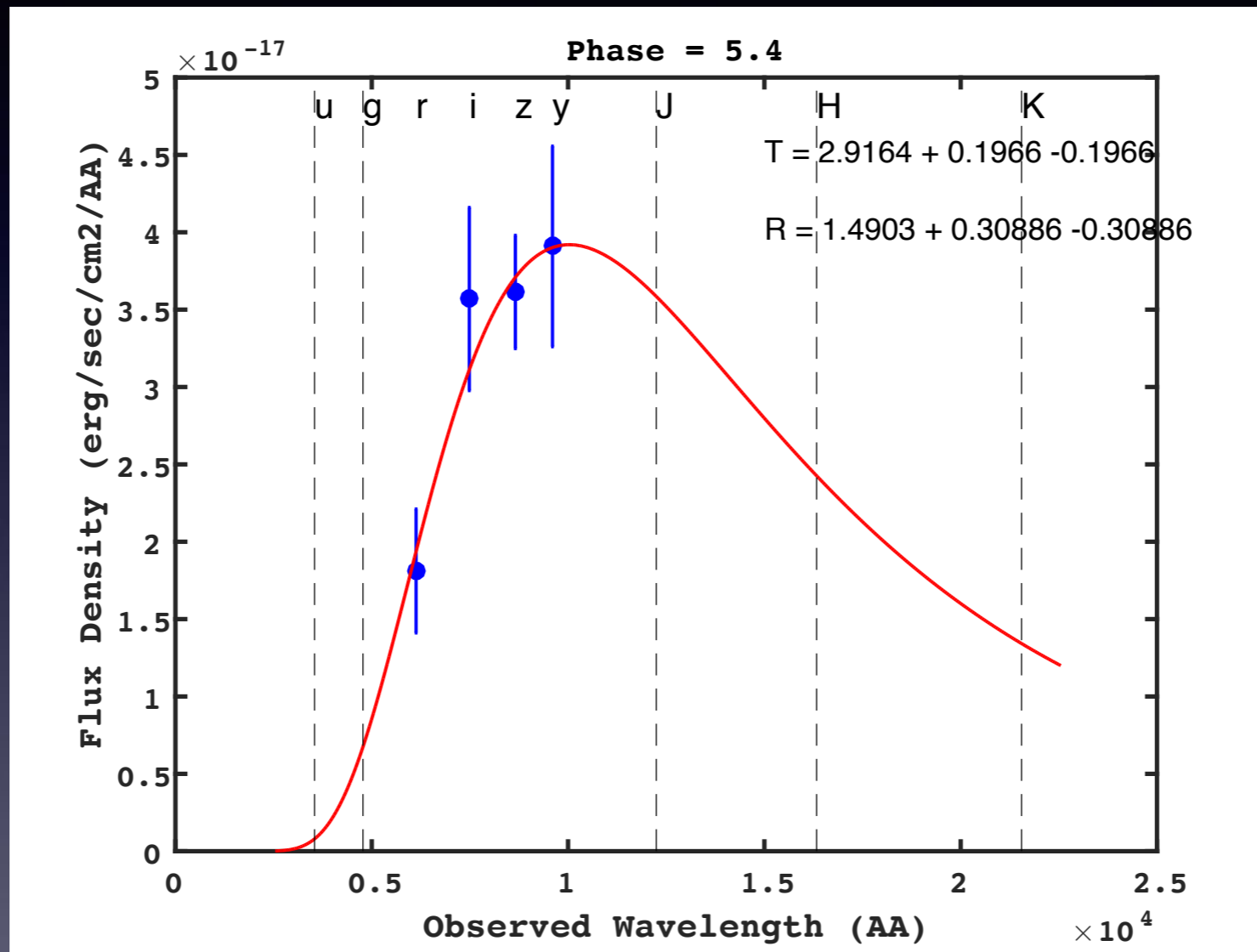
Opt: GROND, DECam

NIR: GROND

Smartt et al. 2017
Cowperthwaite et al./Soares-Santos et al. 2017

Smartt et al. 2017

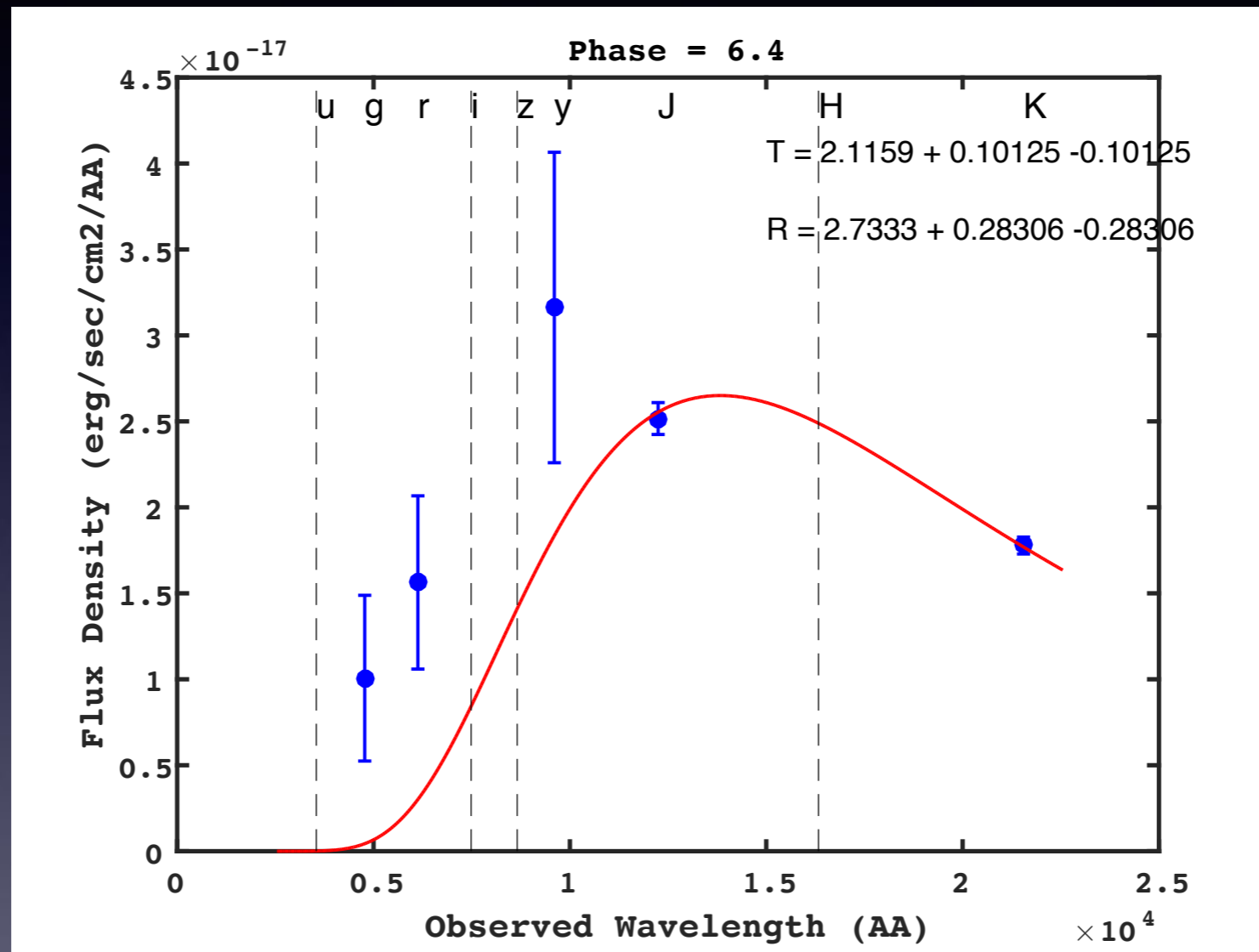
+5.4d Chile



Opt: DECam

Cowperthwaite et al./Soares-Santos et al. 2017

+6.4d Chile



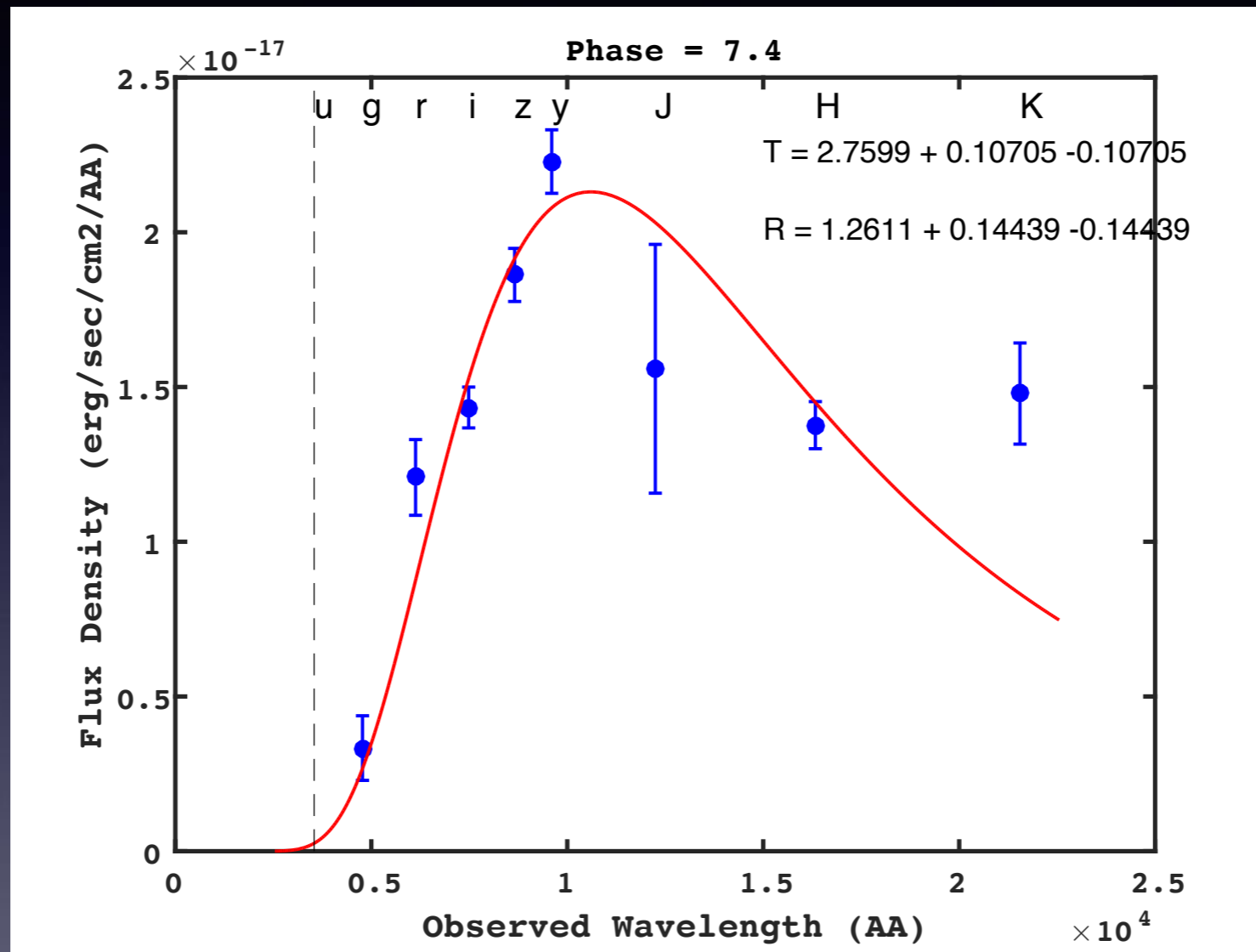
Opt:DECAM

Cowperthwaite et al./Soares-Santos et al. 2017

NIR: VISTA

Tanvir et al. 2017

+7.4d Chile



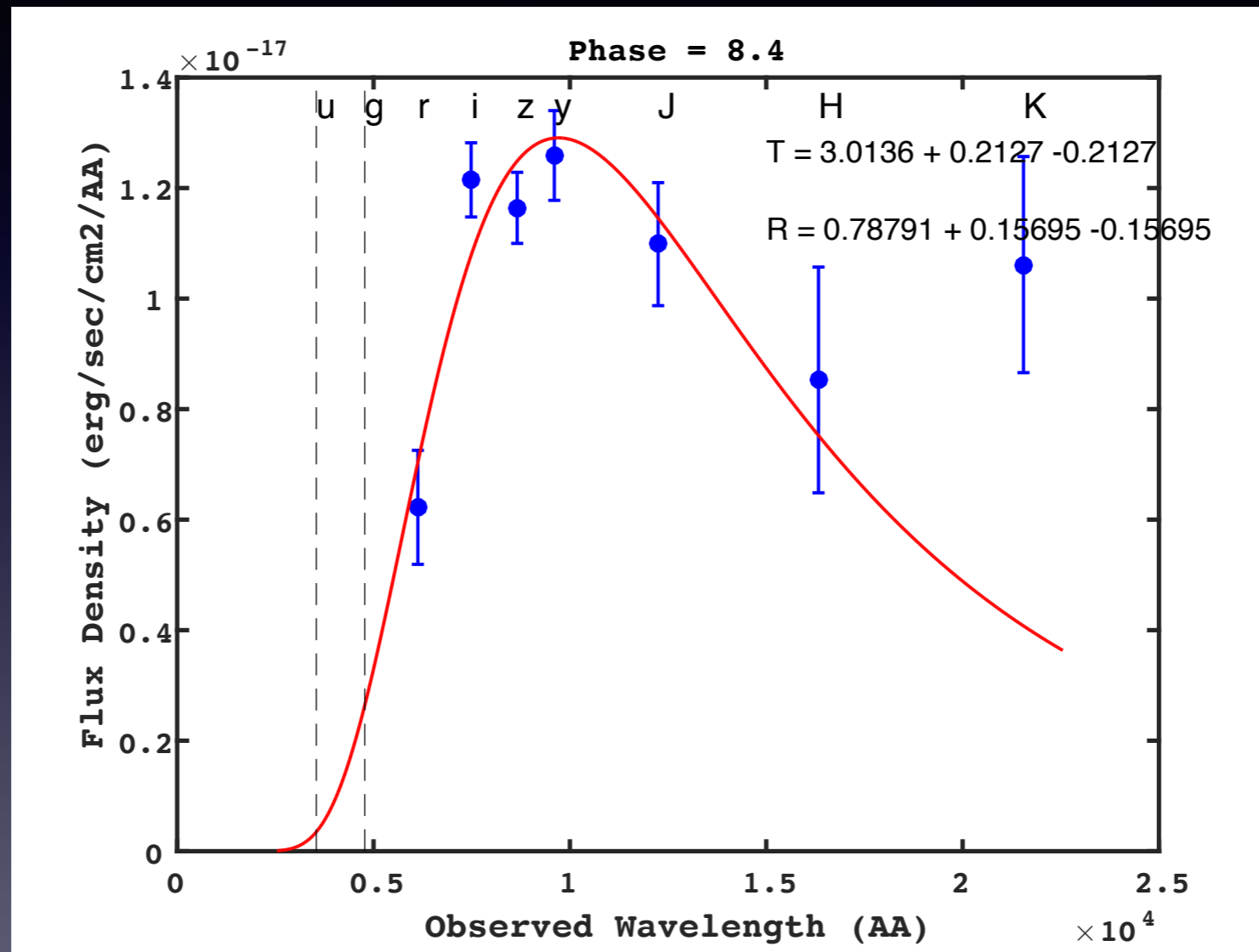
Opt:DECAM

Cowperthwaite et al./Soares-Santos et al. 2017

NIR: GROND

Smartt et al. 2017

+8.4d Chile



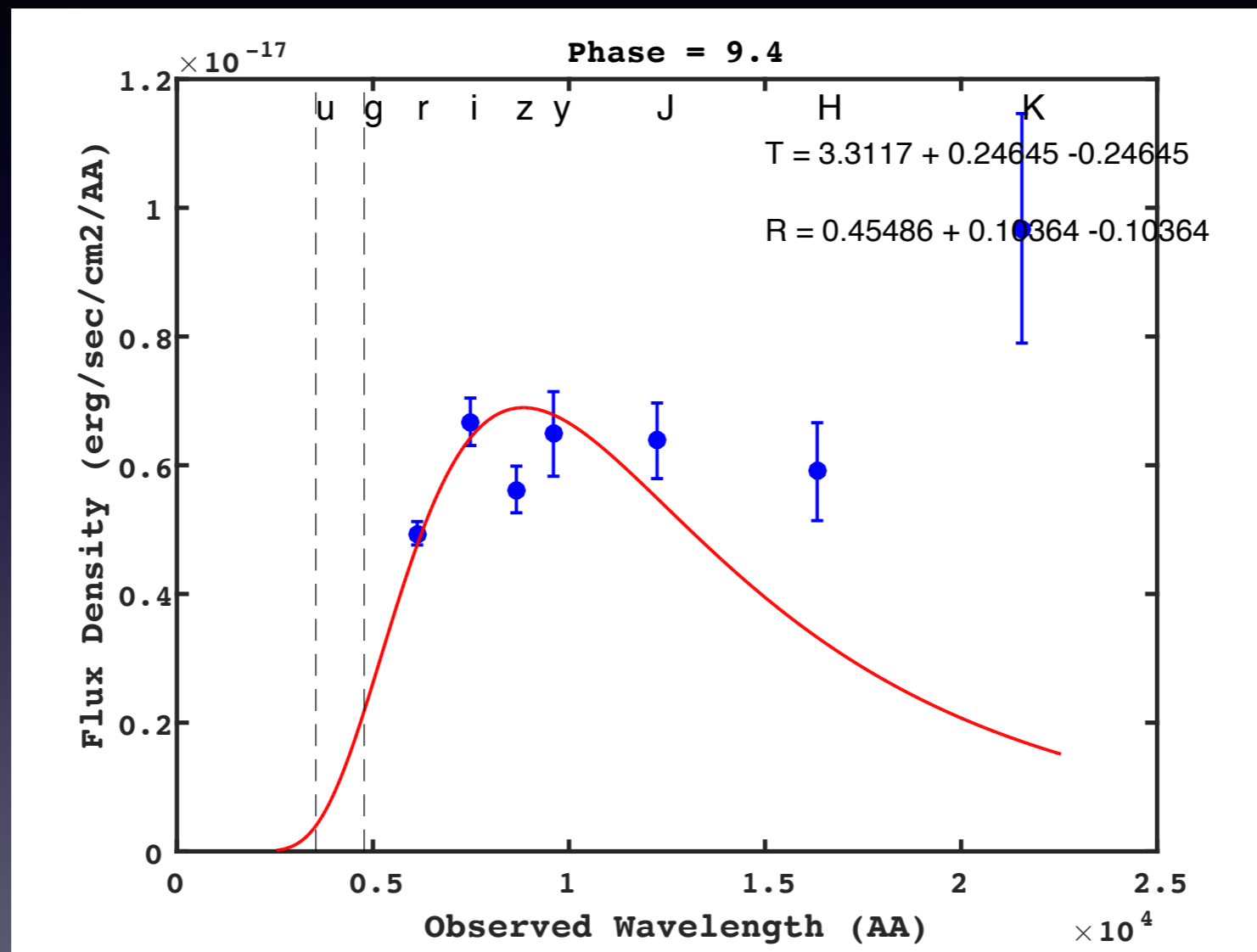
Opt:DECam

Cowperthwaite et al./Soares-Santos et al. 2017

NIR: GROND

Smartt et al. 2017

+9.4d Chile



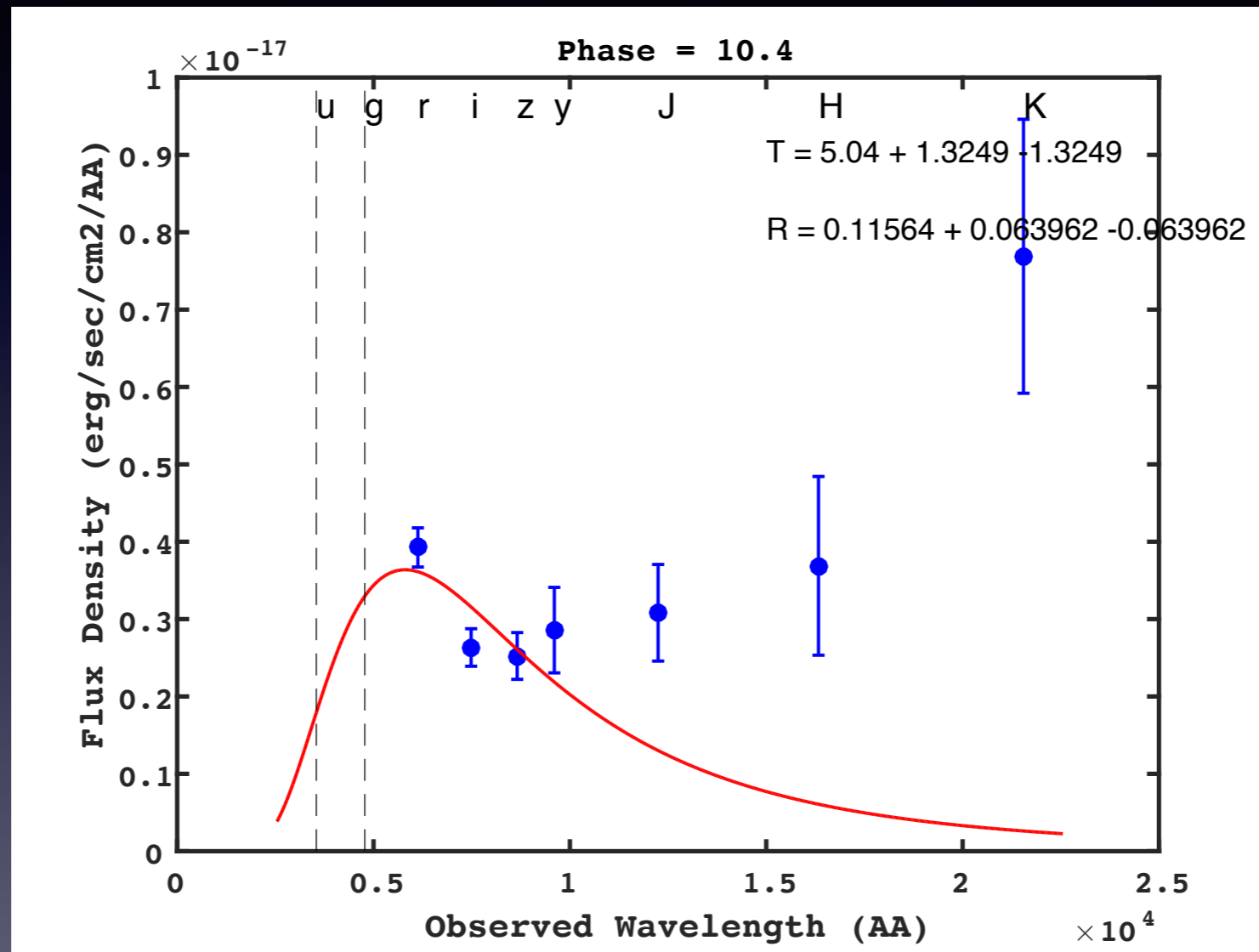
Opt:DECam, VIMOS

Cowperthwaite et al./Soares-Santos et al. 2017
Tanvir et al. 2017

NIR: GROND

Smartt et al. 2017

+10.4d Chile



Opt:DECam, VIMOS

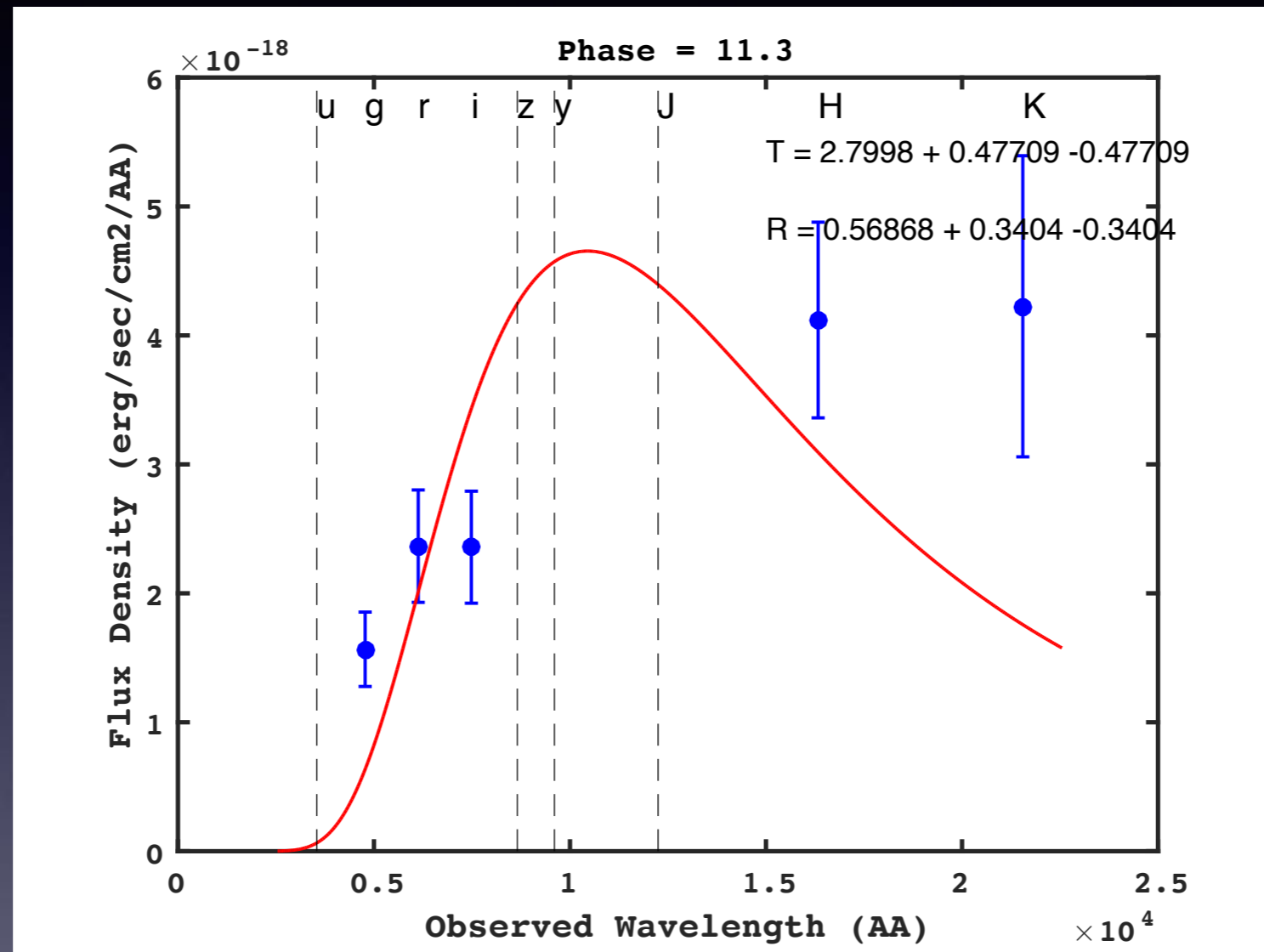
Cowperthwaite et al./Soares-Santos et al. 2017

Tanvir et al. 2017

NIR: GROND

Smartt et al. 2017

+11.3d Chile + Space (HST)



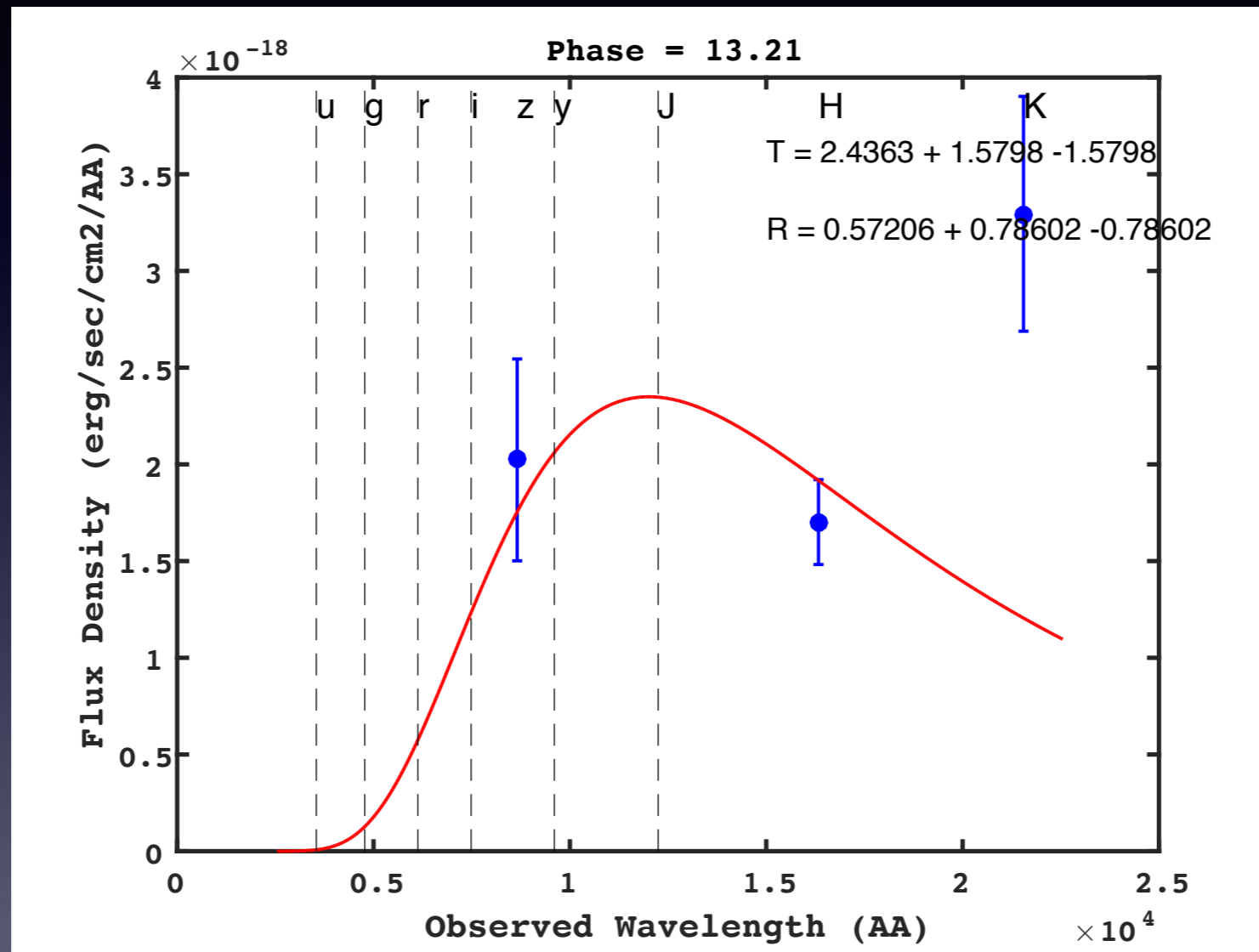
Opt: HST

Tanvir et al. 2017

NIR: GROND + NTT

Smartt et al. 2017

+13.2d Chile



Opt: VIMOS

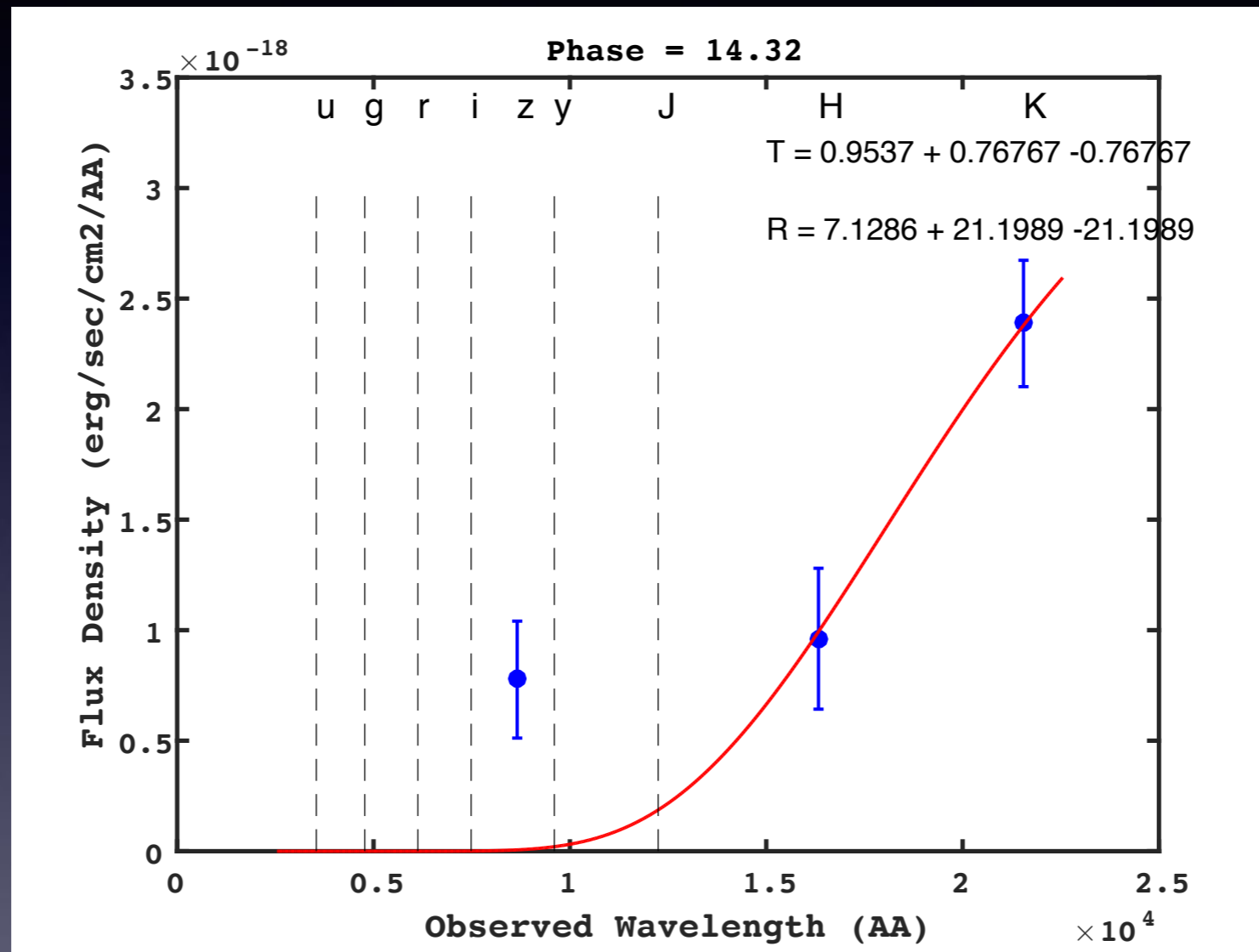
Tanvir et al. 2017

NIR: NTT and Gemini South

Smartt et al. 2017

Chornock et al. 2017

+14.3d Chile



Opt: FORS2

Pian et al. 2017

NIR: VISTA and Gemini South

Tanvir et al. 2017,

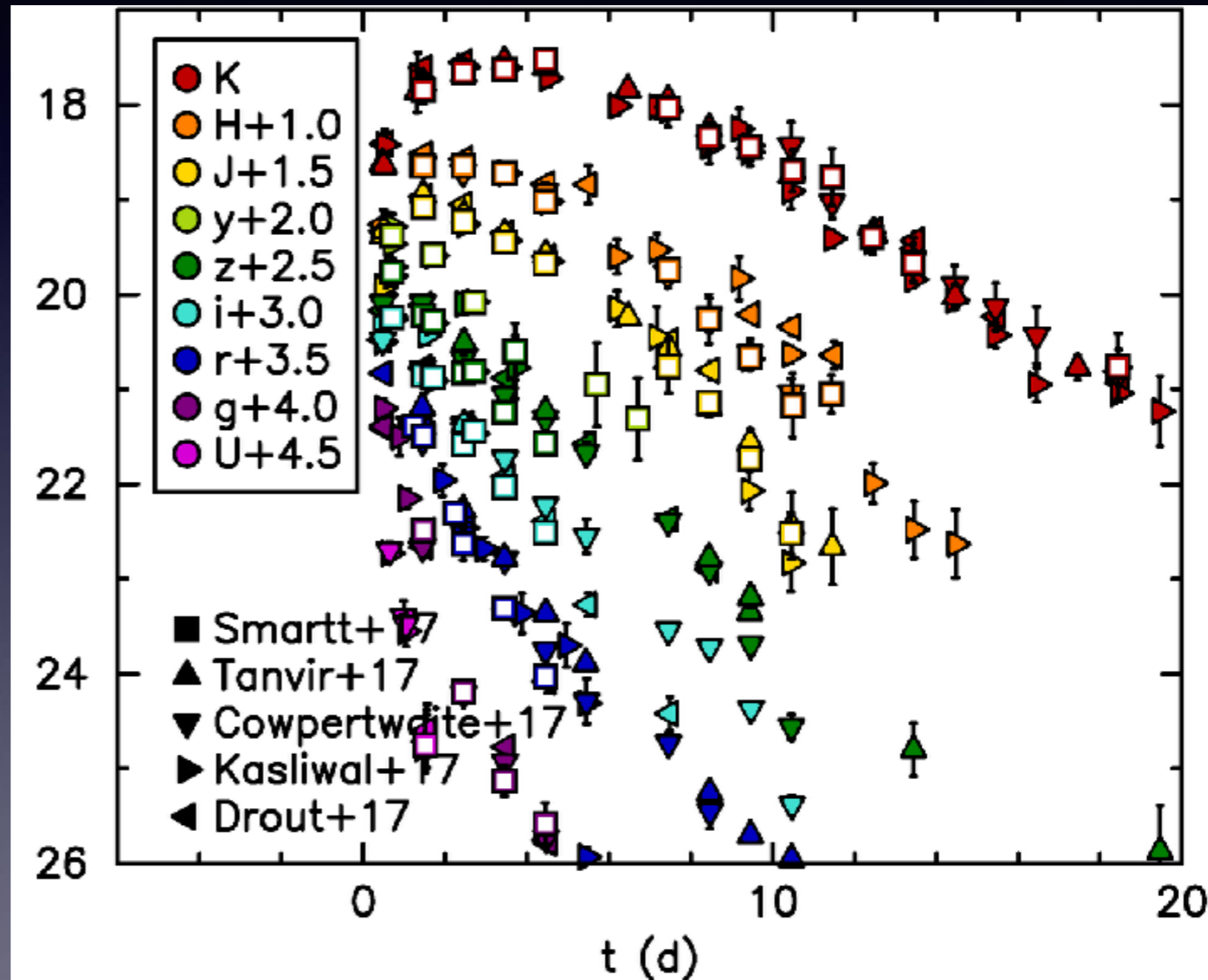
Chornock et al. 2017

Kasliwal et al. 2017

Troja et al. 2017

Unconstrained beyond +15d

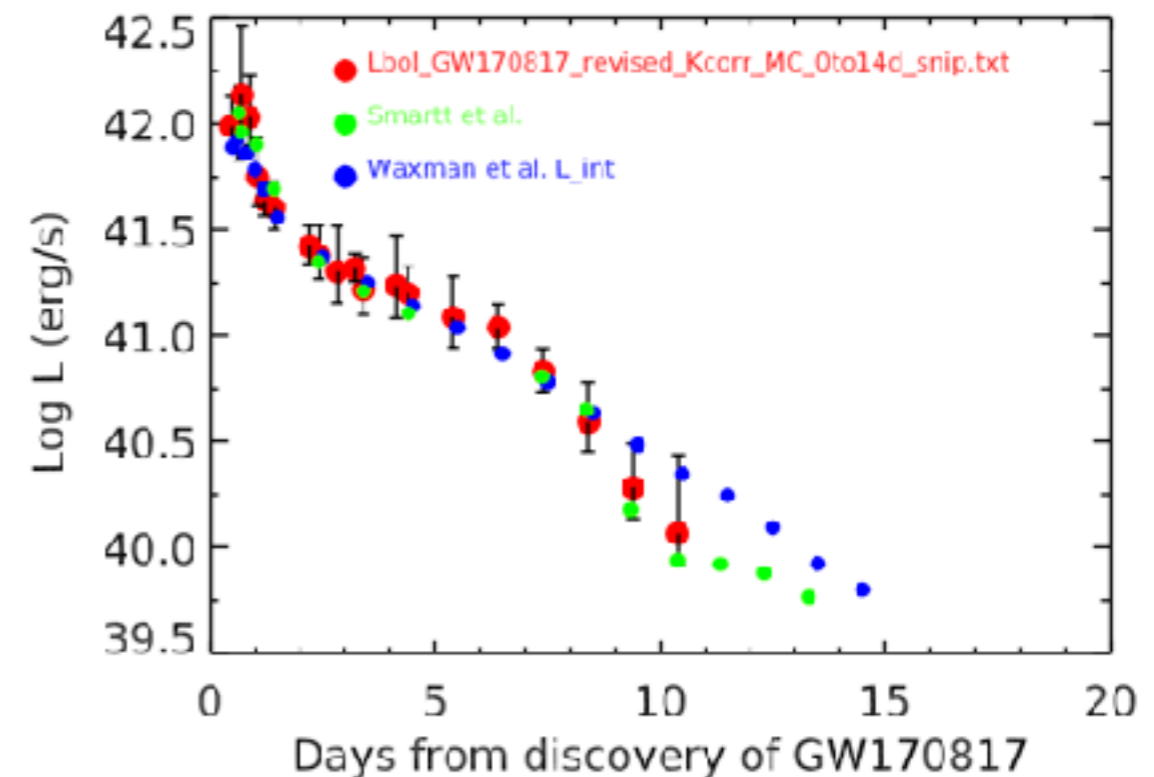
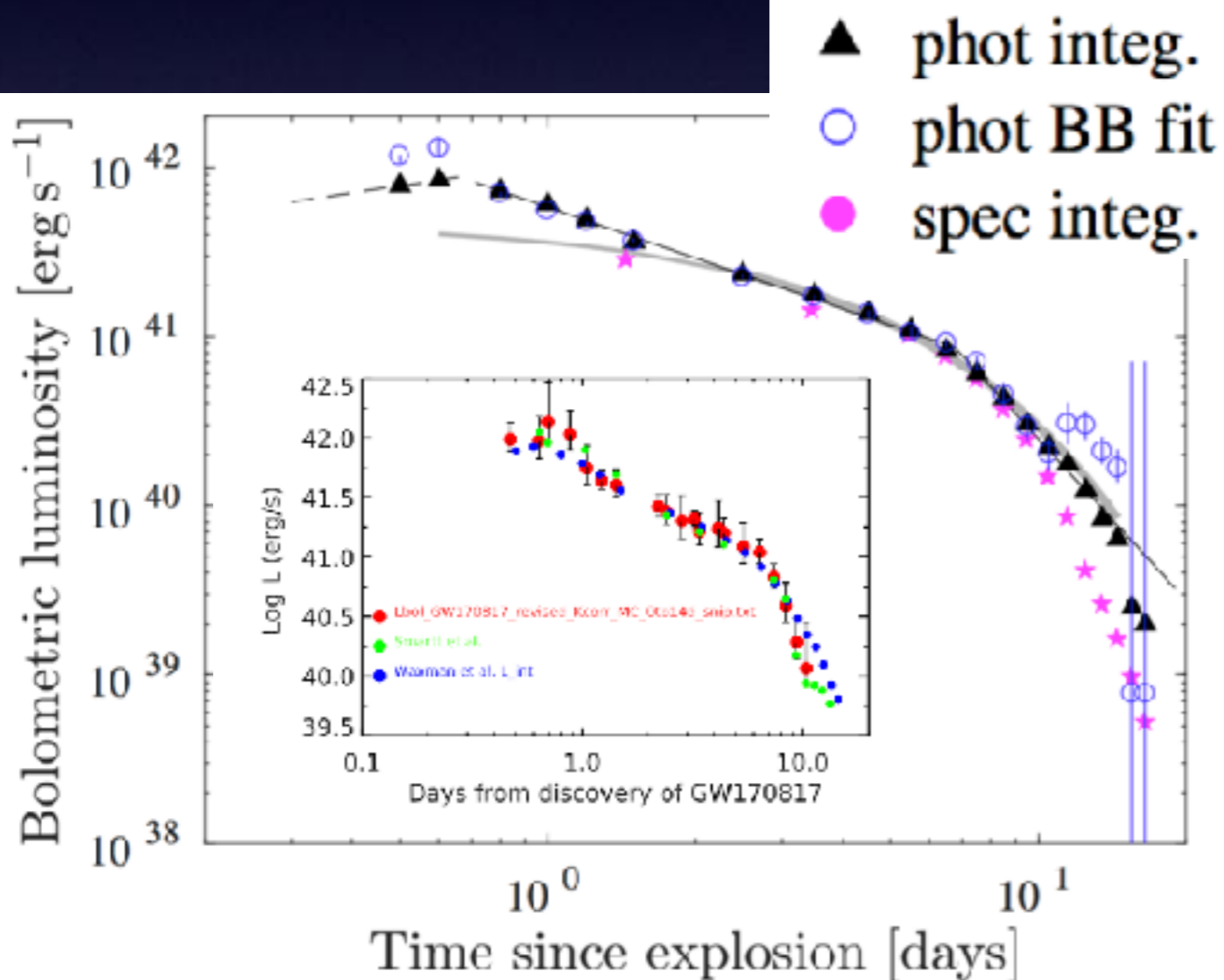
- K-band only beyond +15d
- SED unconstrained, can't say if it is compatible with $T \approx 2500$ K



L_{bol} : reasonable agreement

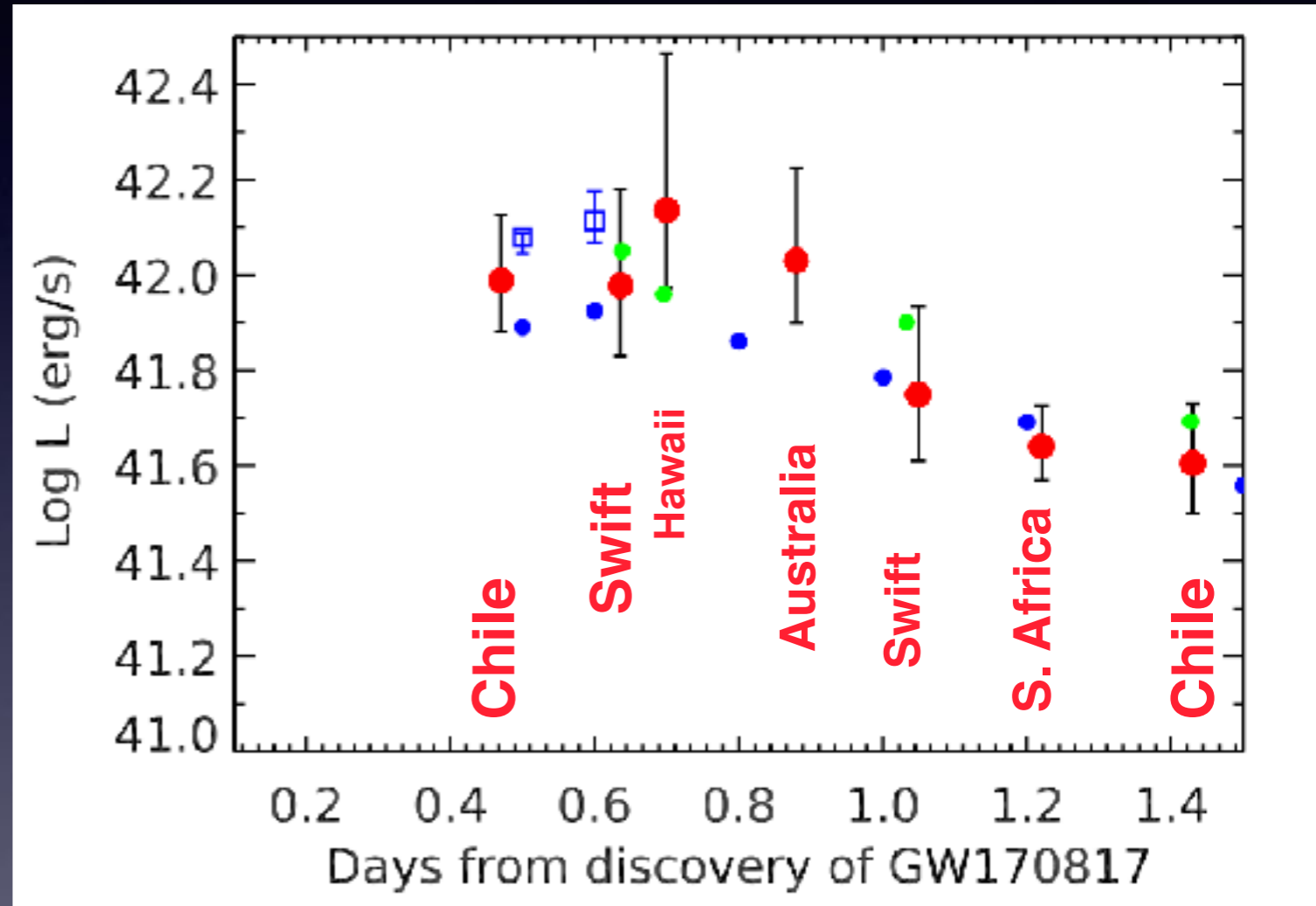
Waxman et al.
arXiv:1711.09638

Beyond 2.5m
add Rayleigh-Jeans
tail $f(\lambda) \sim \lambda^{-4}$



Peak luminosity

- “Peak” resolved within first 24hrs
- $0.4 < t_{\text{peak}} < 0.9$ days
- $\text{Log } L_{\text{peak}} = 42.0 \pm 0.1$
- $L = 1^{+0.26}_{-0.21} \times 10^{42}$ ergs/s



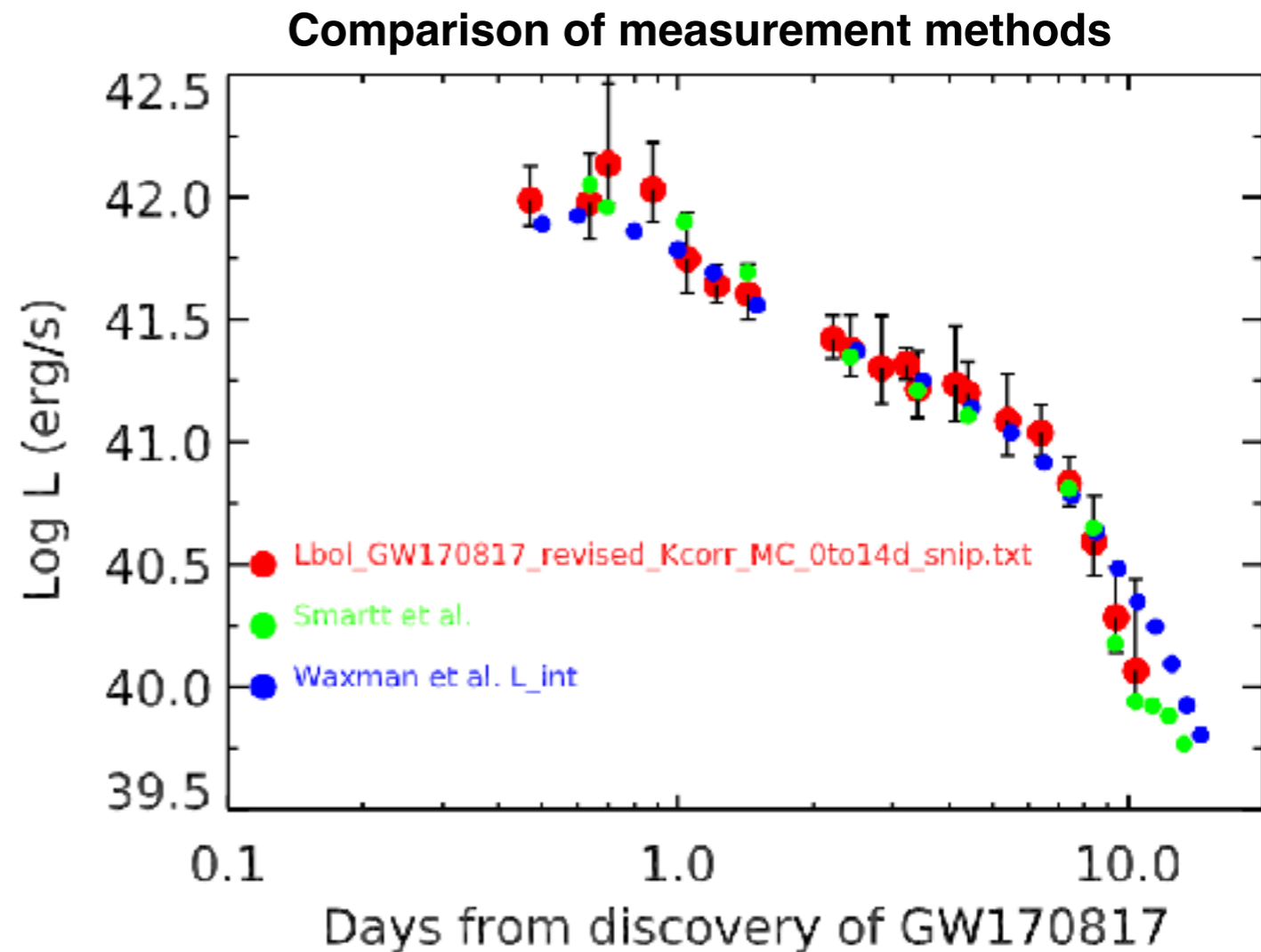
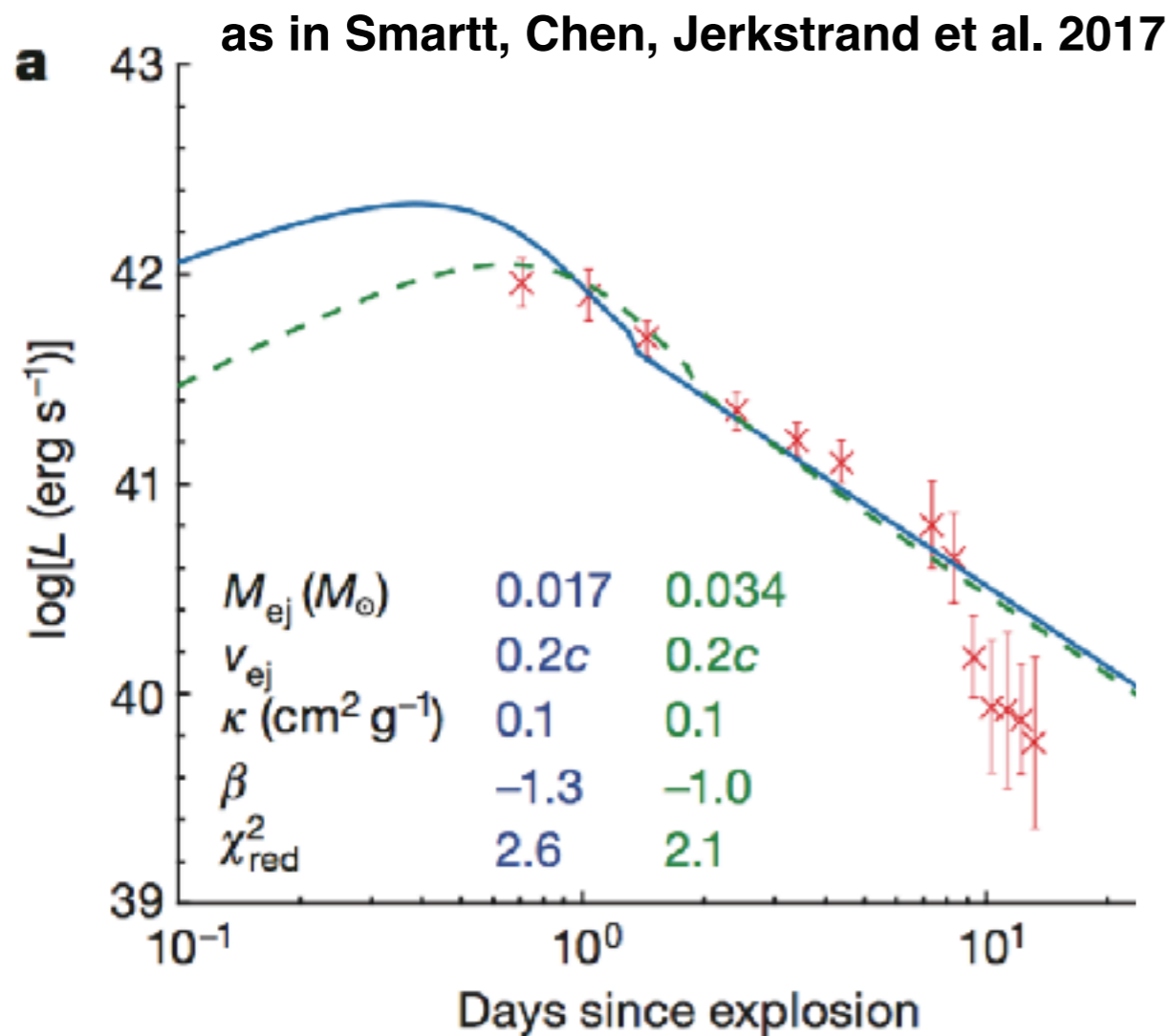
New - BB integration from all data
Smartt et al.
Waxman et al

Reasonable criticisms - and implications for future

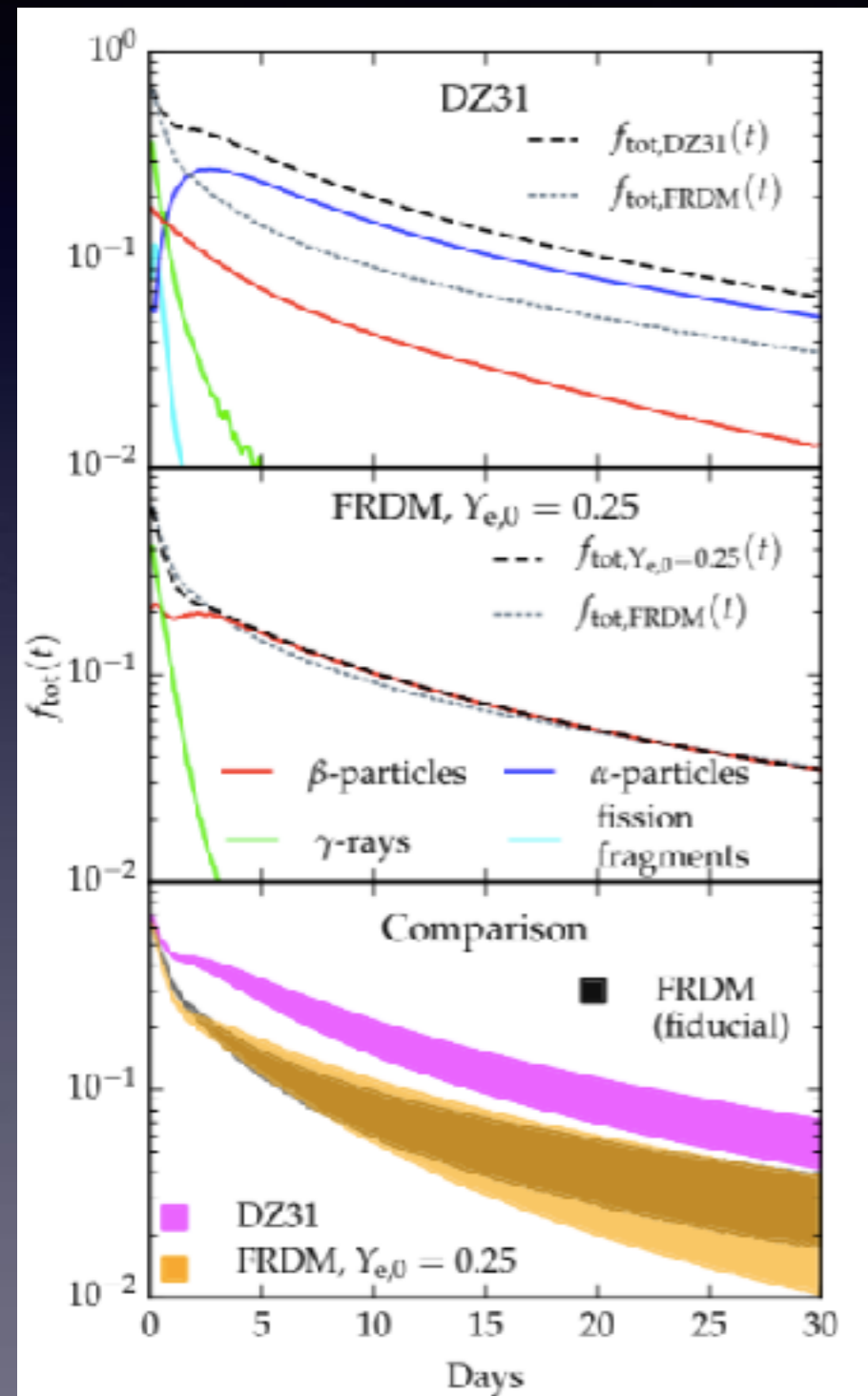
- Our models are too simple - Metzger 2017 “toy model” and Arnett-Jerkstrand semi-analytic model
- We do not use the SED/spectral information available when fitting the lightcurve (L_{bol} only)
- We have underestimated K-band at $> 10\text{d}$. Therefore underestimated the contribution to a high opacity component
- We have only integrated our L_{bol} out to 2.5microns, there is clearly **(some)** flux beyond that. Therefore underestimated the contribution to a high opacity component
- **The thermalisation function and/or heating rate we apply for radioactive decay particles (leptons) are either wrong or unknown**

Arnett-Jerkstrand model

<https://star.pst.qub.ac.uk/wiki/doku.php/users/ajerkstrand/>

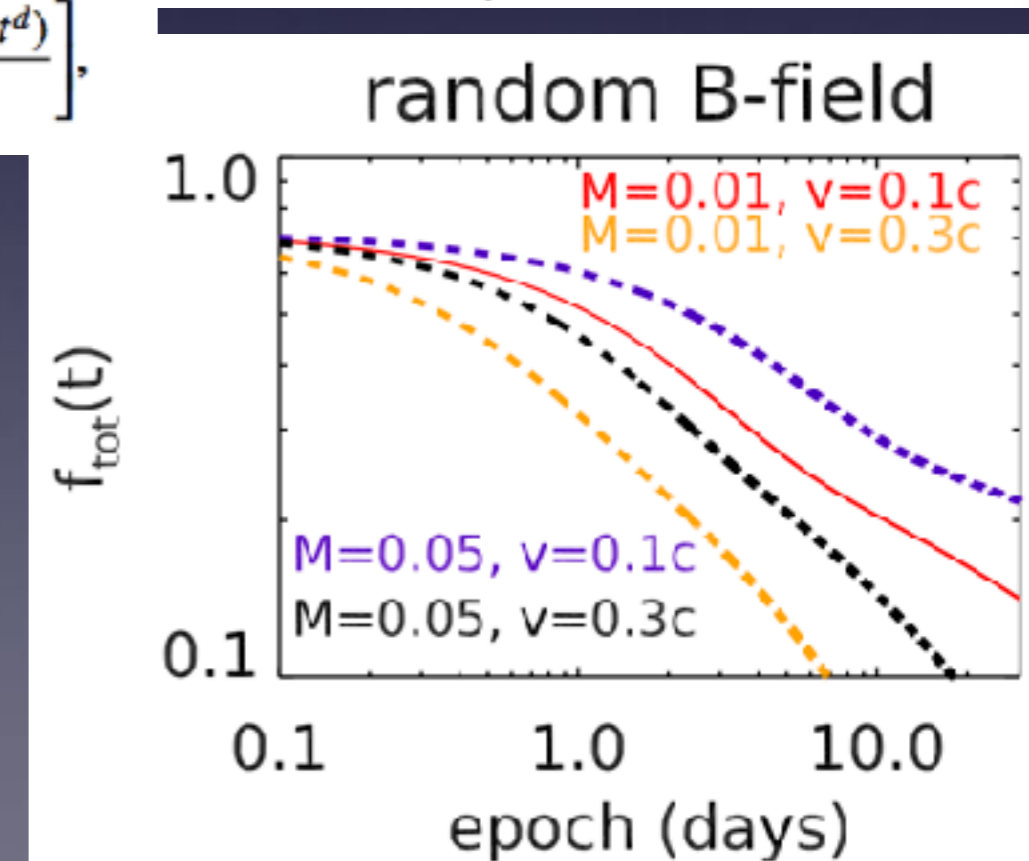
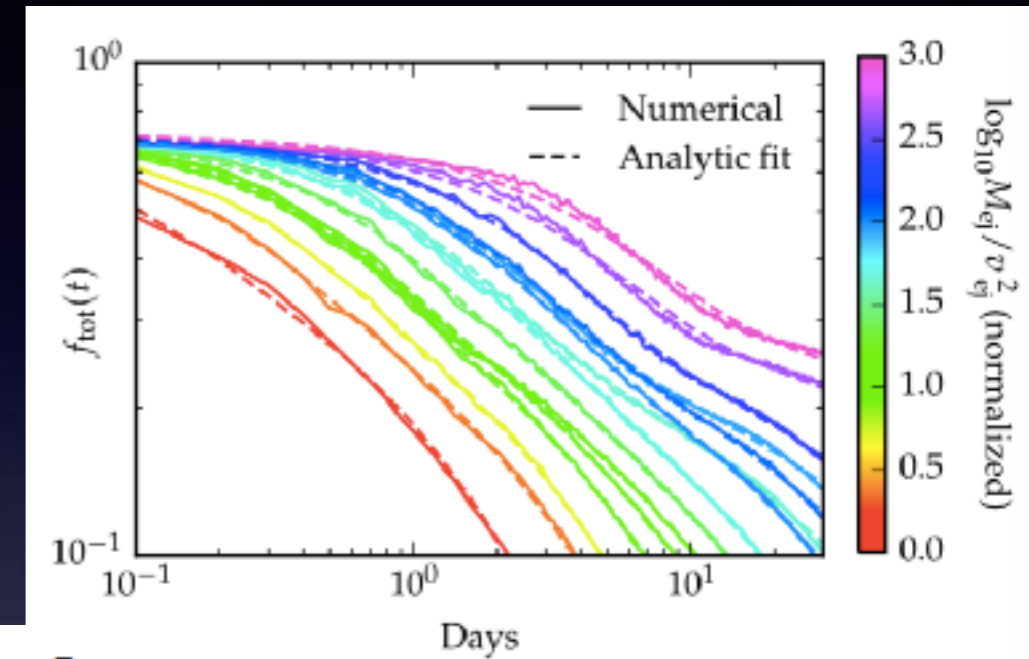


Barnes et al. : thermalisation efficiency



$$f_{\text{tot}}(t) = 0.36 \left[\exp(-at) + \frac{\ln(1 + 2br^d)}{2br^d} \right]$$

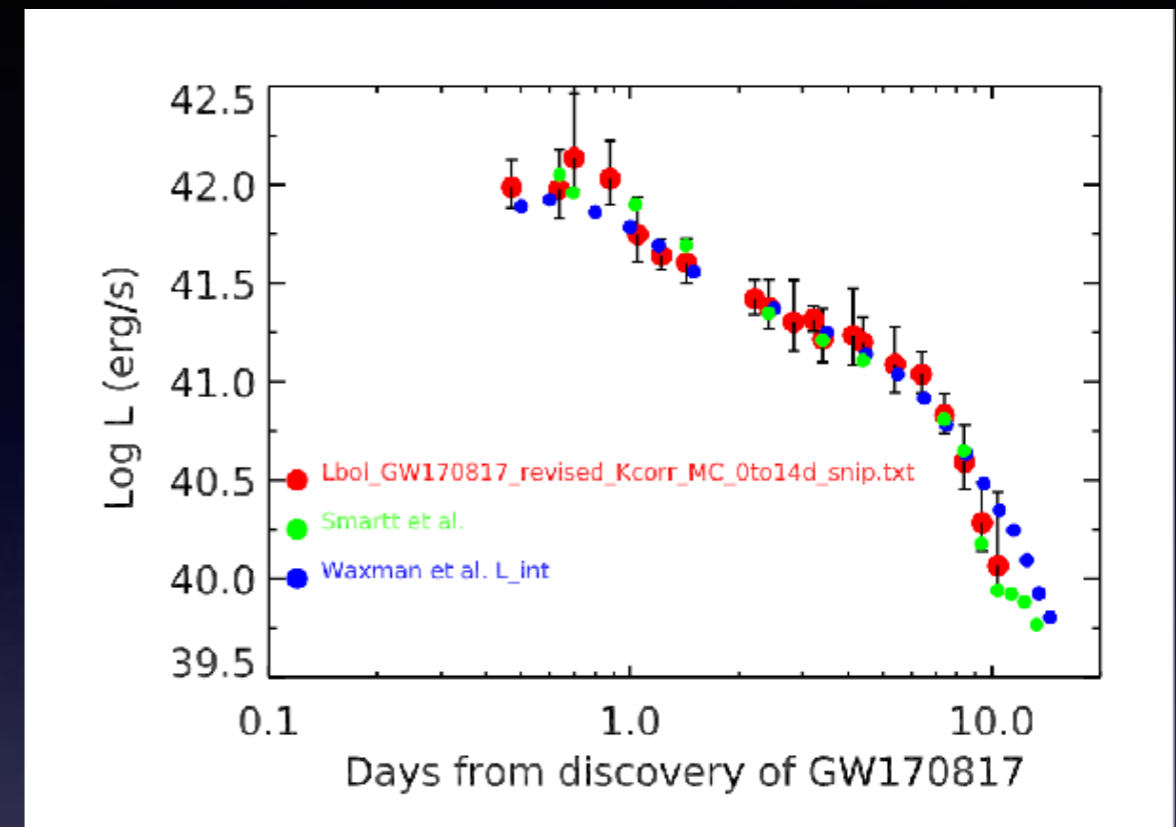
Barnes et al. 2016



1-component fits

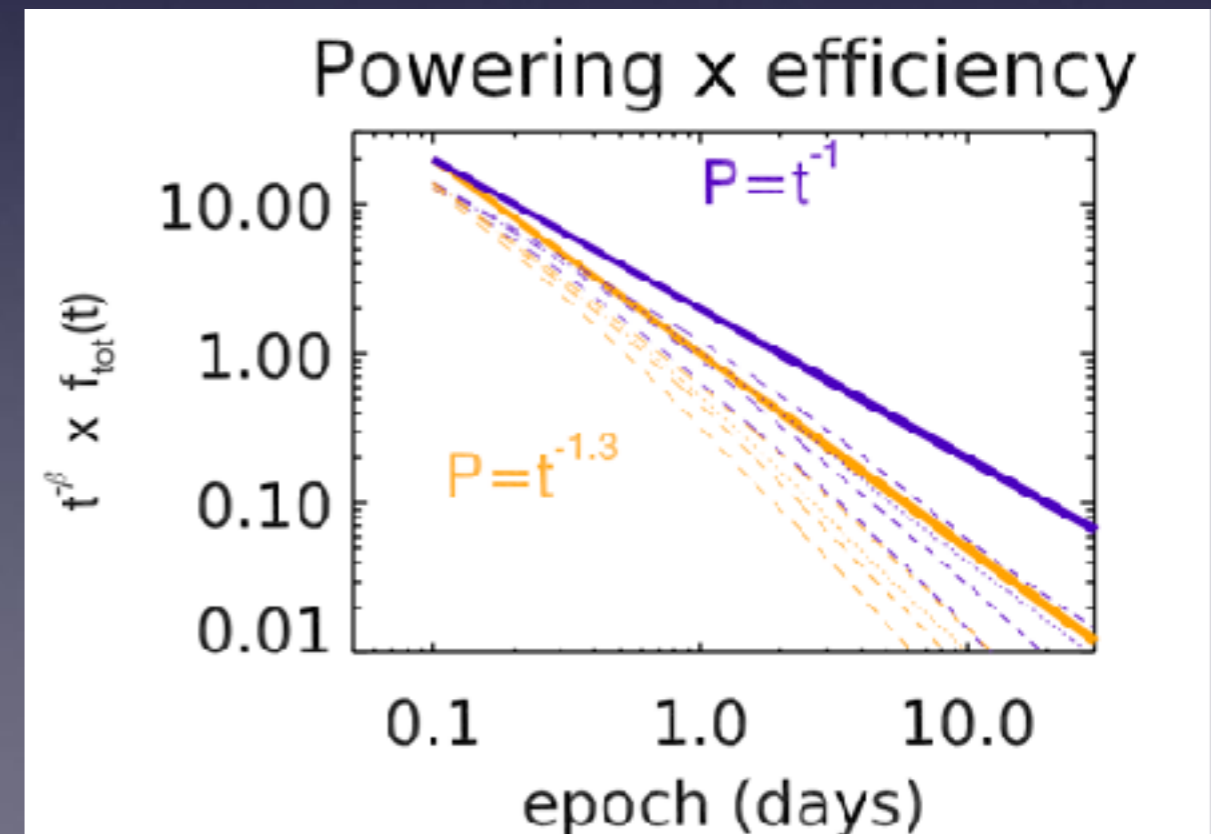
Data :

- Up to 6-7 days : reproduce all photometric data
- SED is (approximately) black body
- L_{bol} after that - uncertain
- No 2nd component **required**



Model :

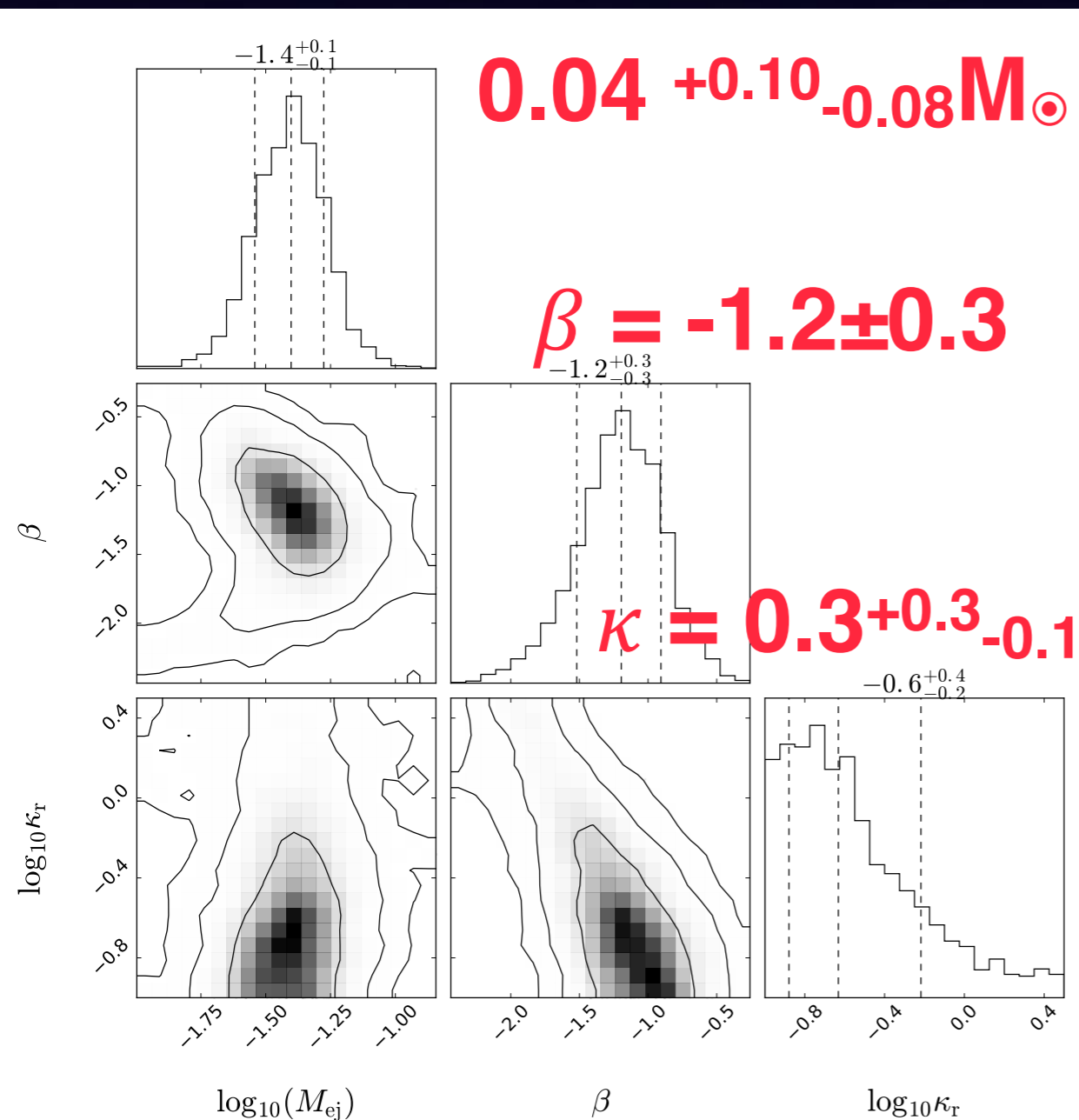
- Within the uncertainties of powering exponent (beta) and efficiency (Barnes et al.)
- Deposited energy does **not require** 2nd component
- Choices can allow it



Arnett-Jerkstrand posteriors



Michael Coughlin: <https://github.com/mcoughlin>

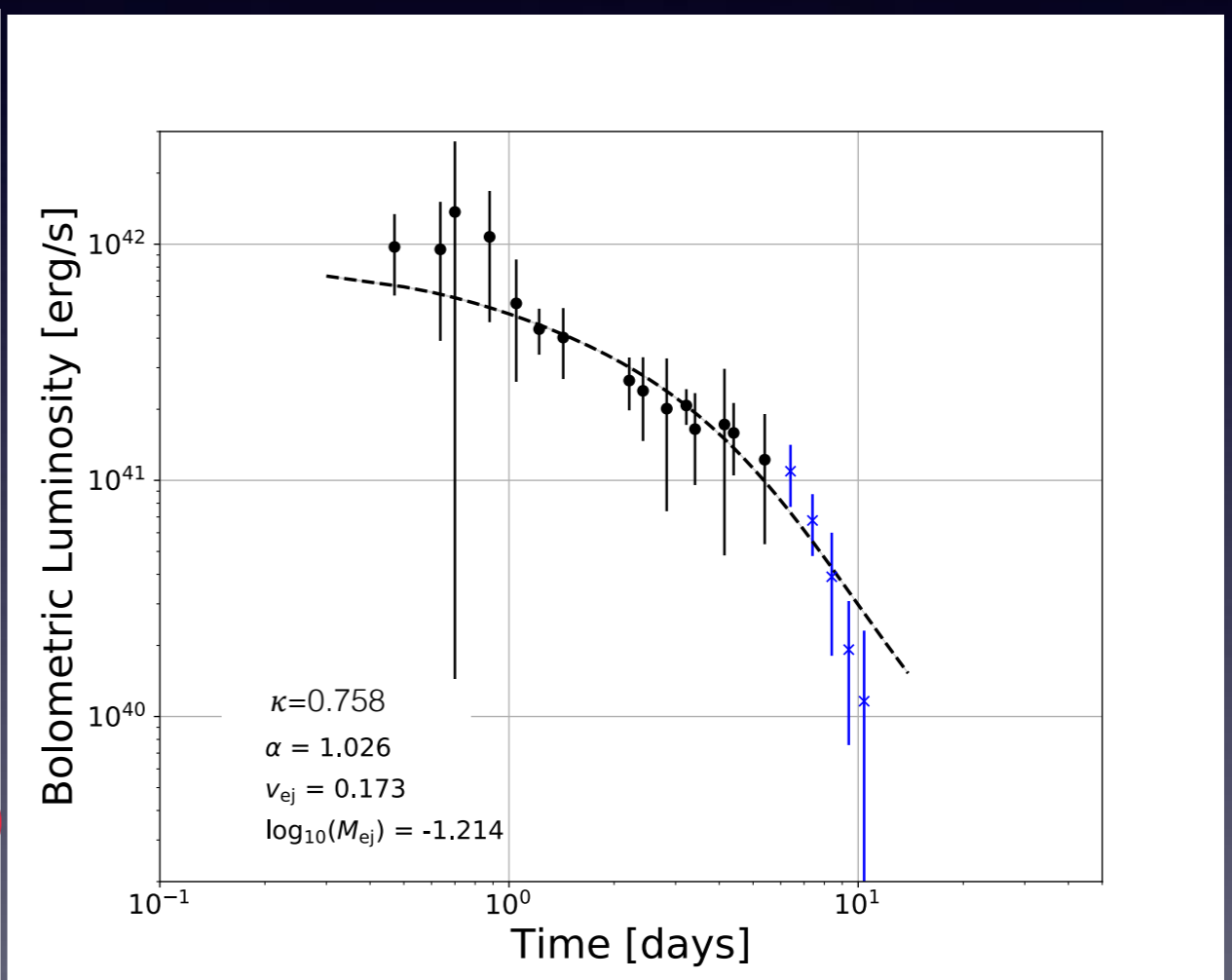
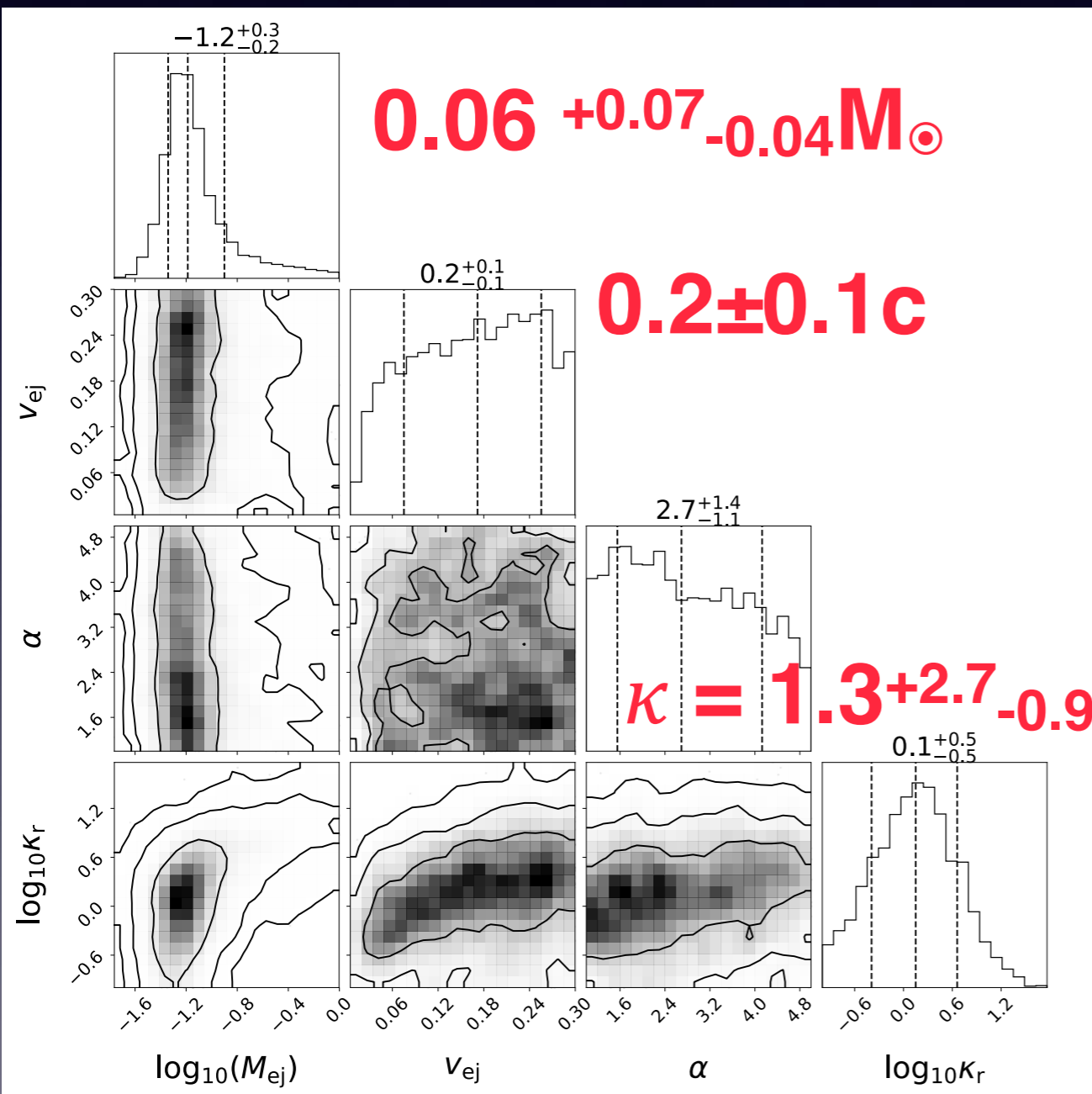


Compare with
Recent analysis by
Waxman et al. 2017
 $M \approx 0.05 M_{\odot}$
 $\kappa \approx 0.3 \text{ cm}^2 \text{ g}^{-1}$
 $v(m) = v_M m^{-\alpha}$
for $(0.1c < v < 0.3c)$

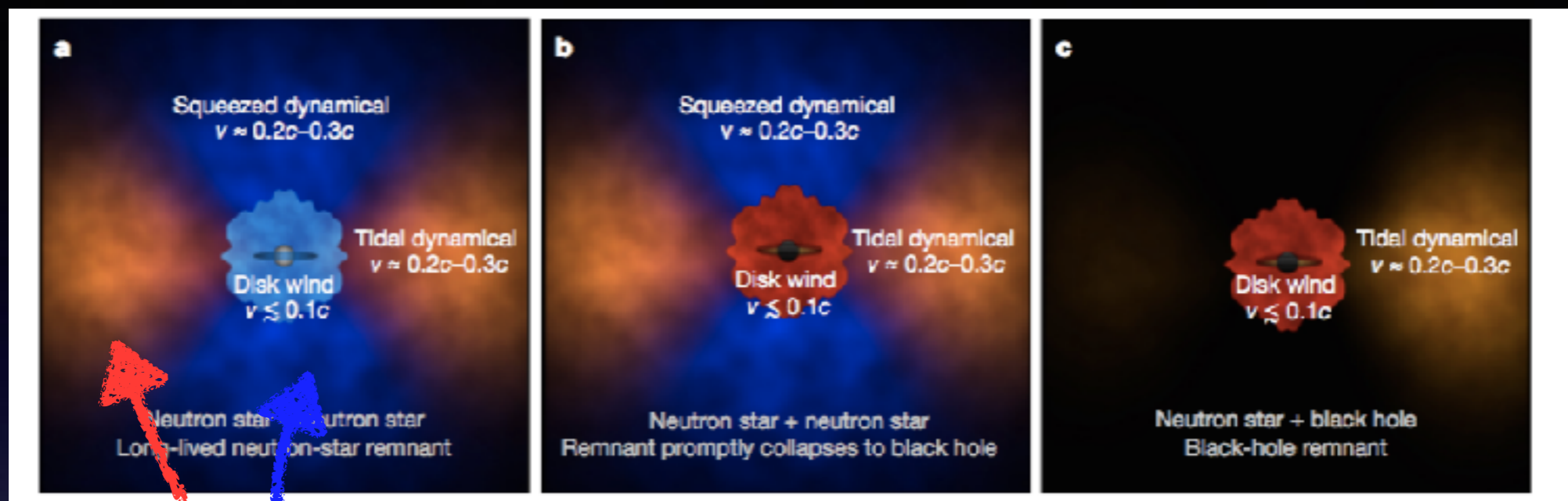
Updated Metzger posteriors



Michael Coughlin: <https://github.com/mcoughlin>

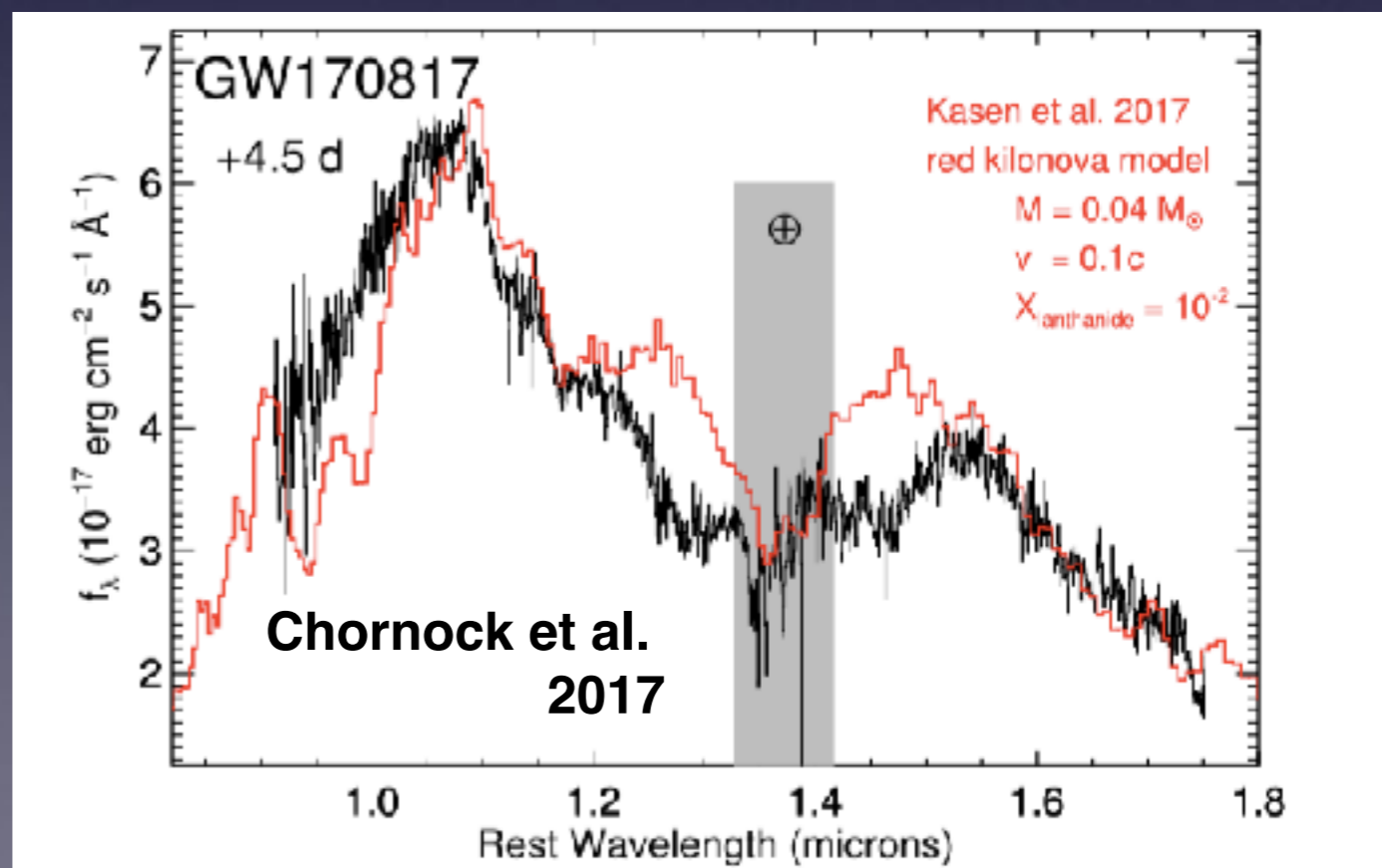
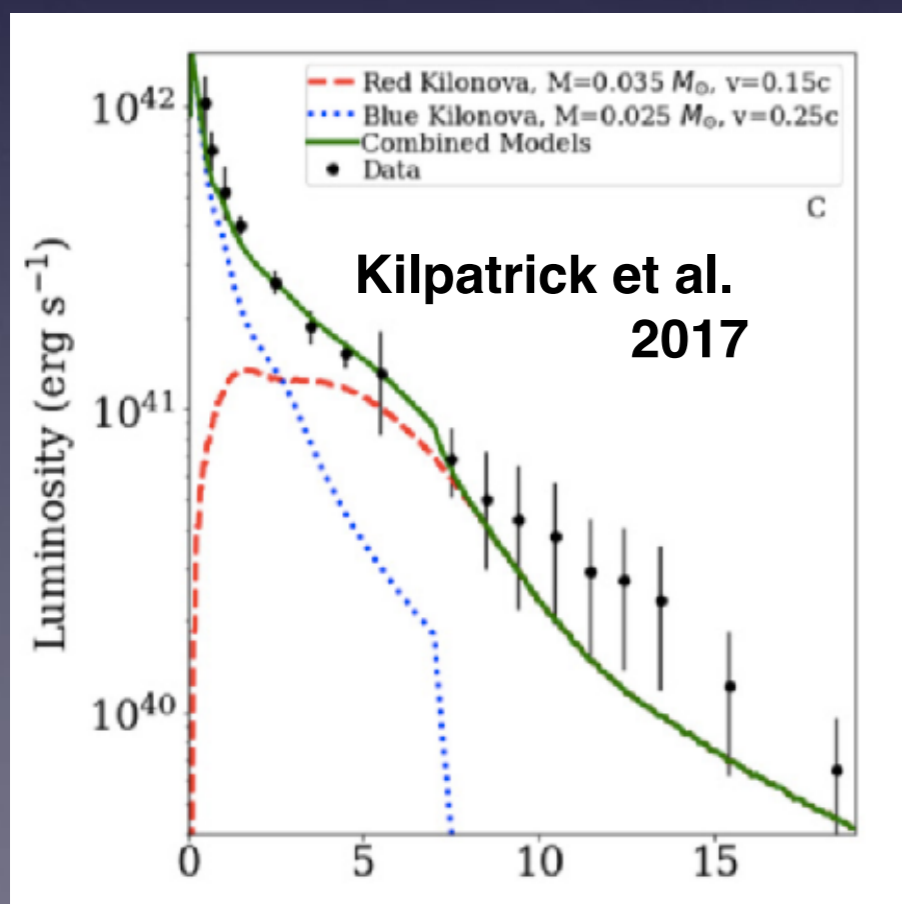


Kasen, Metzger, Barnes, Quartet, Ramirez-Ruiz 2017



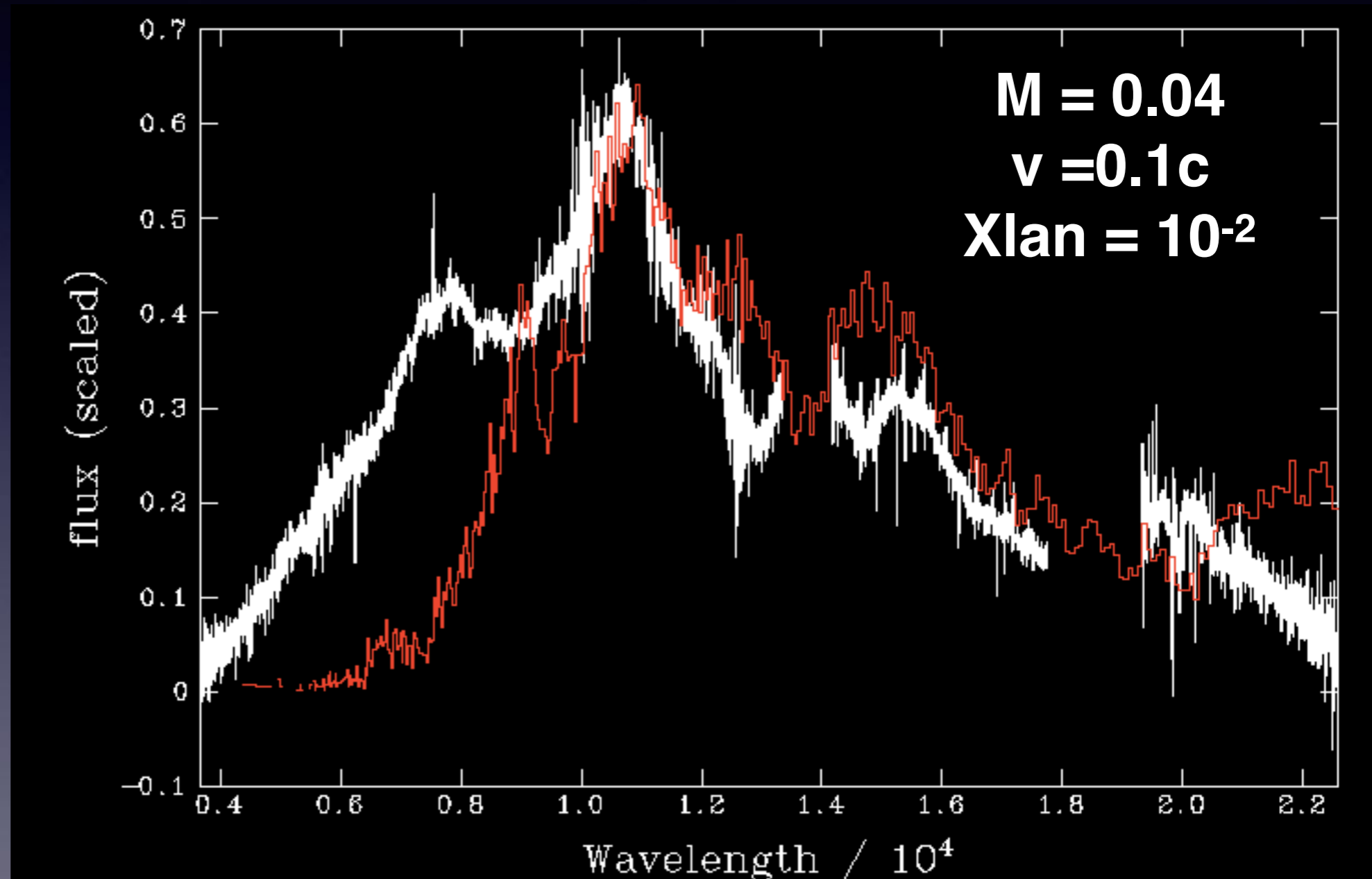
$M = 0.025 M_{\odot}, v_k = 0.3c$ and $X_{\text{lan}} = 10^{-4}$

$M = 0.04 M_{\odot}, v_k = 0.15c$ and $X_{\text{lan}} = 10^{-1.5}$

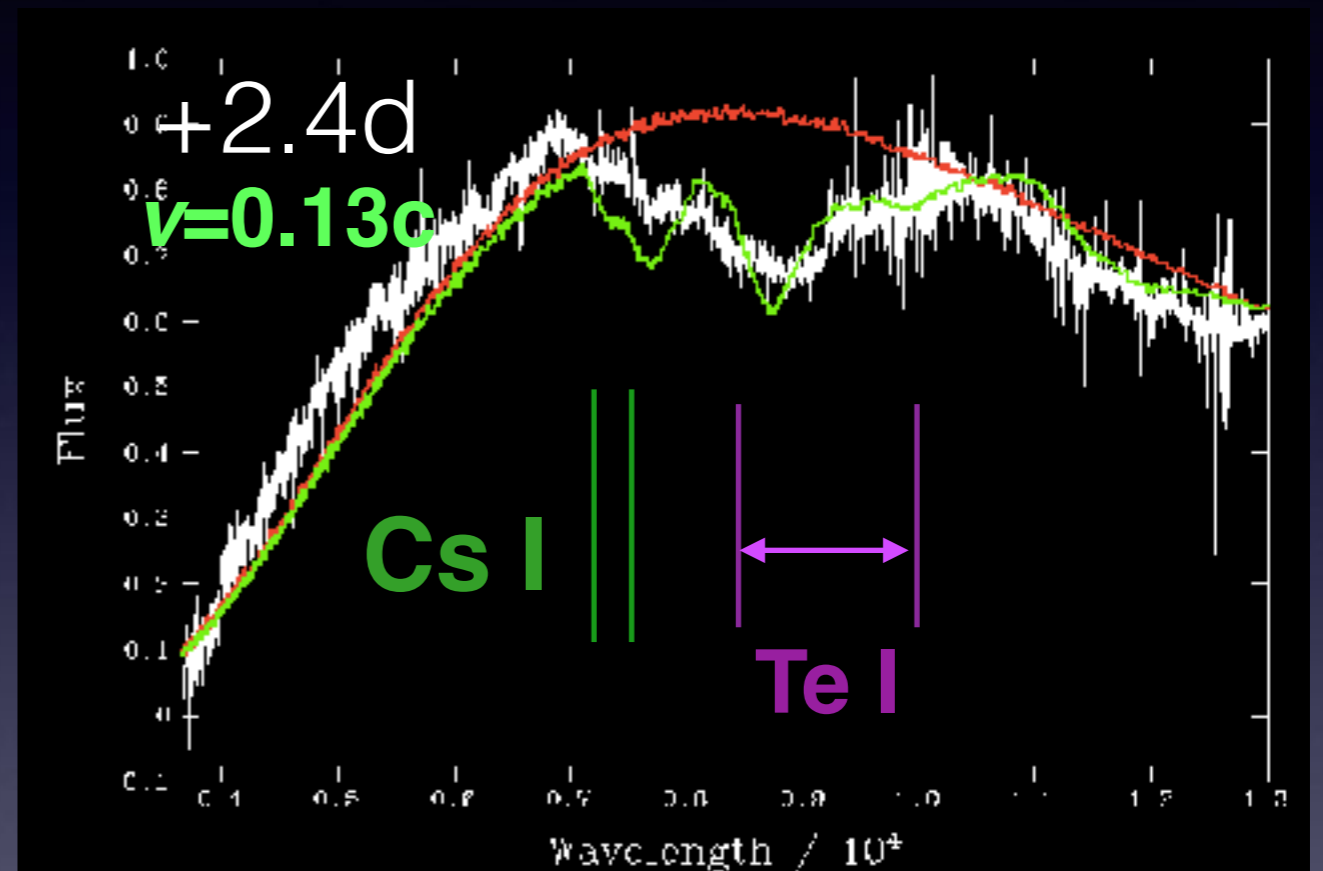
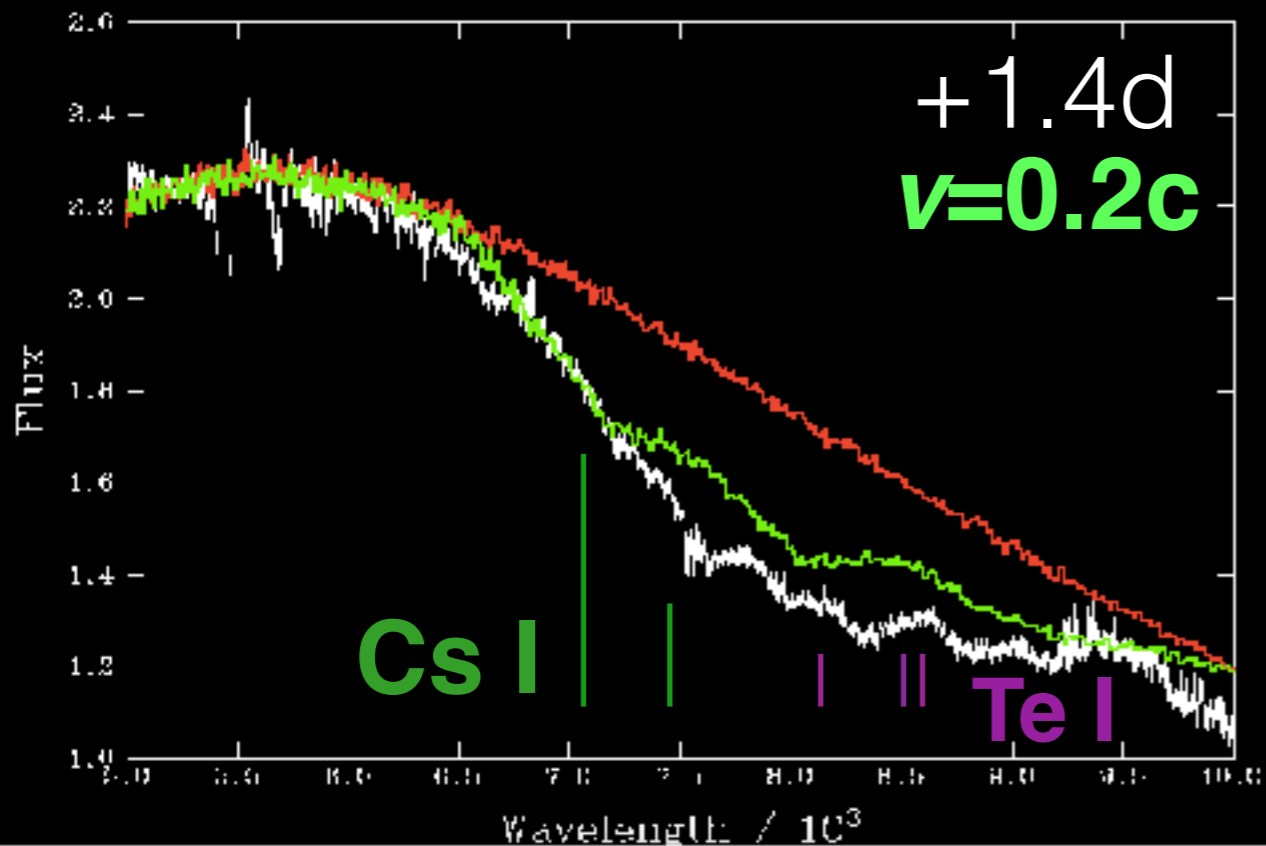


Kasen et al. vs xshooter +4.5d

- Same model - full optical and NIR
- Lacking optical
- Blue component: if thermal would dilute NIR flux



Xshooter spectra - early



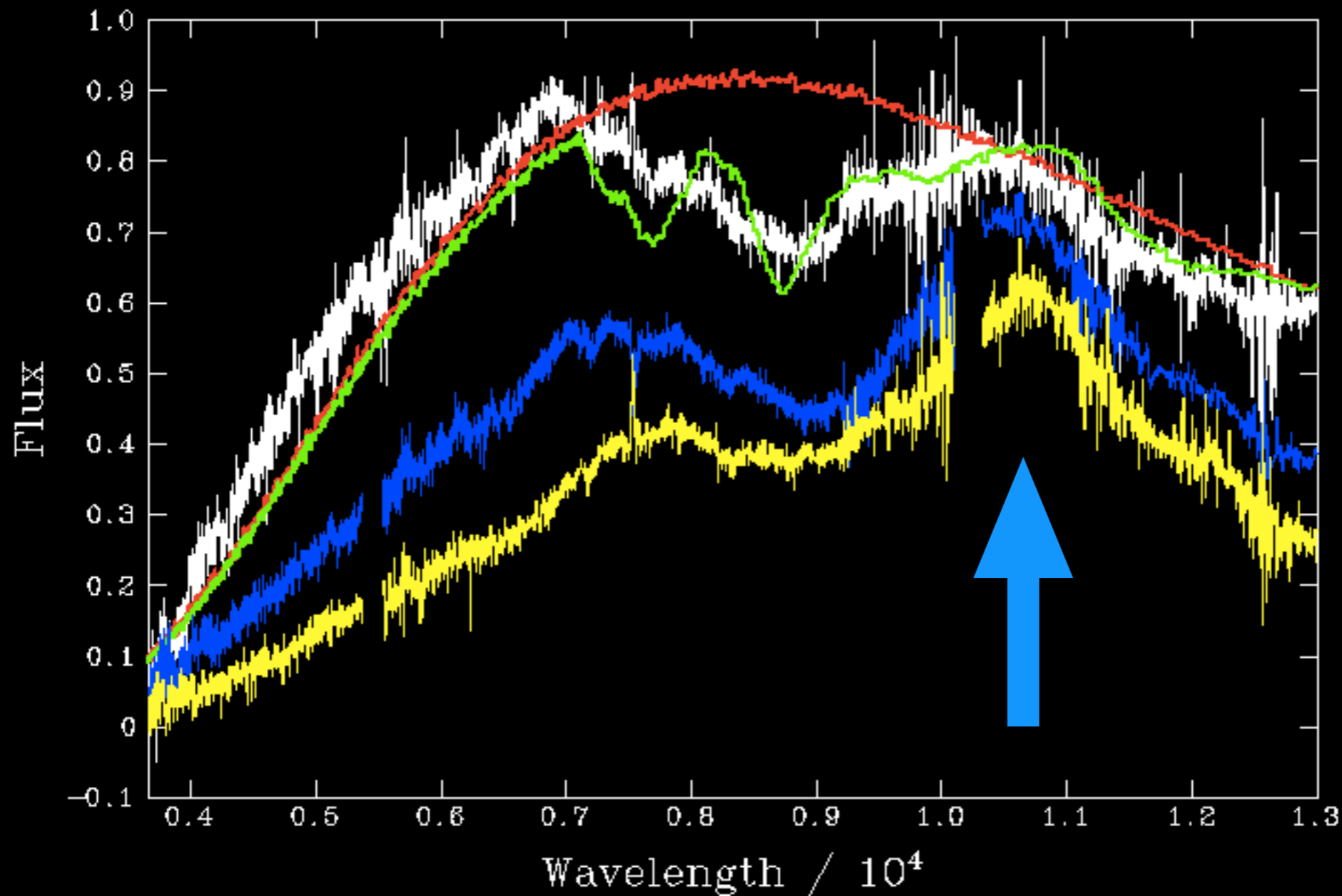
Cs I : resonance doublet
8521, 8943 Angs

Te I : $\log(gf) = 0$

Pian et al. 2017, Smartt et al. 2017



Diffusion phase or optically thin transition



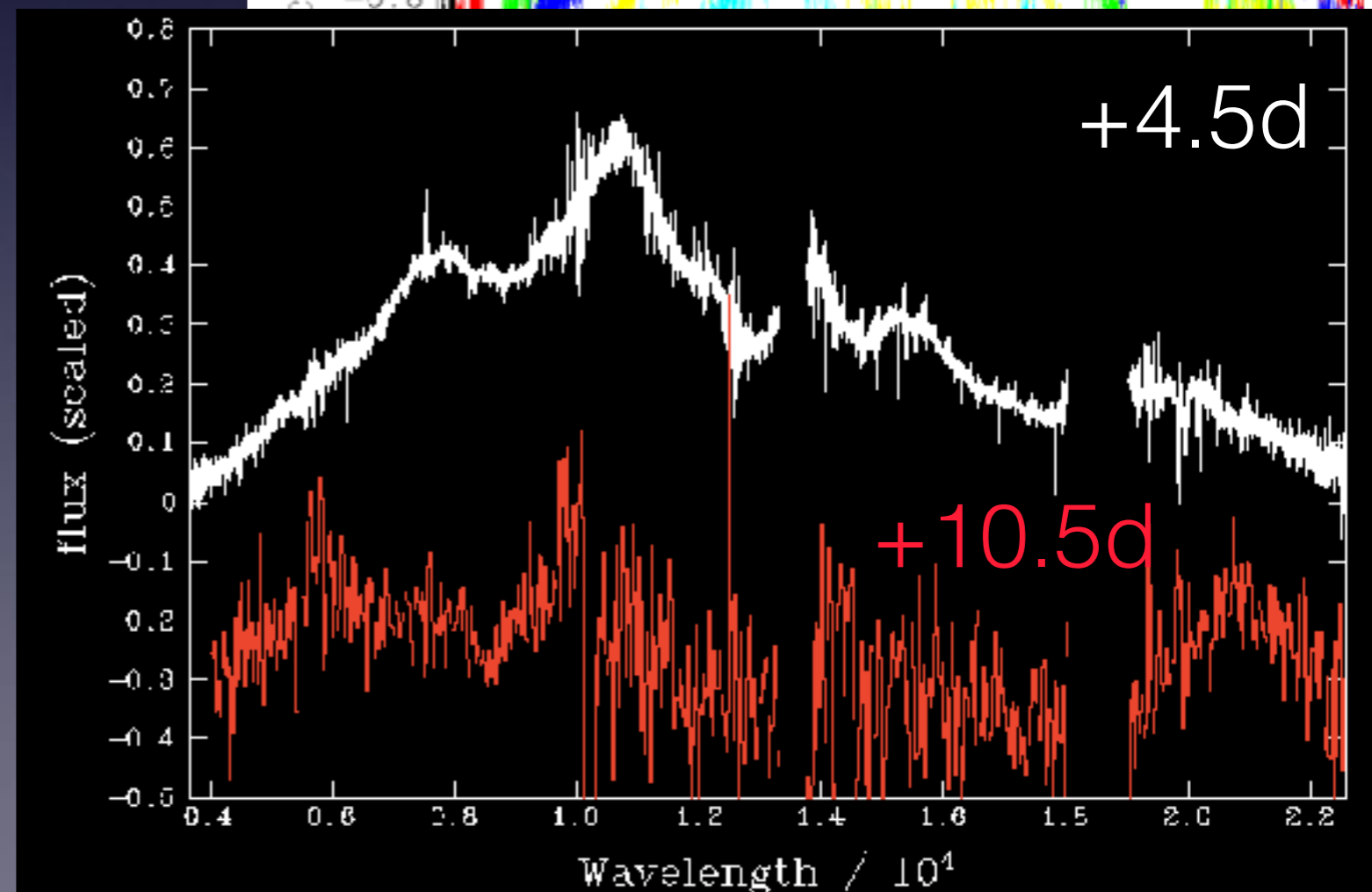
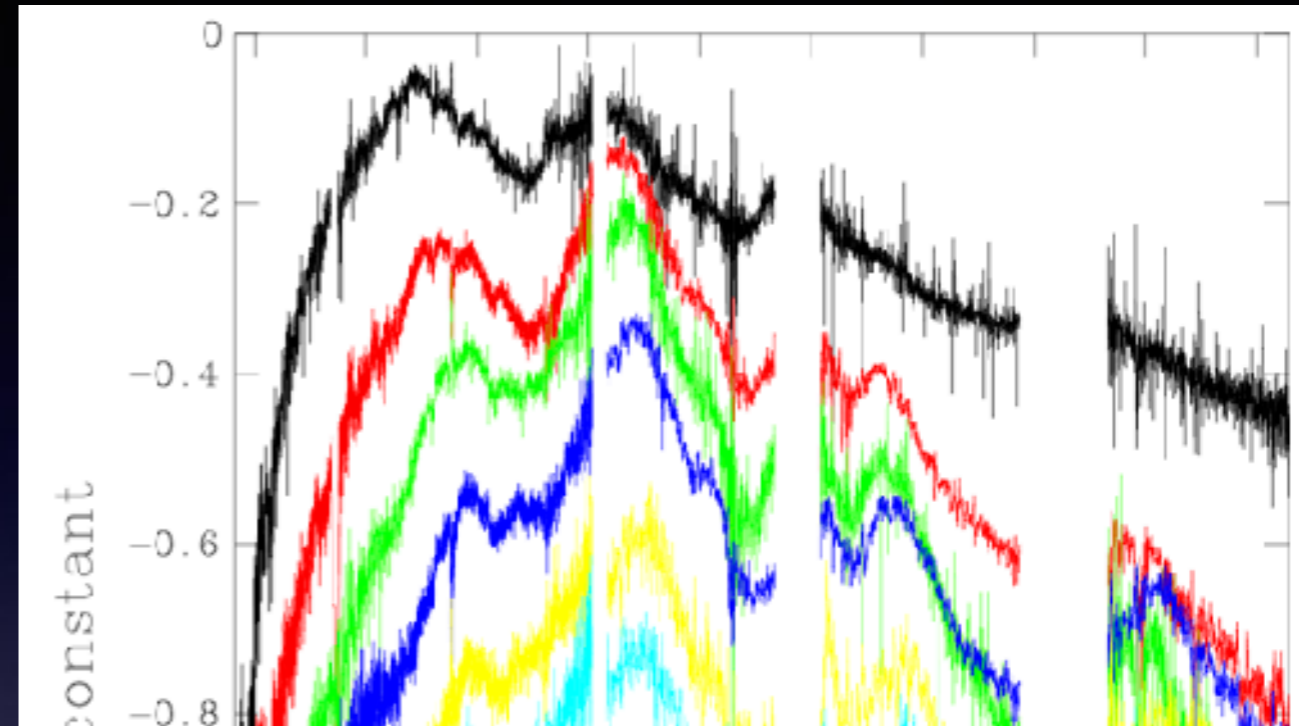
+2.4d

+3.4d

+4.4d

ESO xshooter spectra sequence

- Are all of these optically thick, diffusion phase spectra ?
- Not convincing BBody fits with single T_{eff} beyond about 6 days
- Are we seeing “nebular” phase spectra between 6 to 10.5 days ?



Rates are biggest uncertainty for future

LIGO - Virgo rate of NS-NS mergers

$$R = 1540_{-1220}^{+3200} \text{ Gpc}^{-3} \text{ yr}^{-1}$$

Abbott et al. 2017

O3 sensitivity
D < 100 Mpc

7⁺¹²₋₅
per yr

~0 to 1
per month

Design sensitivity
D < 200 Mpc

52⁺¹⁰⁷₋₄₁
per yr

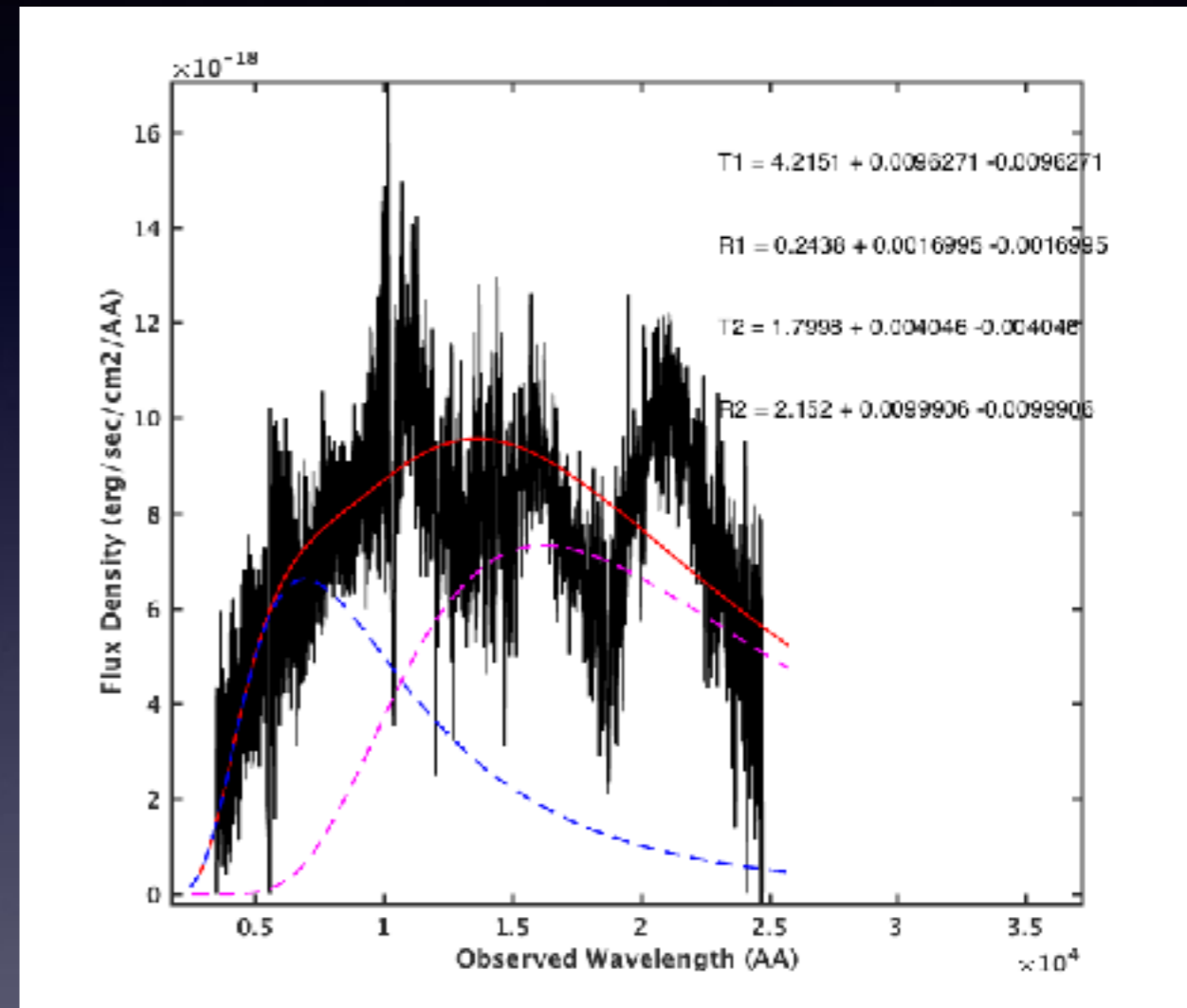
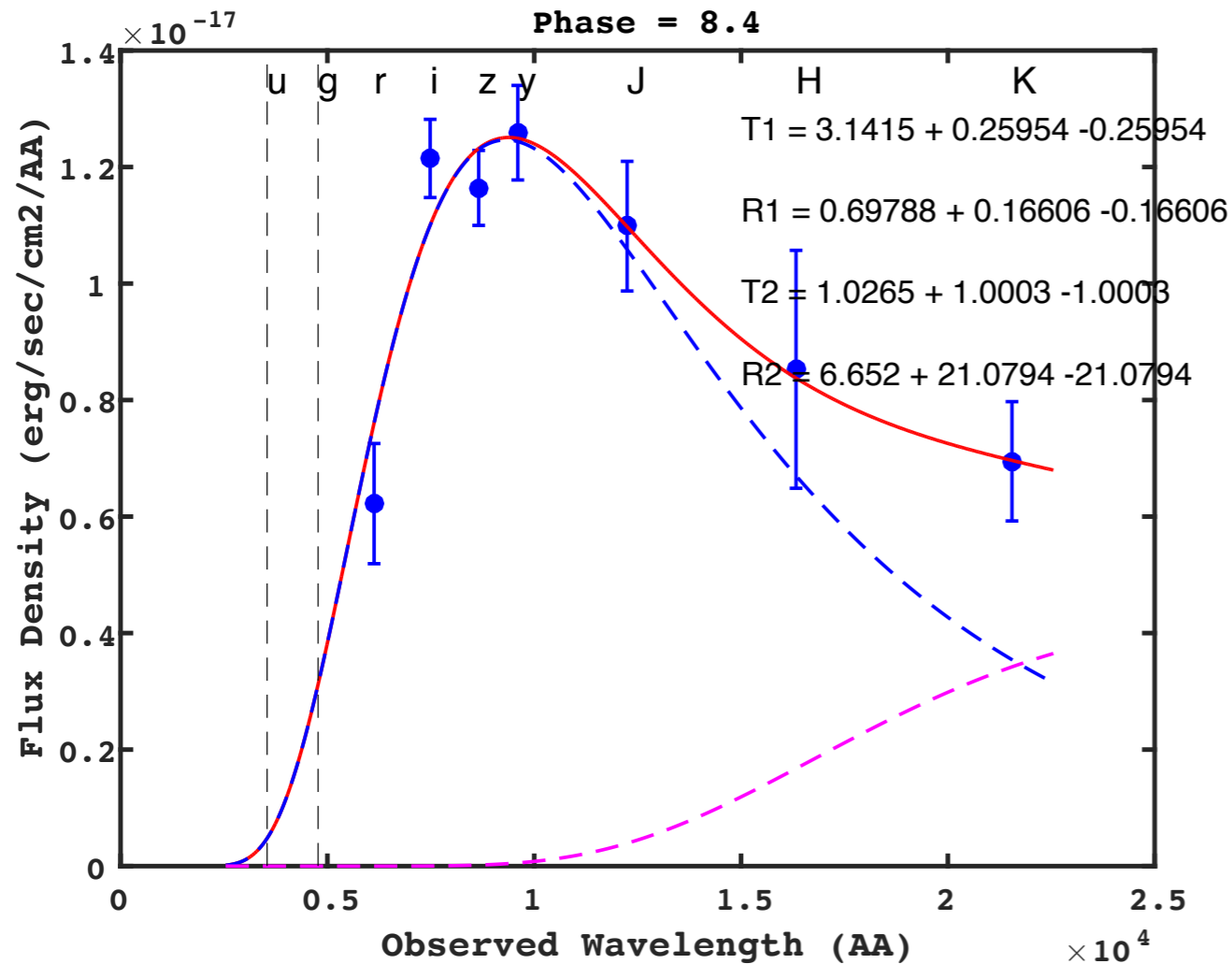
4⁺⁹₋₃
per month

Lowest: 1 per month in 2020+

Conclusions

- L_{bol} recalculated : ok up to 10 days, very uncertain beyond
- Two component models already shown to be plausible - physically motivated, Kasen et al. models (see Monday talks)
- Blue component may be the sole dominant component
- Quantitative fits (simple models) to L_{bol} account for all observed luminosity with one component which is lanthanide free, moderate opacity
- **Simple lesson for O3 - observe early, observe often, observe widely (wavebands)**
- **Open question - rates are biggest uncertainty**

2-component fits - example at +8.4d



- Reasonable fits at some epochs
- But cool component is not $T \sim 2500\text{K}$ (lanthanide recombination)
 - Consistency calculations needed for R , V_{cool} , V_{hot} , T_{cool} , T_{hot}
- Spectra do not appear photospheric after +3-4 days

GW20170814 (BBH)

Sky location : 3 detectors

1160 square degrees shrinks to 60

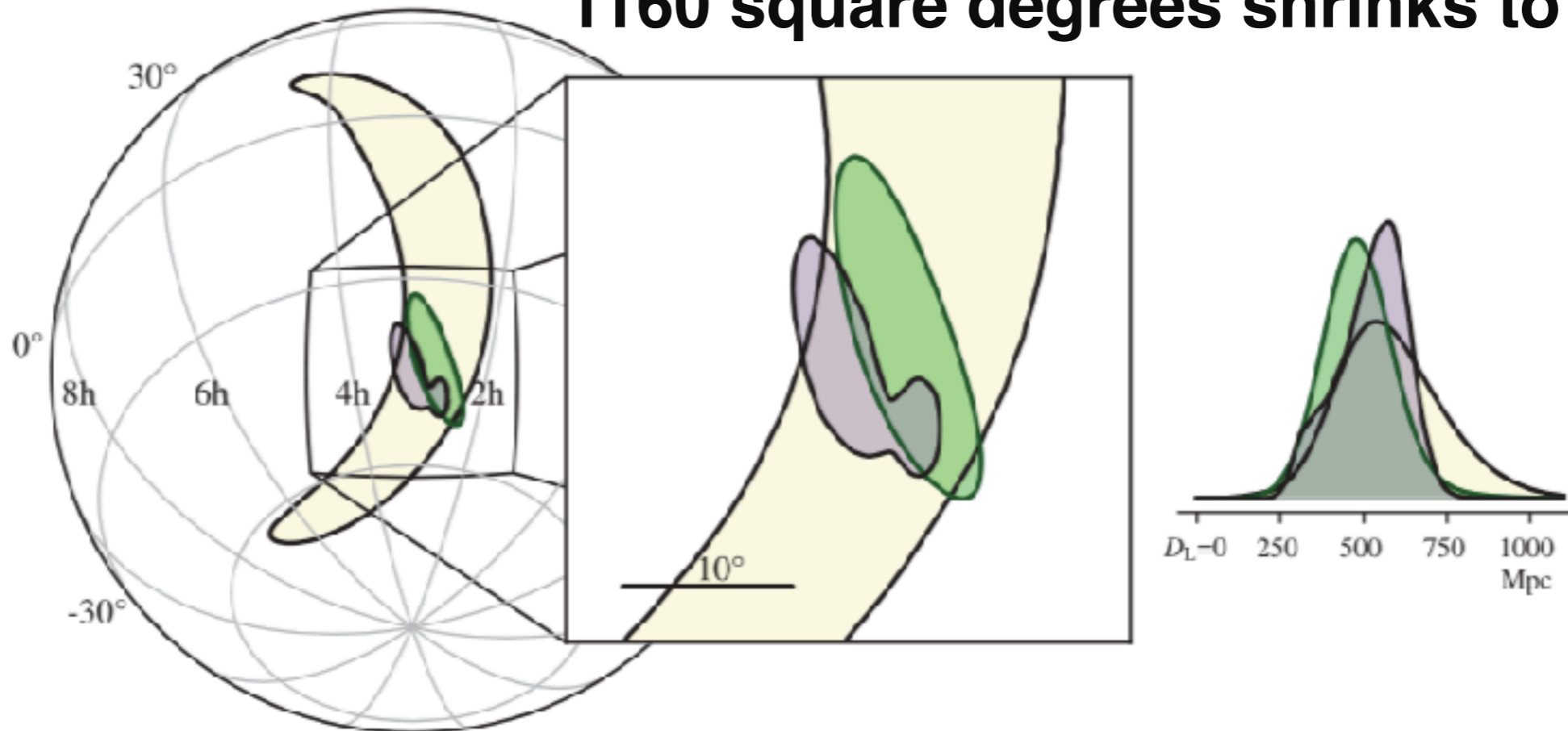
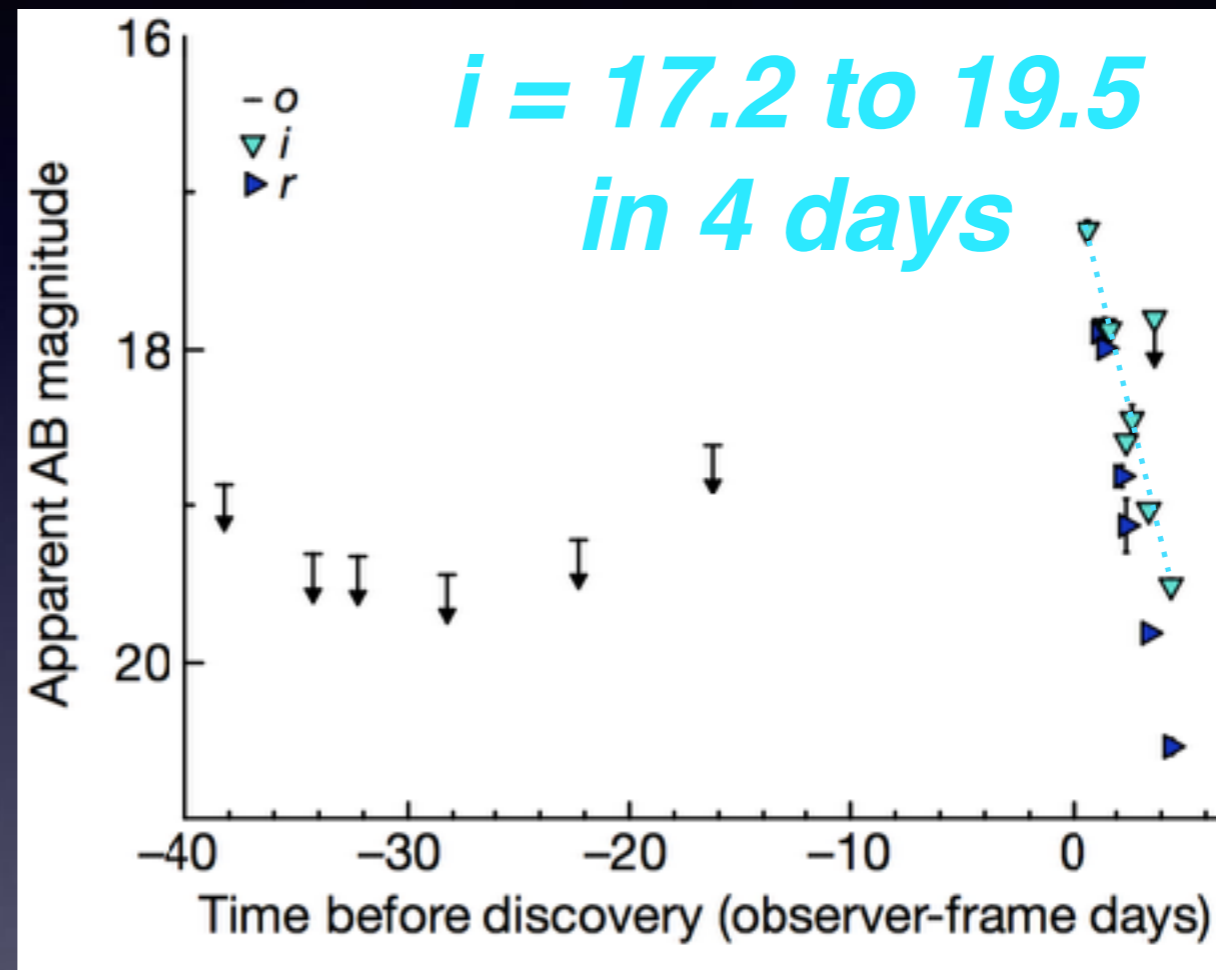
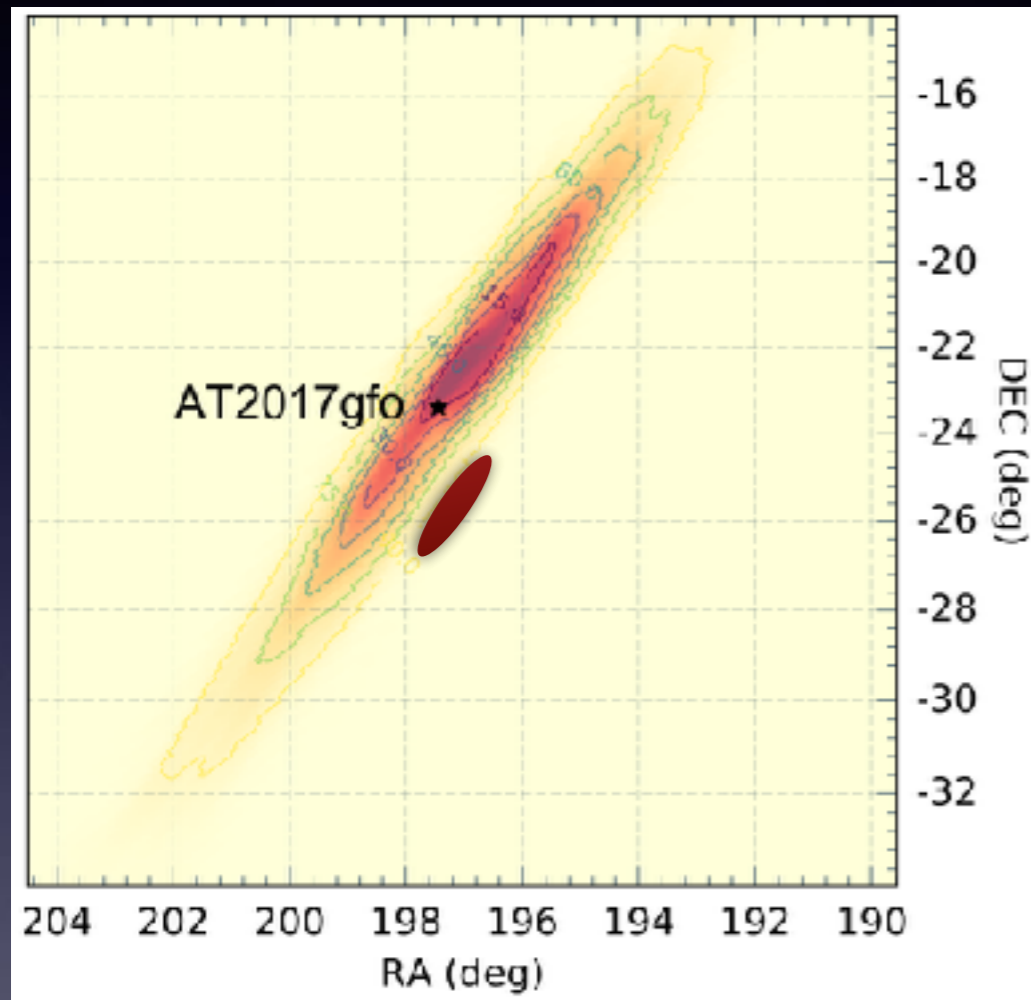


FIG. 3. Localization of GW170814. The rapid localization using data from the two LIGO sites is shown in yellow, with the inclusion of data from Virgo shown in green. The full Bayesian localization is shown in purple. The contours represent the 90% credible regions. The left panel is an orthographic projection and the inset in the center is a gnomonic projection; both are in equatorial coordinates. The inset on the right shows the posterior probability distribution for the luminosity distance, marginalized over the whole sky.

..... as of 2017 Aug 14

Skymap movement



- **Skymaps from LIGO-Virgo Collaboration - 3 degree offset !**
- Smartt S.J. et al. Nature, 2017, 551, 75 : ATLAS upper limits, GROND, ESO-NTT, Pan-STARRS, 1.5m Boyden,

Implications for chemical evolution

Total mass of r-process in Milky Way

$$M_r \sim 17\,000 M_\odot \left(\frac{\mathcal{R}_{\text{NSNS}}}{500 \text{ Gpc}^{-3} \text{ yr}^{-1}} \right) \left(\frac{\bar{m}_{\text{ej}}}{0.03 M_\odot} \right) \left(\frac{\tau_{\text{gal}}}{1.3 \times 10^{10} \text{ yr}} \right).$$

LIGO - Virgo rate of NS-NS mergers

$$R = 1540_{-1220}^{+3200} \text{ Gpc}^{-3} \text{ yr}^{-1}$$

Can account for **all** r-process abundances with AT2017gfo type objects

We may have over-production problem !

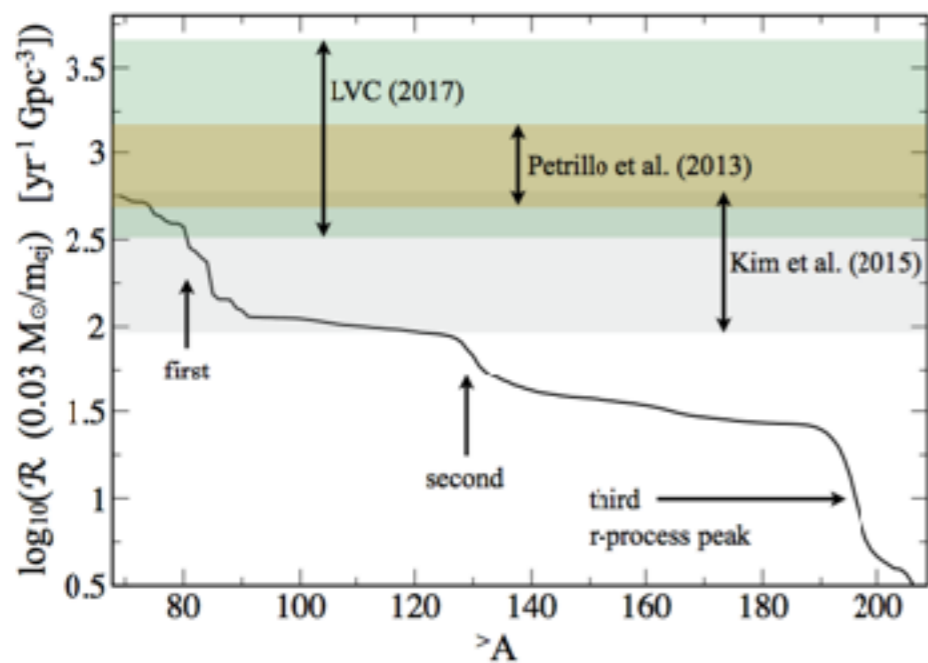


Fig. 5. Needed event rates, scaled to an ejecta mass of $0.03 M_\odot$, if NSNS mergers are to produce all r-process (in solar proportions) *above a minimum nucleon number* $>A$ (solid black line). Also shown are the estimated rates (90% conf.) for NSNS mergers from the population synthesis study of Kim et al. (2015), the sGRB rates based on SWIFT data from Petrillo et al. (2013) and the LVC estimate based on the first detected NSNS merger event.

Rosswog et al. 2017

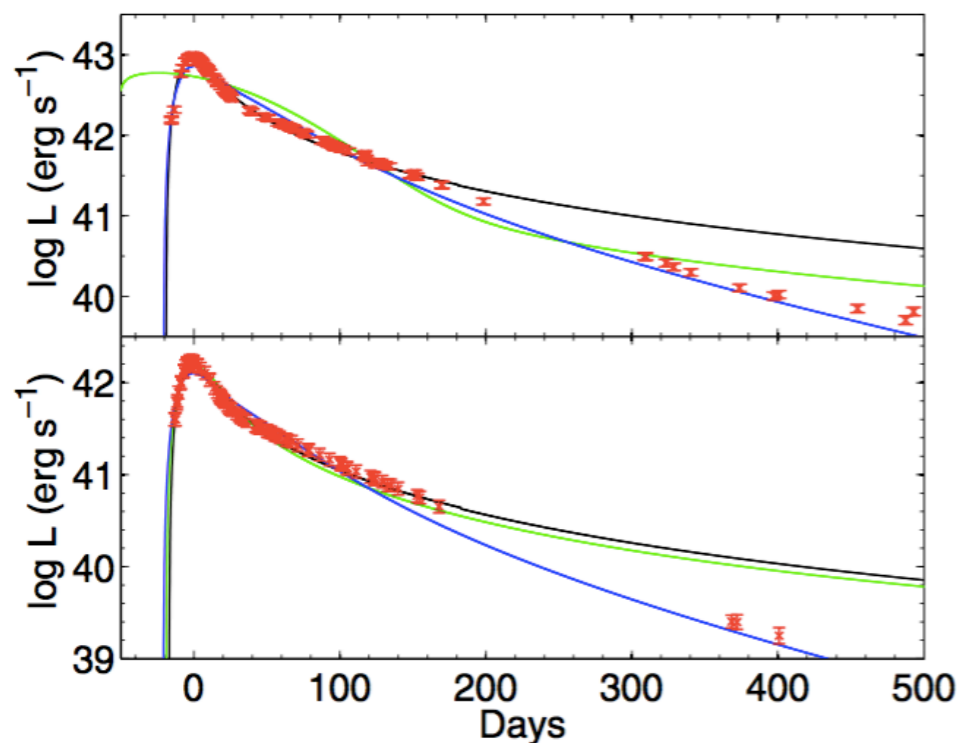
Fin

Semi-analytic models “Arnett-Jerkstrand”

$$L_{\text{SN}}(t) = e^{-(t/\tau_m)^2} \int_0^{t/\tau_m} P(t') 2(t'/\tau_m) e^{(t'/\tau_m)^2} \frac{dt'}{\tau_m} \text{ erg s}^{-1}, \quad (\text{D1})$$

where τ_m is the diffusion timescale parameter, which in the case of uniform density ($E_k = (3/10)M_{\text{ej}}V_{\text{ej}}^2$) is

$$\tau_m = \frac{1.05}{(\beta c)^{1/2}} \kappa^{1/2} M_{\text{ej}}^{3/4} E_k^{-1/4} \text{ s}. \quad (\text{D2})$$



Can vary
 $M = \text{mass}$
 $E = \text{energy (velocity)}$
 $\kappa = \text{opacity}$
 $P(t) = \text{power source function}$

Inserra, Smartt, **Jerkstrand** et al 2013

<https://star.pst.qub.ac.uk/wiki/doku.php/users/ajerstrand/>